Terms and Conditions of Use of Digitised Theses from Trinity College Library Dublin

Copyright statement

All material supplied by Trinity College Library is protected by copyright (under the Copyright and Related Rights Act, 2000 as amended) and other relevant Intellectual Property Rights. By accessing and using a Digitised Thesis from Trinity College Library you acknowledge that all Intellectual Property Rights in any Works supplied are the sole and exclusive property of the copyright and/or other IPR holder. Specific copyright holders may not be explicitly identified. Use of materials from other sources within a thesis should not be construed as a claim over them.

A non-exclusive, non-transferable licence is hereby granted to those using or reproducing, in whole or in part, the material for valid purposes, providing the copyright owners are acknowledged using the normal conventions. Where specific permission to use material is required, this is identified and such permission must be sought from the copyright holder or agency cited.

Liability statement

By using a Digitised Thesis, I accept that Trinity College Dublin bears no legal responsibility for the accuracy, legality or comprehensiveness of materials contained within the thesis, and that Trinity College Dublin accepts no liability for indirect, consequential, or incidental, damages or losses arising from use of the thesis for whatever reason. Information located in a thesis may be subject to specific use constraints, details of which may not be explicitly described. It is the responsibility of potential and actual users to be aware of such constraints and to abide by them. By making use of material from a digitised thesis, you accept these copyright and disclaimer provisions. Where it is brought to the attention of Trinity College Library that there may be a breach of copyright or other restraint, it is the policy to withdraw or take down access to a thesis while the issue is being resolved.

Access Agreement

By using a Digitised Thesis from Trinity College Library you are bound by the following Terms & Conditions. Please read them carefully.

I have read and I understand the following statement: All material supplied via a Digitised Thesis from Trinity College Library is protected by copyright and other intellectual property rights, and duplication or sale of all or part of any of a thesis is not permitted, except that material may be duplicated by you for your research use or for educational purposes in electronic or print form providing the copyright owners are acknowledged using the normal conventions. You must obtain permission for any other use. Electronic or print copies may not be offered, whether for sale or otherwise to anyone. This copy has been supplied on the understanding that it is copyright material and that no quotation from the thesis may be published without proper acknowledgement.

Biomechanical origins of osteoporosis

by

Laoise Maria McNamara, BE

A thesis submitted to the University of Dublin in partial fulfilment of the requirements for the degree of

Doctor in Philosophy

Trinity College Dublin

March 2004

Supervisor
Professor P.J. Prendergast

External Examiner
Professor. H. Weinans
(Erasmus University Rotterdam)

Internal Examiner
Professor. T.C. Lee

DECLARATION

I declare that I am the sole author of this thesis and that the work presented in it, unless otherwise referenced, is my own. I also declare that the work has not been submitted, in whole or in part, to any other university or college for a degree or other qualification.

I authorize the library of Trinity College Dublin to lend or copy this thesis on request.

Laoise McNamara

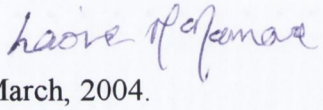

March, 2004.

ACKNOWLEDGEMENTS

I am extremely grateful for the guidance and encouragement I have received from my supervisor Professor Patrick Prendergast throughout the course of my PhD research. I have been fortunate to have had a thoroughly challenging and inspiring experience and enjoyed it above all.

I would like to thank the partners of the MIAB project for a stimulating collaboration from which I received important advice.

I have been extremely fortunate to work with everyone in the Bioengineering group and appreciate all the guidance and assistance I received from Danny, Linda, Triona, Kevin, John B, Alex, Fergal and Damien. I would also like to thank Adriele, Bruce, Richard, Mary Roe, James, Conor, John G, John V, Laura, Paul, Louise and all the other postgrads. It's been fun!

Many thanks to Sheena Browne, Joan Gillen and Nicole Byrne for their assistance whenever it was necessary and also to everybody in the workshop, particularly Gabriel Nicholson, Peter O'Reilly and Alan Reid.

Thanks to all my friends from Galway, my flatmates and the Trinity water polo club for providing all the distractions throughout the years! I am very grateful to Niamh, Cian, Fergal and Adrian for helping me out whenever it was needed and most of all for their tolerance!

Finally I want to thank, my dad and my mum for all their encouragement and support throughout my college years. I would particularly like to thank them for showing such enthusiasm for all my endeavours and providing me with invaluable advice.

This work was funded by the EU project MIAB:

'Mechanical Integrity and Architecture of Bone: '

CONTENTS

Abstract

The contention of this thesis is that a pathological change in bone tissue material properties during osteoporosis alters the mechanical stimuli to bone remodelling cells and drives them to adapt the trabecular architecture resulting in a reduction in bone strength. To argue the case for this thesis, three separate but inter-related hypotheses with respect to the regulatory mechanisms governing bone remodelling are tested. These hypotheses are (1) A pathological change in the material properties of bone tissue occurs during osteoporosis, (2) Bone remodelling is regulated by a combination of strain and damage, and (3) Suppressing bone turnover in drug treated bone results in weaker bone tissue than that of normal and osteoporotic bone

A method to evaluate mechanical behaviour of single bone trabeculae is developed to assess the mechanical properties of normal, osteoporotic and drug treated bone tissue. A micro-tensile testing apparatus is developed that minimizes errors due to misalignment and stress concentrations at the grips. The method is used to test the hypothesis that the strength of single trabeculae will differ for normal, ovarectomized, and drug treated rat bones over the course of ageing (hypotheses 1 and 3).

A method of producing accurate solid models of individual trabeculae, through the use of serial sectioning at micro resolutions and micro-CT scanning, is developed. These models are used to analyse the stress distribution within trabeculae and the effects of the presence of resorption lacunae on these distributions in order to determine whether the structure of the individual trabecula may be maintained by strain or by the presence of microdamage, or a combination of both (hypothesis 2).

A mechano-regulation rule for bone remodelling is developed that relates the mechanical stimuli to the change in bone mass. This rule is applied to a computational model of a bone trabecula to predict bone remodelling along trabecular surfaces. These simulations reveal the regulatory mechanisms that govern initiation, propagation and termination of the normal bone remodelling process (hypothesis 2).

Finally, this rule is applied to models with material properties of osteoporotic bone tissue to investigate the main contention of this thesis.

LIST OF FIGURES

LIST OF TABLES

1. Introduction

1.1 General introduction

The methods of engineering and physics can be used to assess the degeneration of living materials with disease and age. Of particular interest to the ageing population is the degeneration of the bone comprising the human skeleton. The skeletal system gives the body its form, facilitates movement, and protects the internal organs. The composition of bone and its micro-structural organisation create the material properties that allow bone to serve these functions under loading conditions experienced during life (Currey, 1984). Bone has been described as a dynamic material because it has the capacity to renew itself, and adapt its architecture, so that it continues to serve its functions. However with age and disease, in particular the disease of osteoporosis, the ability of the skeleton to perform fundamental mechanical functions is impaired. A particular problem is that bone strength is reduced causing an increase in susceptibility to bone fractures. Osteoporotic fractures frequently require hospitalization, often lead to permanent disability, and are a major contributor to medical care costs worldwide. In fact it is estimated that, of women who have an osteoporotic hip fracture, around 10-20% more die within a year than would be expected for their age group (Cummings and Melton, 2002).

Because of the importance for quality of life in an ageing population, the processes by which osteoporosis and ageing lead to a reduction in bone strength are the subject of intense scientific investigation. In recent years the advances in health-care provision in many countries and an increased expectation for quality of life have increased life expectancy of the population. As osteoporosis is a disease that prevails with older people it is clear that the consequences of osteoporotic bone fracture are set to become even more relevant in the future. In order to address this problem it is imperative that biomechanical engineers develop an understanding of how the normal bone renewal process maintains bone strength and the mechanism by which a breakdown in this process occurs during osteoporosis. Also of importance is the extent to which conventional drug treatments are capable of halting osteoporosis.

1.2 Bone remodelling, osteoporosis and drug-treatment

There are two main types of bone found in the human skeleton; cortical bone and trabecular bone. Cortical bone has low porosity and is primarily found in the shafts of long bones and forms a shell around bones such as the vertebrae, scapula and pelvis. Trabecular bone is a highly porous network of interconnected rods and plates called trabeculae. The pores are filled with bone marrow and trabecular bone is primarily found in the ends of long bones such as the femur, and also in the vertebrae.

Bone modelling is the process that involves growth and adaptation of bones to produce a mechanically-functional architecture (Jee, 2001). Bone *re*modelling is a process whereby bone is renewed continuously throughout life in order to continue to fulfil its function in the human body. It is carried out by a group of cells known collectively as a Basic Multi-cellular Unit (BMU), consisting mainly of osteoclasts and osteoblasts. The action of these cells appears to be coupled, with osteoclasts travelling along the surface of bone trabeculae resorbing the tissue and forming a resorption cavity and osteoblasts subsequently filling in the cavity with new tissue. (Parfitt, 1984), see Figure 1.1. The exact nature of the regulatory mechanisms governing this cellular coupling is not fully understood.

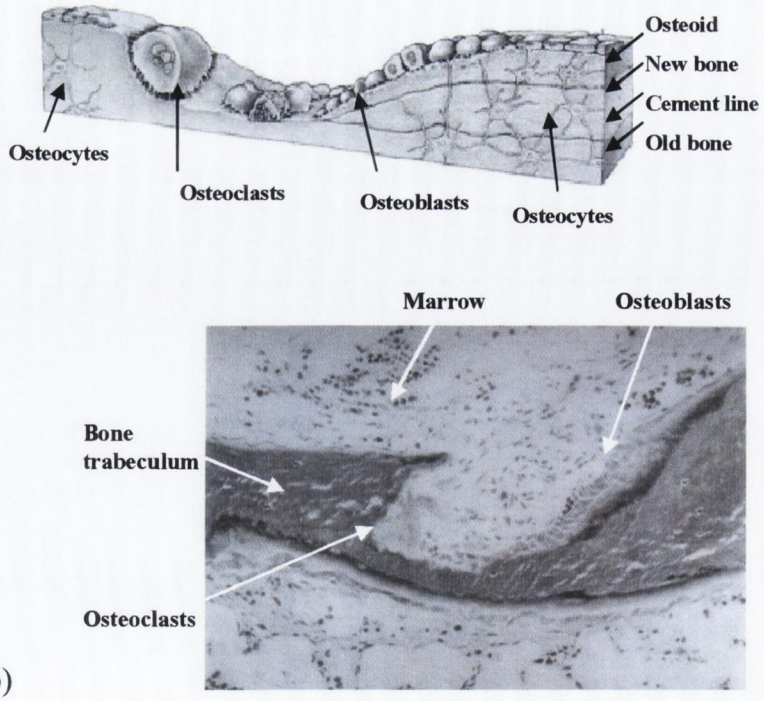

Figure 1.1: *Bone Multi-cellular Unit (BMU) (a) schematic of BMU activity (b) Histological image of BMU activity (from Jee, 2001)*

Osteoporosis is caused by pathological remodelling whereby an imbalance of the cellular coupling leads to excessive osteoclast resorption without adequate new bone formation. This results in the deterioration of the trabecular architecture and leads to fractures of bones (most commonly the hip and the wrist bones in the elderly). This issue has been addressed to a certain extent through the use of conventional anti-resorptive drugs. These drugs prevent this osteoclast/osteoblast imbalance by inhibiting osteoclast activity, which reduces bone resorption and suppresses the normal bone turnover process (Kloosterboer and Ederveen, 2003). Drug treatments have been shown to maintain bone mass and trabecular architecture, and thus serve to restore bone strength to a certain extent. However, even with drug treatment, fractures often occur and the quality of life of a sufferer of osteoporosis cannot be fully restored. A concern with some anti-resorptive drugs is that they inhibit the remodelling process resulting in an increase in the amount of old bone tissue, so that, although bone mass is maintained, bone strength of the tissue may be reduced because fatigue damage will have accumulated within it.

1.3 Biomechanics of bone remodelling and osteoporosis

1.3.1 Mechano-regulation of bone remodelling

The function of the bone remodelling process is not fully agreed. A number of researchers propose that the purpose of the bone remodelling process is to optimise the architecture of trabecular bone so that there is minimum stress in the bone tissue relative to its weight, see Hart (2001) for a review. This process requires that bone cells be regulated by the strain distribution in their immediate vicinity in the bone tissue. This theory has been investigated both experimentally (Lanyon, 1993; Carter *et al*, 1994) and computationally (Burger *et al*, 2002). Theoretical models have proved capable of qualitatively predicting certain aspects of bone adaptation using strain as a stimulus (Huiskes et al, 2000).

An alternative view is that bone remodelling may be targeted to maintain bone strength by resorbing mature bone and replacing it with new bone thereby preventing accumulation of damage (Carter *et al.*, 1987; Frost, 1986; Martin and Burr, 1989; Prendergast and Taylor, 1994; Prendergast and Huiskes, 1996; Martin, 2002). This is based on the observations that microdamage is generated in bone under everyday

physiological loading conditions, for example by Frost (1960), Lee *et al.* (2002) and Vashishth *et al.* (2000). Damage based theoretical models have also proved capable of successfully predicting some aspects of bone remodelling (Prendergast and Taylor, 1994; Prendergast and Huiskes, 1996). If damage repair was the purpose of bone remodelling, then the activity of the cells would need to be regulated by signals due to damage, but the precise nature of such a signal has yet to be identified.

Important progress has been made in understanding how bone cells may sense the effect of mechanical loading, and how mechanical signals may be transduced into cellular signals (el Haj *et al*, 1990; Chambers *et al*, 1999; Burger and Klein-Nulend, 1999). However, many details of the biological process whereby bone tissue responds to loading are still vague. Much of the insight into bone cell biology has been derived from *in vitro* experiments that have shown, for example, that strain derived fluid flow activates osteocytes to produce anabolic factors such as prostaglandin's and nitric oxide. However, difficulties associated with reproducing the *in vivo* cellular environment have limited the ability of such experiments to provide a complete picture of the *in vivo* bone cellular activity.

Many theoretical adaptation models have been developed and the application of such models to finite element representations of bone has produced simulations that are qualitatively reasonable and fit with experimentally reported results (Hart, 2001). These simulations help to further understand bone as a mechanical structure, but do not provide useful information about the physiological process of adaptation. In order for these models to provide more insight and be more useful the modelling assumptions should be more tightly coupled to biological parameters that can be histologically measured and manipulated.

There exists experimental evidence in support of both strain (Carter, 1984) and damage (Burr et al, 1985; Lee et al, 2002) as mechano-regulatory stimuli for bone remodelling and it is plausible that bone remodelling is in fact regulated by signals due to both strain and microdamage (Prendergast and Huiskes, 1996). If bone remodelling is regulated by strain or by microdamage, or a combination of both, then the signal should not only activate a Bone Multicellular Unit (BMU), but also stimulate the BMU to traverse a trabeculum, as is seen *in vivo* and illustrated in Figure 1.1.

Several theories have been developed regarding what initiates the bone remodelling process, but there is little understanding of what causes it to continue

resorption and ultimately terminate on the surface of a trabeculum. If the regulatory mechanisms governing the cellular activity during trabecular remodelling were better understood then, since osteoporosis is associated with dysfunctional remodelling, it might be possible to develop an understanding of the pathology of osteoporosis, and also of the biomechanical treatment required to inhibit osteoporosis and maintain bone mass.

1.3.2 Mechanical testing of osteoporotic and drug-treated bone

Measurement of the consequences of osteoporosis on the mechanical behaviour of bone has been carried out previously using whole bone testing (Kasugai et al, 1998; Yoshitake et al, 1999; Ederveen et al, 2001; Hirano et al, 2000; Bourrin et al, 2002) or testing of volumes of cancellous bone (Mosekilde et al, 1995; Hu et al, 2002; Teramura et al, 2002). Using ovariectomy to induce osteoporosis in the rat, it has been found, for example, that the compressive strength of rat vertebral bodies and the bending strength of rat femora decrease due to osteoporosis. However, significant decreases in trabecular bone volume occurred in these experiments and thus it cannot be determined whether changes were due only to the reduction in bone mass or whether a reduction in strength of the mineralized tissue constituting this matrix also contributed.

A number of studies have been carried out that describe the effects of osteoporosis on the mineral content of the bone tissue; some reveal that the mineral content is unchanged or slightly lower in the osteoporotic bone tissue (Li and Aspden, 1997) and others have found an increase in the mineral content and a lack of collagen (Dickenson et al, 1981; Zioupus et al, 2000; Birkenhager-Frenkel, 1987). Such microstructural changes suggest that a corresponding change in the mechanical behaviour of the tissue could ensue during osteoporosis. However, to date, the tissue level properties of osteoporotic trabecular bone have never been quantified and so such ideas remain conjecture.

The efficacy of drug treatments has been measured. It has been found, for example, that treatment with Tibolone (Kasugai et al, 1998; Yoshitake et al, 1999; Ederveen et al, 2001), estrogen and other anti-resorptive drugs such as, Risedronate, Alendronate, and Incandronate (Hirano et al, 2000; Bourrin et al, 2002; Mosekilde et al, 1995; Hu et al, 2002; Teramura et al, 2002) increases the structural or bulk trabecular bone strength and the whole bone strength by maintaining bone mass and

trabecular architecture. However, in what may seem to be a contradictory finding, it has been found that treatment with high doses of certain anti-resorptive drugs was associated with an increase in spontaneous fractures of the thoracic spinous process, ribs and pelvic fractures (Hirano et al, 2000; Flora et al, 1981; Parfitt et al, 1987). While these studies indicate that the structural mechanical behaviour is maintained using HT drugs, they do not reveal anything about the properties of the mineralised tissue itself.

1.4 Summary

While a vast amount of research has been undertaken to understand the biomechanics of bone during normal physiology and under pathological conditions such as osteoporosis, there still remains a number of unanswered questions. The importance of differences in bone size, cortical thickness, trabecular number, trabecular thickness, trabecular connectivity, tissue mineral content, microdamage burden, osteocyte density, porosity, for determining bone strength is not fully understood.

Although a number of researchers have tested the strength and stiffness of individual trabeculae from healthy bone, their results are rather inconclusive, as will be reviewed in Chapter 2. Also, the effects of ageing, osteoporosis and drug treatment on the strength of individual trabeculae remain an open question.

The bone remodelling process has been studied experimentally and theoretical models of its adaptation mechanisms have been derived. However, it is still unclear what the exact molecular signalling cascade is between bone mechanics and the adaptive responses that drive bone cells to maintain a homeostatic bone mass throughout life. The function of bone remodeling is not fully agreed and most importantly no clear understanding of the cellular imbalance during osteoporosis has been achieved.

The challenge is to measure the specific material and structural determinants of bone strength (Seeman, 2003) and to develop a comprehensive knowledge of the molecular biology and physiology of bone remodelling. Whether a combination of this information will lead to a better understanding of osteoporosis and assist more accurate identification fracture risk or improve approaches to drug therapy is unknown.

1.5 Objectives of this thesis

It can be summarised from section 1.3 above that the effects of ageing, osteoporosis, and drug treatment on cancellous bone trabeculae remain to be discovered. In this thesis the author will propose that there is a pathological change in bone tissue material properties during osteoporosis, and that this alters the mechanical stimuli to bone remodelling cells causing them to adapt the trabecular architecture resulting in a loss of bone mass and consequent reduction in bone strength. If this were true then the mechanism by which conventional drug treatments for osteoporosis suppress bone turnover may not be the best intervention required to prevent loss of bone mass during osteoporosis. To argue the case for this thesis, three separate but inter-related hypotheses with respect to the regulatory mechanisms governing bone remodelling are tested. The aim is to discover the possible causes for the degenerative process occurring during osteoporosis and the extent to which drug treatments address these issues. The hypotheses are as follows:

1. Damage occurs local to resorption cavities in bone trabeculae due to the stress elevations caused by the reduced trabecular thickness. This damage acts in combination with local strains as stimuli to initiate and drive bone multi-cellular units (BMUs).
2. There is a pathological change in the material properties of bone tissue during osteoporosis (stiffness and strength) and this leads to a change in the mechanical stimuli on bone remodelling cells.
3. Suppressing bone turnover in drug treated bone results in weaker bone tissue than that of both normal *and* osteoporotic bone by allowing damage to accumulate within the bone tissue.

These hypotheses are tested through a combination of (a) finite element analyses, (b) mechanical testing and (c) computational simulations.

If this set of hypotheses can be confirmed then it would be clear that, aside from the consequences of osteoporosis on the architecture of bone tissue, there are also more subtle processes ongoing that affect bone strength at the level of material composition. It may then be possible to develop an understanding of the optimal interventions that are necessary for an effective drug treatment to maintain bone strength during osteoporosis, such as inhibiting/promoting bone cell activity or perhaps attempting to change the composition of the tissue.

2. Literature Review

2.1 Introduction

Biomechanical problems associated with osteoporosis and loosening of prosthetic implants are manifested in both cortical and trabecular bone. Due to the fact that the strength behaviour of trabecular bone is integral to musculoskeletal applications, such as bone fracture, extensive research has been dedicated to understanding its mechanical behaviour (Keaveny, 2001). In this chapter, the research to date is presented. This includes analyses of the trabecular architecture, mechanical testing at the macro and micro-structural levels, and development of computational analyses of trabecular bone mechanical behaviour.

As mentioned in Chapter 1, it has been found that osteoporosis is manifested initially at the cellular level through a breakdown in the coordinated activity of bone remodelling cells and therefore, in this chapter, normal bone physiology and the pathophysiology of osteoporosis are first described. A review of the methods that have been applied to develop an understanding of the mechanical behaviour of trabecular bone during osteoporosis is presented. The means by which conventional drug treatments attempt to combat loss of bone strength during osteoporosis, and the studies that have assessed the efficacy of these drug treatments for improving bone strength, are reviewed. Finally the experimental and computational research that has been performed to investigate the mechanisms that drive the normal bone remodelling process is presented.

2.2 Bone structure and biomechanics

2.2.1 Bone structure and organization

Bone is a specialized heterogeneous anisotropic material, whose fundamental function in the body is to bear load (Wolff, 1892). Bone architecture is hierarchical and complex, consisting of component phases at different levels of structural organization (Rho *et al*, 1998). At the macrostructural level in the skeleton, bone is organized into two main types; namely cortical bone and trabecular bone, also known as cancellous or spongy bone. Cortical bone is characterized by low porosity, approximately 5-10% and is most commonly found in the shafts of long bones (Fig. 2.1(a)), and also forms a shell around the ends of bones. Trabecular bone conversely is characterized by high

porosity, typically 75-95%, and is found at the ends of long bones, in vertebral bones and in flat bones, as can be seen from Fig. 2.1- (a) and (b). The structure of trabecular bone is a matrix of bone struts, known as trabeculae, which are believed to be oriented along the stress trajectories in the femur (Wolff, 1892). The adult human skeleton is comprised of approximately 80% cortical bone and 20% trabecular bone.

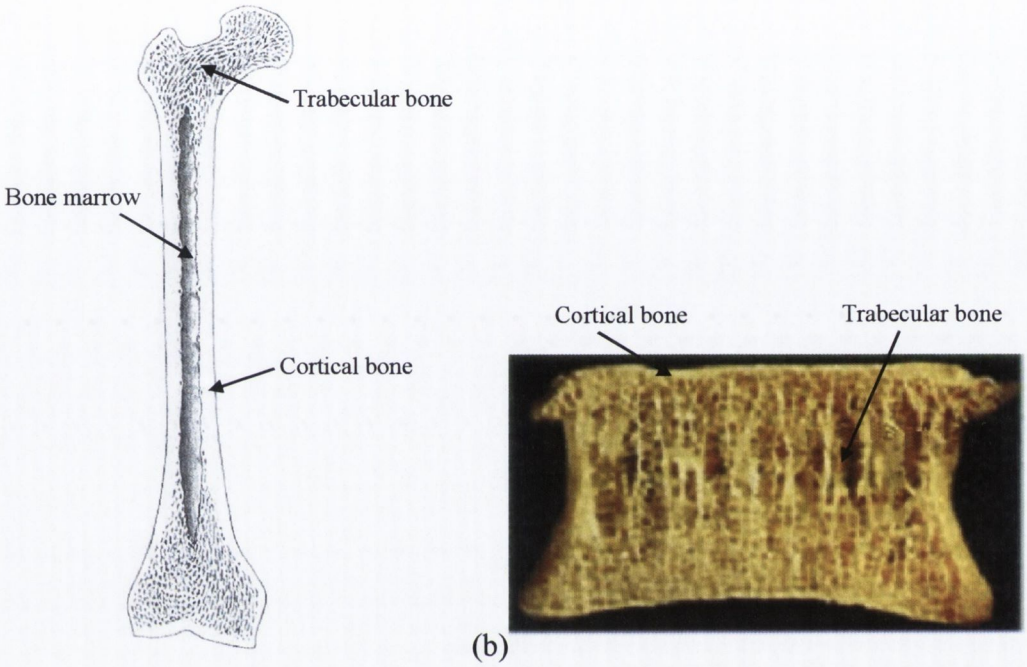

Figure 2.1: *Trabecular bone in (a) a long bone and (b) a vertebral body*

The microstructure of bone is organized differently depending on the anatomical location and the type of bone involved; however, the basis of the differences between bone types involves the organization of layers, or lamellae, of bone tissue. In cortical bone, the bone tissue is organized either into circumferential layers of bone or into osteons (Haversian systems), which surround the vascular supply to the blood, see Fig. 2.2, Fig 2.3(a). In trabecular bone, the lamellae are organized into single trabeculae, which are the structural units of trabecular bone, and are not vascularized, see Fig. 2.3 (b). The intervening space between these trabeculae is filled with bone marrow. Human trabeculae are typically 150-300μm in diameter and can be up to 2000μm in length; their shape is determined by their anatomical location and loading situation.

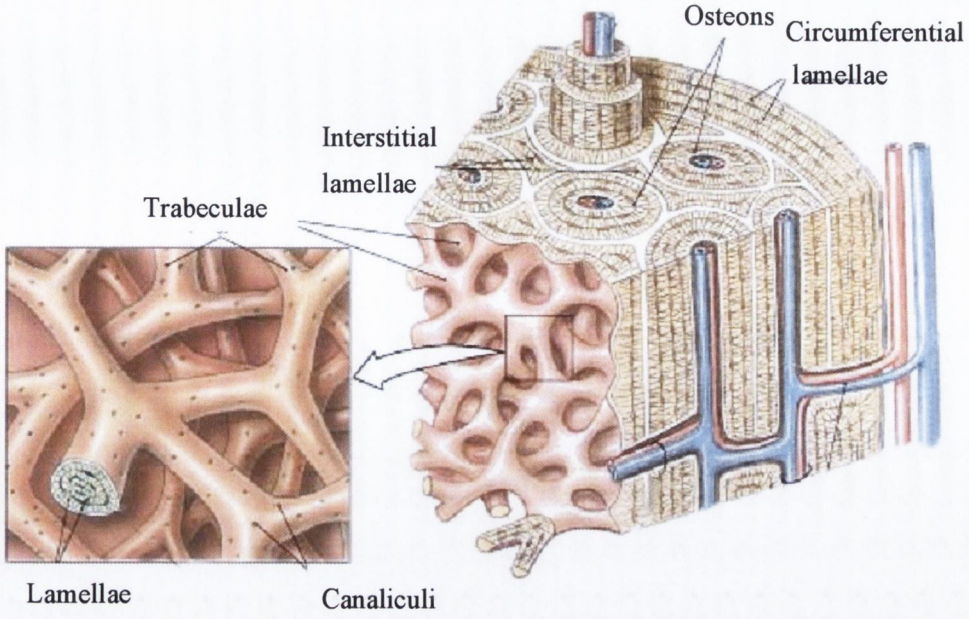

Figure 2.2: *Schematic of bone tissue organisation in cortical and trabecular bone (Martini, 1998)*

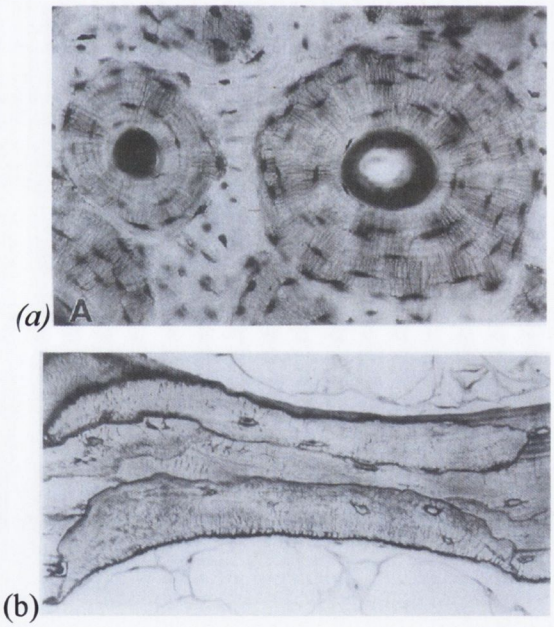

Figure 2.3: *Histological image of bone tissue organisation showing (a) concentric arrangement of cortical bone tissue and (b) lamellar organisation of trabecular bone tissue (Jee, 2002)*

At the nano-structural level, bone tissue is in essence a composite material comprised of an organic matrix, consisting of proteoglycans and type I collagen fibrils, and a mineral phase, consisting of bone crystals composed of calcium phosphate hydroxyapatite, see Figure 2.4.

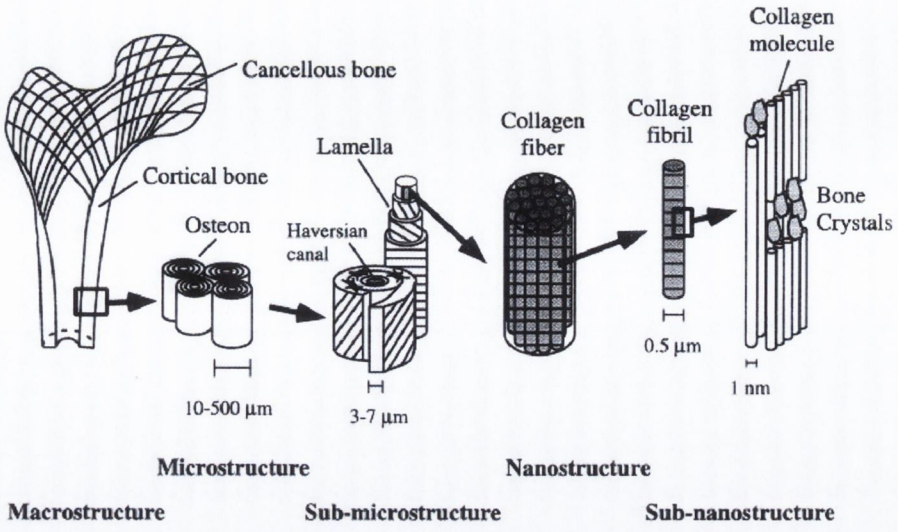

Figure 2.4: *Organisation of collagen and mineral (bone crystal) phases in bone tissue (Rho et al, 1998)*

The composite nature of bone tissue is largely responsible for its mechanical behaviour. The mineral phase is an important determinant of bone elasticity, whereas the organic phase is responsible for the bone post-yield behaviour (Reilly and Burstein, 1975). The noncollagenous proteins and proteoglycans have many functions, including organization of the collagenous matrix, mediating cell attachment, regulating the rate of growth and regulating the stability of the mineral phase crystals (Luchinetti, 2001). The proteoglycans have a high negative fixed charge density and readily bind to Ca^{2+} ions. They are believed to be responsible for regulating the mechanical properties of the interface between the collagen and mineral by modulating the formation of bonds between collagen and mineral (Luchinetti, 2001).

Trabecular bone tissue is a porous material, and the degree of porosity varies with anatomical location. Besides the porosity associated with the marrow-filled cavities in the trabecular structure, there are three other important fluid-filled compartments of bone that enable the transport of nutrients and mineral ions to the bone tissue. These three porosities are the vascular porosity, the lacunar-canalicular porosity and the collagen-apatite porosity (Cowin, 1999). These different levels of porosity serve to exchange bone fluid with vascular fluid, to provide mechanical stimuli for bone cells, and to transport nutrients and waste products to and from the vascular system to the bone cells.

2.2.2 Biomechanical properties of trabecular bone

Trabecular bone is a highly specialized tissue, and its biomechanical behaviour is accordingly intricate. As detailed in section 2.2.1, it has a complex hierarchical structure, and analyses of the behaviour at each level are essential for a holistic understanding of its biomechanical behaviour. As noted by Rho *et al* (1998)

> "Every technique of assessing bone architecture or the properties of a given structure has its own resolution, and therefore a combination of techniques is required to reveal the material structures and properties at the many different length scales"

Given its structural and material complexity, a variety of studies have been carried out to assess the biomechanical behaviour of trabecular bone. These studies have concentrated on determining the architecture of trabecular bone, its structural mechanical behaviour and its material mechanical behaviour.

2.2.2.1 Architecture of trabecular bone

The architecture of trabecular bone is believed to be essential for its ability to withstand the complex loading to which it is subjected to during normal activities. It has long been hypothesised that trabeculae are directed along the force trajectories created by weight-bearing forces (Wolff, 1892). Extensive research has been carried out to characterize the exact morphology of trabecular architecture (Nicholson *et al*, 1997; Odgaard, 1997; Kothari *et al*, 1999). These researchers have sought to characterise the structure of trabecular bone by defining certain parameters for the matrix, such as bone volume, trabecular thickness, trabecular separation, number of trabeculae/mm^2 and trabecular length in various animals including humans, cattle and rats. Techniques used include serial sectioning and micro-CT scanning which have allowed the morphology of trabecular bone to be analysed at resolutions ranging from 14 -250 μm. It has been reported that more than 80% of the variance of trabecular bone strength and modulus can be explained by measures of density and trabecular orientation (Goldstein *et al*, 1993).

2.2.2.2 Structural mechanical behaviour of trabecular bone

The majority of research performed to determine the mechanical behaviour of trabecular bone has been concerned with determining the material properties of the

trabecular matrix. A variety of mechanical testing has been undertaken to characterize the structural behaviour, also known as the apparent behaviour of trabecular bone. In order to assess this behaviour, test specimens must be chosen, which represent the continuum mechanical properties of the bone tissue. In trabecular bone limitations of the continuum assumption appear in two areas: near biologic interfaces, and in areas of large stress gradients. The work of Harrigan and Mann (1988) demonstrated that the continuum assumption is suspect within three to five trabeculae of an interface. Therefore the standard samples for testing are cylinders, typically 5 mm in diameter, or cubes (5 mm^3) of trabecular bone from the proximal and distal femur, the vertebral body or the proximal tibia (Keaveny *et al*, 1993; Keaveny *et al*, 1997; Nicohlson *et al*, 1997; Koperdahl and Keaveny, 1998).

It has been reported that the apparent elastic modulus of trabecular bone is anisotropic with values ranging from 165 MPa in the supero-inferior direction to 43 MPa in the lateral direction (Nicholson *et al*, 1997). Keaveny *et al* (1994) reported that the mean yield strength of trabecular bone in tension is 15.6 MPa and that this is 30% lower than the yield strength under compressive loading. The apparent yield strain of trabecular bone is approximately 0.8% (Koperdahl and Keaveny, 1998).

The fatigue failure criterion of the trabecular bone matrix has also been investigated (Michel *et al*, 1993). Fatigue testing is typically carried out at 2 Hz, which is within normal physiological frequencies that range from 0.5 and 3 Hz. Michel *et al* (1993) reported that the number of cycles to failure ranged from 20 cycles at 2.1% strain to 400,000 at 0.8% strain.

Due to the structure of trabecular bone, the material properties obtained using these test methods are highly dependant on the architecture of the matrix and do not represent the properties of the mineralised tissue itself.

2.2.2.3 Material behaviour of trabecular bone tissue

The mechanical behaviour of trabecular bone has been assessed at the level of the bone tissue by a number of researchers using different approaches. The majority of these studies have concentrated on determining the elastic modulus of bone tissue through experimental testing, however an approach involving the use finite element analysis has also been employed.

2.2.2.3.1 Experimental testing of trabecular bone tissue

A variety of micro-mechanical experiments have been performed to measure the mechanical properties of single bone trabeculae; test methods applied have included 3/4-point bending studies (Choi *et al.*, 1990), buckling studies (Runkle and Pugh, 1975; Townsend and Rose, 1975), cantilever beam tests (Mente and Lewis, 1989) and micro-tensile testing (Ryan and Williams, 1989, Rho *et al.*, 1993, Samelin *et al.*, 1996). The aim of the majority of these tests was to assess whether trabecular bone tissue and cortical bone tissue have the same stiffness. Reported values for the elastic modulus of an individual trabecula from these studies have conflicted, with values ranging from 0.75GPa to 20GPa. In this review the methods of micro-specimen preparation and gripping techniques that have previously applied to test single bone trabeculae are presented. The possible sources of error of these test methods are outlined, which might explain the wide range of values previously reported.

Two separate research groups first carried out mechanical testing of individual trabeculae excised from trabecular bone specimens in 1975 (Runkle and Pugh, 1975; Townsend and Rose, 1975). Prior to that date, the mechanical properties of trabecular bone were assumed to be the same as cortical bone at a microstructural level, and that it was their architecture only that distinguished between them.

Runkle and Pugh (1975) constructed a micro-mechanical tester to obtain the elastic modulus of an individual trabecula by means of uniaxial compressive buckling. Plate-like trabeculae were excised from human subchondral bone located under stereomicroscopy. The test specimens were dehydrated in alcohol and tested dry. The ends of the trabeculae were trimmed square and cemented to ceramic rods, and this assembly was then placed in a glass sleeve. Load was applied via a pan balance, through loading one pan with water and thus allowing the other pan to act as a moving platen, to transfer the load to the specimen. The unloaded end of the trabecula was cemented to a fixed wall. The load was of the order of 0.45N and displacement was measured. The buckling point was observed from the load-deflection curve obtained from the test results. The dimensions of trabeculae were measured after testing, by embedding in MMA and observing under light microscopy. The mean elastic modulus, determined using buckling theory, was found to be 8.3 GPa.

Townsend and Rose (1975) also determined the elastic modulus of an individual trabecula through a buckling study. The specimens were excised from human tibiae under stereomicroscopy and dehydrated in alcohol for dry testing. A

number of specimens were also tested wet. The ends of the trabeculae were mounted on ceramic rods using epoxy and surrounded by a glass tube. This assembly was placed in a testing machine and tested in compression. They observed that dry trabeculae were brittle under a buckling load, whereas wet trabeculae were very ductile. The estimated value for the elastic modulus of dry trabecular bone tissue was reported as 14 GPa and that of wet trabeculae as 11 GPa.

Kuhn *et al* (1987, 1989) undertook studies to produce and mechanically test microspecimens of trabecular tissue and cortical tissue. Thin serial sections of trabecular bone were cut using a diamond blade saw. These were cleared of marrow and segments deemed of adequate length were dissected from the specimens. A miniature-milling machine was used to mill the trabecula to a thickness of 50-200 μm. Three-point bending tests were carried out and the bending modulus was calculated. The mean trabecular modulus was calculated as 3.17 GPa. They concluded that the difference between cortical and trabecular stiffness was insignificant at a microstructural level.

Ryan and Williams (1989) performed tensile testing of individual trabeculae, in order to determine their elastic modulus. The test specimens were rod-like trabeculae from bovine femora. The bone sections were cleaned of marrow using a water jet and uniform trabecular rods were removed with a scalpel blade and forceps. The trabeculae were on average 5mm long with diameters of approximately 500μm. Gripping of test specimens was achieved with clamp plates faced with 320-grit emery paper and tightened with thumbscrews, see Figure 2.5. The value for elastic modulus of rod-like trabeculae that was estimated by this method was 0.75 GPa.

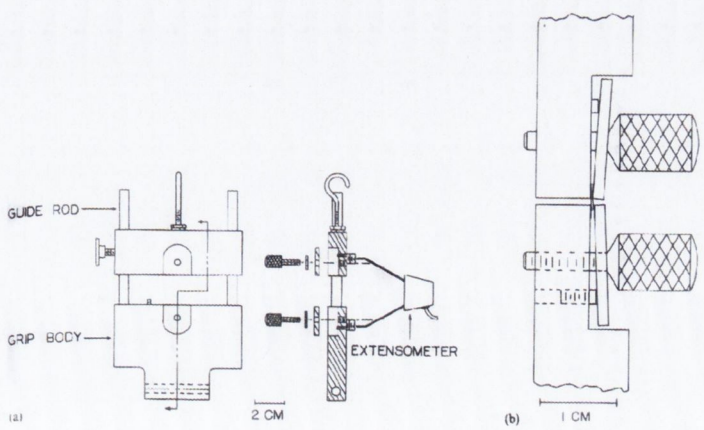

Figure 2.5: *Grip assembly for testing trabeculae (Ryan and Williams, 1989)*

Mente and Lewis (1989) carried out cantilever beam testing of single bone trabeculae to measure the elastic modulus of trabecular bone tissue. After testing, specimens were ground down sequentially and photographs of the trabecular cross-sections were obtained to develop geometry for finite element modelling. The tissue was modelled as a linear elastic isotropic material. The material properties used for this model were 15 GPa for the elastic modulus and 0.28 for Poisson's ratio. The glue was modelled as linear elastic with an elastic modulus of 3.1GPa and a Poisson's ratio of 0.36. The displacement observed in the finite element model was compared to that observed during experimental testing and the elastic modulus was adjusted until correspondence between FE and experimental results were obtained. The calculated elastic modulus for trabecular bone tissue was 6.2 ±1.8 GPa.

Rho *et al* (1993) compared the elastic modulus of individual trabeculae and microspecimens of cortical bone by microtensile testing and using an ultrasonic technique. Individual trabeculae were obtained from a human tibia with average diameters of 0.18 mm and lengths of 2.3 mm. Microspecimens of cortical bone were obtained from the same tibia and 0.3x0.3x2.2 mm specimens were produced using a diamond blade saw. The trabeculae were tested in tension by gluing the specimen ends using cyanoacrylate into brass grip rods under a stereomicroscope. The effect of gluing the specimens to the tensile grips was investigated by an ultrasonic technique, whereby the moduli obtained for unglued and glued were compared and no significant difference was observed ($p=0.15$). They concluded that cortical and trabecular bone are not mechanically the same material with the elastic modulus of individual trabeculae (10.4 ± 3.5 GPa) being significantly lower ($p<0.0001$) that that of the microspecimen of cortical bone (18.6 ± 3.5 GPa).

Trabeculae have also been tested in tension by Samelin *et al* (1996), in a study that investigated the effects of tensile and compressive forces on trabeculae. A 5mm slice of trabecular bone was cut from the proximal human femur with a Bandsaw. Trabecular struts were excised under microscopy using an electrically propelled dental miller, a thin scalpel and a watchmaker's pin. The ends of the trabeculae were embedded in cylinders of methylmethacrylate and assembled in the custom-made test system, see Figure 2.6.

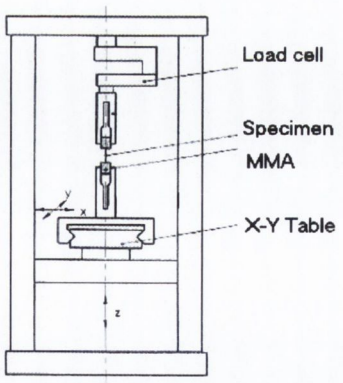

Figure 2.6: *Test apparatus for testing trabeculae (Samelin et al, 1996)*

Choi *et al* (1990) used an Isomet low speed Diamond Blade Saw to cut bone specimens from trabecular bone obtained from the medial side of the proximal tibia. Bone marrow was removed using a needle and continuous segments were cut from the sections using a scalpel blade. A specially designed miniature milling-machine was then used to produce (100 – 170) x (100 – 170) x (1500) μm^3 beam specimens. The elastic modulus was measured through a three-point bending test and the mean value reported was 4.59 GPa. Choi and Goldstein (1989,1992) have also investigated the fatigue properties of individual trabeculae; this was performed through three and four-point bending tests of individual trabeculae excised from the human proximal tibia. They estimated that the fatigue strength of trabecular bone tissue is 100 - 140 MPa and that at these stress levels the number of cycles to failure is approximately 100,000 cycles.

Nano-indentation (1-5 μm resolution) is a technique that can be used to calculate the elastic modulus of a material under the assumption that the material is elastically isotropic. The technique involves determining the hardness of an indented material by observation of an indented area. The load and indenter displacement are recorded in situ to obtain an indentation hysteresis curve and the elastic properties can be derived from the curve. Rho et al (1997) used this technique and calculated that the elastic modulus of trabecular bone tissue in the transverse direction is approximately 13.5GPa.

Acoustic microscopy (30-60 μm resolution) can also be used to evaluate the elastic properties of human bone at a microstructural level. This method involves producing an acoustic wave in a tiny area just in the vicinity of surface (near-field area) through different interaction mechanisms. The acoustic properties of materials

can be determined at a high resolution from the acoustic wave detected. Turner *et al* (1999) used both nano-indentation and acoustic microscopy to compare the Young's moduli of trabecular and cortical bone tissues from a common human donor. They reported that the Young's modulus of cortical bone in the longitudinal direction was about 40% greater than ($p<0.01$) the Young's modulus in the transverse direction. The Young's modulus of trabecular bone tissue was slightly higher than the transverse Young's modulus of cortical bone, but substantially lower than the longitudinal Young's modulus of cortical bone. These findings were consistent for both measurement methods and suggest that elasticity of trabecular tissue is within the range of that of cortical bone tissue.

2.2.2.3.2 Finite element calculations of bone tissue elastic modulus

Van Rietbergen *et al* (1995) used a finite-element strategy to estimate the Young's modulus of trabecular bone tissue. They constructed a large-scale FE model of a 5 mm cube of trabecular bone using three-dimensional serial reconstruction techniques. The results of their model were compared to experimental data taken from literature and an estimate of elastic modulus of the bone tissue was obtained by adapting the FE tissue modulus so that the FE model results corresponded to the experimental results. Using this technique, the upper and lower boundaries for the tissue modulus of trabecular bone were reported to be 10.1 and 2.23 GPa, respectively.

Table 2.1 summarises the aspects of each of the methods outlined above for ease of comparison and compares the elastic moduli obtained where available.

Study	Property	Mechanical Test	Specimen Origin	Elastic Modulus (GPa) Mean (SD)
Townsend and Rose (1975)	Elastic Modulus	Buckling	Human medial tibia	14.1 (dry); 11.3 (wet)
Runkle and Pugh (1975)	Elastic Modulus	Buckling	Human subchondral bone	8.7 (3.2)
Mente and Lewis (1989)	Elastic Modulus	Cantilever beam	Dried human femur	6.2 (1.2)
			Fresh human tibia	11.2 (10.1)
Ryan and Williams (1986)	Elastic Modulus	Tensile	Bovine distal femurs	-
Ryan and Williams (1989)	Elastic Modulus	Compression	Bovine femora	0.8 (0.4)
Kuhn *et al* (1989)	Elastic Modulus	Three-point bending	Human iliac crest	3.8
Choi and Goldstein (1989)	Fatigue strength	Three-point bending	Proximal tibia	-
Choi *et al* (1990)	Elastic Modulus	Three-point bending	Proximal tibia.	4.6 (1.3)
Rho *et al* (1993)	Elastic Modulus	Ultrasonic / Microtensile	Proximal human tibia	10.4 (3.5)
Choi and Goldstein (1992)	S-N curve	Four-point bending	Proximal tibia	-
Van Rietbergen *et al* (1995)	Elastic Modulus	High-resolution FE modelling	Proximal human tibia	5.91
Rho *et al* (1997)	Elastic Modulus	Nanoindentation	Human vertebrae	13.5 (2.0)
Turner *et al* (1999)	Elastic Modulus	Nanoindentation	Human distal femur	18.14 (1.7)
		Acoustic Microscopy		17.5 (1.12)

Table 2.1: *Previous studies to determine the mechanical properties of bone tissue*

2.2.2.4 Possible sources of error in previous reports of bone tissue mechanical behaviour

As is evident from this review, conflicting results have been obtained from previous test methods, perhaps due to the difficulty of developing a reliable, consistent experimental test method or due to inaccurate assumptions employed during finite element analyses.

The small size of test specimens and irregularity of their geometry has meant the repeatability of mechanical test methods was a challenge. A review by Lucchinetti *et al* (2000) of the different methods of micro-mechanical testing of individual trabeculae postulated on the possible sources of error associated with the different test methods that may explain the range in reported elastic moduli. They noted that, due to the extremely small and irregular shape of test specimens, reconstruction of sample geometry for calculation of the elastic modulus might be a source of error. They noted that resulting uncertainties in reported results has a worse impact on bending tests than on tensile test results. Their review also noted that the presence of glue in tensile tests might be a source of error, due to the fact that the displacement recorded during testing may be a combination of the glue displacement and the sample displacement. This may result in inaccuracies in calculating the strain experienced by the specimen during testing. Another error postulated by this review was that of alignment inaccuracies during tensile testing.

The method of preparation of specimens for nano-indentation involves embedding them in epoxy, a process that dehydrates the bone tissue considerably. Additionally, nano-indentation calculates the elastic modulus of a material under the assumption that the material is elastically isotropic. Turner *et al* (1999) concluded that that this assumption does not limit nanoindentation as a technique for measurement of Young's modulus, due to the fact that results obtained by nano-indentation were similar to those obtained by acoustic microscopy. However, both techniques involved dehydrating the bone tissue in ethanol and embedding in polymethylmethacrylate. Therefore, given the drying effects associated with embedding techniques, concerns exist regarding the accuracy of this technique for estimating the elastic modulus of bone tissue.

Finite element analysis is limited by the assumptions that are required to make models computationally efficient and as such may introduce a number of potential

errors in estimating bone tissue elastic properties. Firstly, the most common assumption made in finite element modelling of bone is that the material is isotropic. Bone tissue is a viscoelastic and anisotropic material (Gottesman and Hashin. 1980) and as such this assumption may have an effect on the calculations of tissue elastic properties. Secondly, the elastic modulus is estimated by comparing FE results to experimental results obtained from literature. The geometry of the trabecular architecture from the experimentally tested specimen was unknown. Also, the exact loading conditions of the bone tissue are approximated, as the exact loading conditions experienced during testing is not readily reproducible. Therefore, the accuracy of this technique for estimating the elastic modulus of trabecular bone tissue is contentious.

Given the variety of potential errors and limitations of previous methods applied to determine bone tissue elastic properties it is clear that, in order to fully understand the mechanical behaviour of bone tissue, a reliable, consistent method is needed. It is required to develop a method to test single bone trabeculae that minimizes errors due to,

1. Damage during extraction and preparation,
2. Stress concentrations during gripping,
3. Inaccuracies in displacement data,
4. Alignment of test specimens.

2.2.2.5 Stress analyses of trabecular bone

The complexity of bone structure and organisation has made it difficult to develop a detailed understanding of the biomechanical function of trabecular bone. One method of addressing this issue has been to use finite element analyses of trabecular bone volumes (Guo *et al*, 1994; Muller and Ruegsegger, 1995; Van Rietbergen *et al*, 1995; Pidaparti, 1997; Ulrich *et al*, 1998; Van der Linden *et al*, 2001b; Homminga *et al*, 2003). In order to perform these analyses, solid models of trabecular architecture have been developed either by treating the matrix of trabecular bone as a repeating unit or by obtaining the geometry of cubes of trabecular bone through micro-CT scanning. The approach to developing finite element models from the obtained solid models has been to use either hexagonal or tetrahedral elements, see Figure 2.7.

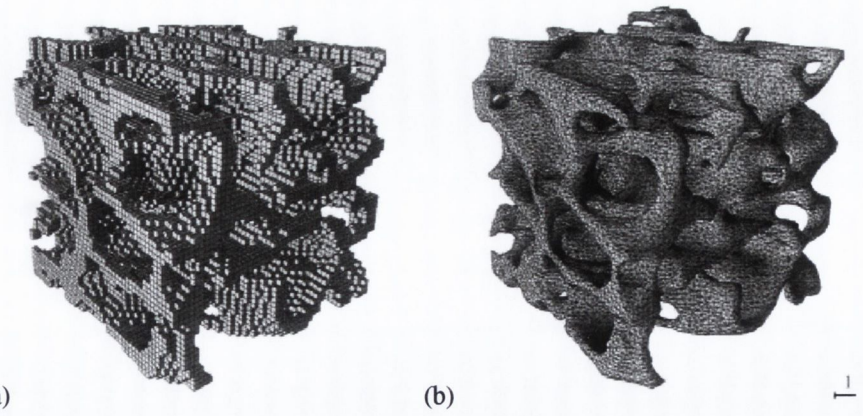

Figure 2.7: *Finite element models of trabecular bone architecture using (a) hexagonal and (b) tetrahedral elements (Ulrich et a, 1998)*

Stress analyses have been performed using these solid models in which it is assumed that the mechanical properties of trabecular bone are the same as cortical bone at the microscopic level, or using values reported from testing of cancellous bone tissue. These models have been used to estimate the elastic properties of bone tissue (Van Rietbergen *et al*, 1995, Ulrich *et al* 1998; Homminga *et al*, 2003) and to analyse the fatigue behaviour of trabecular bone (Guo *et al*, 1994; Pidaparti, 1997). Other applications include analyses of the effects of loss of bone mass on the structural behaviour of the matrix (Muller and Ruegseggger, 1996, Van der Linden *et al*, 2001b). A model by Van Rietbergen *et al* (1999) was used to analyse the distributions of stresses and strains in the trabecular matrix under physiological loading conditions and found that the distributions were non-uniform.

While this area has been extensively researched, the resolutions at which these models have been developed, which range from 14 μm - 250 μm, are inadequate for carrying out detailed computational analyses of the biomechanics of trabecular bone at the level of the bone tissue, i.e. single bone trabeculae.

A number of different aspects of the material behaviour of trabecular bone, such as composite material behaviour and viscoelasticity, have been included in previous computational analyses (Gottesman and Hashin, 1980; Currey *et al*, 1994b; Pidaparti *et al*, 1996). Of particular interest to the work presented in this thesis are those that have modelled the porous nature of bone tissue. The use of the poroelastic theory to model the porous behaviour of bone has been accepted by various researchers (Weinbaum *et al*, 1994; Manfredini *et al*, 1999; Steck *et al*, 2000; Smit *et al*, 2002; Papathanasopoulou *et al*, 2002). A review of the development of the

poroelasticity theory by Cowin (1999) addressed the question of the most appropriate model for the study of bone fluid movement and bone fluid pressure. It was proposed that the porosity of particular interest with respect to bone remodelling (as will be described in section 2.3) is the lacunar-canalicular porosity and, as such, it is important to model this behaviour in order to accurately simulate bone adaptation. The derivation of the poroelasticity theory is outlined in Appendix A.

2.3 Bone Physiology and remodelling

Bone is a living tissue that has the capacity to continuously adapt and renew its structure throughout life. The process by which bone renewal is accomplished is known as bone remodelling. It is performed by a group of cells known collectively as the Basic Multicellular Unit (BMU). A BMU consists of osteoclasts and osteoblasts working in a coupled action of bone resorption and deposition (Frost, 1986). In trabecular bone osteoclasts travel along the surface of trabeculae, resorbing the tissue and forming a resorption cavity, called a Howship's lacuna, and osteoblasts follow along behind filling in the cavity with osteoid, which subsequently mineralizes (Parfitt, 1984).

Osteoclasts are derived from cells in the mononuclear/phagocytic lineage of the hematopoietic marrow (Jee, 2002). The remodelling process begins when preosteoclasts are recruited from the bone marrow and are differentiated under the influence of cytokine and growth factors to mature into active osteoclasts. The precursor cells are hematopoietic stem cells known as monocytes. Osteoclast differentiation and function is controlled primarily by three factors: Macrophage Colony-Stimulating Factor (M-CSF), Receptor for Activation of Nuclear Factor Kappa B Ligand (RANK-L) and Osteoprotegerin (OPG). M-CSF is produced by osteoblasts and is required for survival and differentiation of osteoclast precursors. RANK is a receptor that is present on the surface of osteoclast precursor cells. RANKL is expressed on the surface of osteoblasts and lining cells and binds to RANK. This leads to the differentiation and maturation of the osteoclast precursor into mature multinucleated osteoclasts, which develop a ruffled border. The mature osteoclasts secrete bone-reabsorbing enzymes, which digest bone matrix. OPG is made by osteoblasts and blocks both osteoblasts formation and bone resorption.

Osteoblasts are responsible for bone matrix synthesis and are derived from mesenchymal progenitors near bone surfaces (Jee, 2002), see Figure 2.8. They secrete a collagen rich ground substance essential for later mineralization of hydroxyapatite and other crystals. The collagen strands to form spiral fibers of bone matrix known as osteoids. Osteoblasts cause calcium salts and phosphorus to precipitate from the blood, these minerals bond with the newly formed osteoid to mineralize the bone tissue. Alkaline phosphatase is contained in osteoblasts and secreted during osteoblastic activity.

The mode of differentiation, recruitment and inhibition of osteoclasts and osteoblasts is controlled by numerous hormonal and growth factors (Jee, 2001). Both osteoclasts and osteoblasts have estrogen receptors. Estrogens can inhibit osteoclast recruitment and conversely increase the number of osteoblasts, which subsequently increases collagen production. Parathyroid Hormone (PTH) can increase the recruitment and the activity of osteoclasts stimulating bone resorption and resulting in an increase in blood calcium levels. PTH also increases the activity of osteoblasts and therefore, if the PTH secretion is too high, there is an acceleration of the bone turnover. If the increase occurs along a Vitamin D deficiency, the bone cycle is accelerated and entails bone loss. Vitamin D tends to increase the recruitment of osteoclasts, and also plays a part in the mineralization of bone matrix. A lack of Vitamin D results in osteomalacia (impaired mineralization) and too much Vitamin D results in bone loss. Many other important factors are involved in bone remodelling such as calcitonin, glucocorticoïds, progesterone and androgens.

Osteoblasts that have been trapped in the osteoids produced by other surroundings osteoblasts are called osteocytes. Osteocytes maintain bones, they play a role in controlling the extracellular concentration of calcium and phosphate, and are directly stimulated by calcitonin and inhibited by PTH (Parathyroid hormone). While osteocytes are believed to play a role in the maintenance of bone mass, their exact role is actually still to be defined.

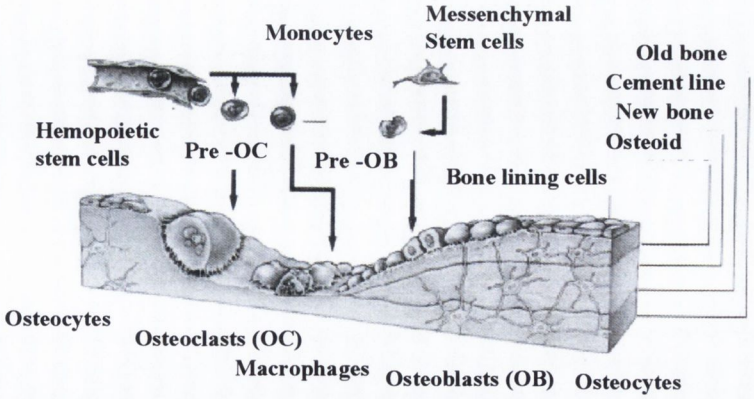

Figure 2.8: *The bone remodelling sequence (Bartl, R., 1998)*

Each of these cell types is recruited at different stages during the bone remodelling process as shown in Fig. 2.9.

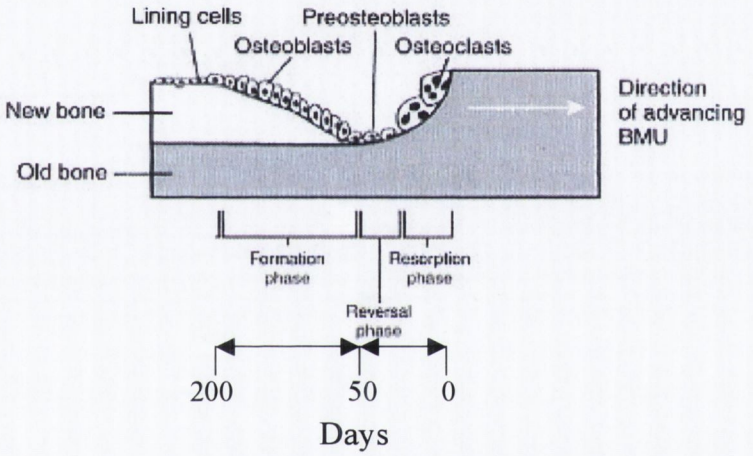

Figure 2.9: *The bone remodelling sequence*

During a remodelling cycle osteoclasts resorb bone, removing unwanted bone and microdamage, at a longitudinal rate of 40μm per day (Jaworksi *et al*, 1975; Eriksen and Kassem, 1992; Martin *et al*, 1998). A typical resorption cavity depth is 40 - 60μm (Jaworksi *et al*, 1975; Cohen-Solal *et al*, 1991; Eriksen and Kassem, 1992) and the resorptive sequence lasts for 40-50 days (Eriksen and Kassem, 1992). After resorption, the osteoclasts disappear, and osteoblasts are recruited to form layers of osteoid and these slowly refill the cavity. The osteoblasts replace bone and the formative period is 100-150 days (Eriksen and Kassem, 1992). In normal remodelling, there is a small bone mass loss with age as osteoblasts deposit less bone tissue than the osteoclasts have resorbed. The change in trabecular thickness due to this is −1μm (Eriksen and Kassem, 1992). At any one spot on the surface the resorption lasts

approximately two weeks (Eriksen and Kassem, 1992). The osteoblasts age and turn into lining cells on the surface and eventually, when successive layers of new bone are laid down on these surfaces, they become osteocytes distributed throughout the bone matrix. It has been reported that 10-15% of the bone surface of trabecular bone is occupied by remodelling activity (Kanis, 1998).

A number of parameters have been defined to quantify the amount of remodelling that occurs in healthy bone. The remodelling activity is defined by the activation frequency, which is the number of activated BMU's per unit volume of bone per unit time. The activation frequency of trabecular bone is different for remodelling of normal and osteoporotic bone. The resorption depth defines the amount of bone removed during resorption, which is the depth of the cavity formed during resorption. Resorption depth is time dependant, and different cells appear at different resorption depths, as can be seen from Fig. 2.9.

2.4 Osteoporosis

Osteoporosis is caused by an imbalance in the normal bone remodelling process whereby excessive osteoclast resorption occurs without adequate new bone formation. The trabecular struts become thin and eventually resorb altogether leading to a reduction in bone strength and an increased likelihood of fractures of the spine, hip and wrist in sufferers (Cummings and Melton, 2002). These fractures are generally attributed to the reduction in the bone mass and trabecular connectivity, see Fig. 2.10.

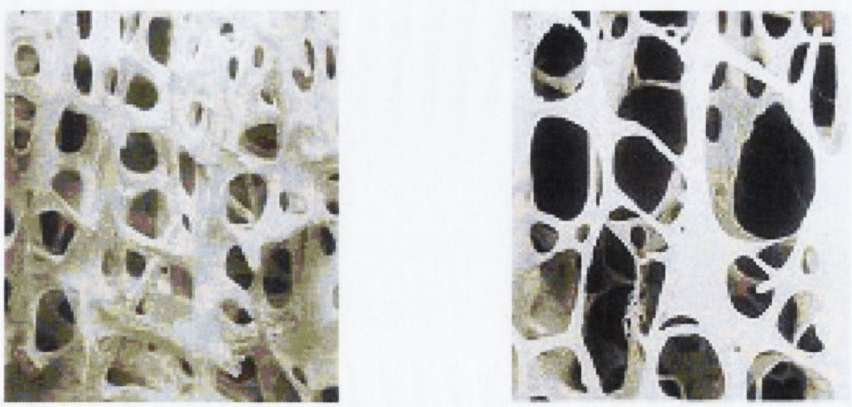

(a) (b)

Figure 2.10: *Structure of trabecular bone in (a) normal and (b) osteoporotic bone (Dempster et al, 1986)*

2.4.1 Pathophysiology of osteoporosis

During menopause the levels of circulating estrogen in the blood are deficient and this deficiency is believed to play a role in the imbalance in the cellular activity during osteoporosis. It has been found that osteoclastic activity is enhanced by estrogen deficiency, and that the reduced levels of circulating estrogen during osteoporosis are associated with increased rates of bone turnover and bone loss due to a relatively high activity and increase in number of both osteoblasts and osteoclasts, with a functional imbalance in favour of the osteoclasts (Bell *et al*, 1996; Rosen, 2000). Osteoblast-like cells from estrogen receptor knockout mice have deficient responses to mechanical strain suggesting that estrogen withdrawal during osteoporosis may inhibit the osteogenic response to mechanical loading (Jessop *et al*, 2004). The osteoblasts may be no longer capable of completely refilling the resorbed space, resulting in irreversible bone loss. The activation frequency increases and resorption cavities become deeper, leading to thinning of trabecular struts and subsequent perforation. The perforated trabeculae are removed by further remodelling and this loss of bone mass, as is illustrated in Figure 2.10, increases the fragility of bones, resulting in a greater propensity for fracture (Recker, 1993; Dalle Carbonare and Giannini, 2004).

2.4.2 Epidemiology and statistics of osteoporosis

Osteoporosis is a disease that is most commonly manifested in elderly people, especially post-menopausal women, see Fig. 2.11. However men and in rare cases younger people are also affected. It has been reported that 96% of fractures of the spine and femur reported in Ireland in 1999 were diagnosed in persons after the age of 45. Of this number approximately 75% of the patients were female and 25% male (HIPE Report 2002). This condition is associated with severe health implications requiring hospitalisation and long-term care at great personal and financial expense. Osteoporosis has a large impact on both the individual sufferer and the healthcare industry. Approximately 4000 osteoporotic fractures occur in Ireland each year (HIPE Report 2002). In the United States this figure is estimated as 1.5 million, of which about 300,000 are hip fractures (Compston and Rosen, 2002). These frequently require hospitalisation and often lead to permanent disability. Within a year following a fracture 25% of survivors will be confined to long-term care facilities,

50% will experience long-term loss of mobility, and 75% never regain the same level of independence. In the US, the direct medical costs of osteoporotic fractures has been estimated at $20 billion/year; in the EU, the hospital costs of hip fractures alone have been assessed as being equivalent to $3.9 billion/year (Compston and Rosen, 2002).

In the UK is has been estimated that 1 in 3 women and 1 in 12 men will have osteoporosis over the age of 50. It has been reported that every 3 minutes someone has a fracture due to osteoporosis and that each year 60,000 hip fractures, 50,000 wrist fractures and 40,000 spinal fractures can be attributed to osteoporosis (Compston and Rosen, 2002). These fractures are estimated to cost the NHS and UK government over £1.7 billion each year, working out at £5 million each day. It is the second most important public health problem for women after breast cancer.

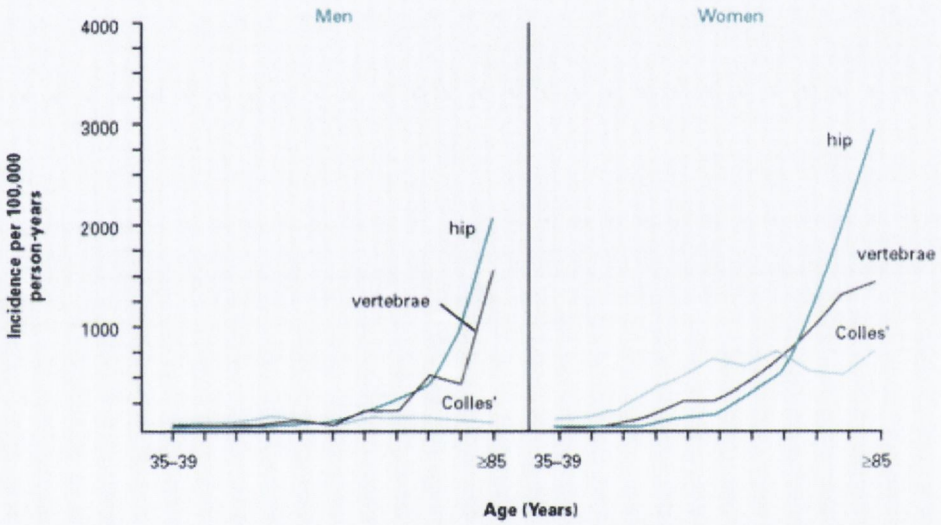

Figure 2.11: *Incidence of hip, forearm and clinically diagnosed spinal fractures. (Cooper and Melton, 1992)*

2.4.3 Biomechanical behaviour of osteoporotic trabecular bone

The main concern with regard to osteoporosis is that bone fractures occur unpredictably and with little force. For this reason, a number of studies have been carried out to develop an understanding of the biomechanical behaviour of bone during osteoporosis. The majority of these studies have been concerned with assessing the effects of the disease on the morphology of the trabecular architecture and the mechanical consequences of its structural degradation. Determination of whether

there is a change in the material behaviour of the tissue constituting the architecture has received much less attention.

2.4.3.1 Structural mechanical behaviour of bone during osteoporosis

During osteoporosis the increased bone turnover leads to trabecular thinning and increases the likelihood of trabecular perforation under physiological loads (Compston *et al*, 1989). There are fewer trabeculae present, and their connectivity is diminished, so there may not be adequate structural support, which would explain the decreased mechanical performance of osteoporotic bone. A study by Lane *et al* (1998) observed that trabecular connectivity decreased 27% by days 5 and 8 post-ovariectomy ($p < 0.01$) and continued to decrease up to day 50 post-ovariectomy ($p < 0.01$). The trabecular bone volume decreased 25% by 8 days post-ovariectomy ($p < 0.01$), and it continued to decrease through day 50.

Due to the relationship between osteoporosis and estrogen depletion (Kimmel, 1996), animals that have become osteopenic following ovariectomy are widely used for research into the effects of osteoporosis on the mechanical performance of bone. The ovariectomised rat model has become the gold standard because it emulates most of the important clinical features of the osteoporotic adult human skeleton. Firstly, following ovariectomy the rat model develops osteopenia, primarily in poorly loaded cancellous bone sites with a rapid phase of bone loss during the early stages of estrogen deficiency. Secondly, increased bone turnover is associated with the initial, rapid phase of bone lone induced by estrogen deficiency.

Assessment of the effects of osteoporosis on the mechanical behaviour of bone has been carried out previously using whole bone testing (Kasugai *et al*, 1998; Yoshitake *et al*, 1999; Hirano *et al*, 2000; Ederveen *et al*, 2001; Bourrin *et al*, 2002) or testing of volumes of cancellous bone (Mosekilde *et al*, 1995; Sugita *et al*, 1999; Hu *et al*, 2002; Teramura *et al*, 2002) from rat and dog models and also from post-mortem human specimens. Using ovariectomy to induce osteoporosis in the rat, it has been found, for example, that the compressive strength of rat vertebral bodies and the bending strength of rat femora is significantly decreased following ovariectomy (Kasugai *et al*, 1998; Yoshitake *et al*, 1999; Ederveen *et al*, 2001). However, these observations were accompanied by significant decreases in trabecular bone volume and thus cannot discriminate whether changes were due only to the reduction in bone

mass and loss of architecture, or whether a reduction in tissue strength also contributed.

2.4.3.2 Material properties

The effects of osteoporosis on the behaviour of the bone tissue itself have not been adequately quantified. Osteoporosis has previously been defined as a "systemic skeletal disease characterized by decreased bone mass and microarchitectural deterioration of bone tissue with a consequent increase in bone fragility and susceptibility to fracture" (cited in Pietschmann *et al*, 2003). However, this definition does not take into account the possibility that there is a change in the material behaviour. As Aspden (2003) acknowledged, changes in material behaviour might also ensue: "Osteoporosis results in a reduction in the quantity of the bone, an alteration in its structural organization, and possibly, changes in the material properties of the bone matrix".

A number of studies have been carried out that describe the effects of osteoporosis on the mineral content in the bone tissue; some of these reveal that the mineral content is unchanged or slightly lower in the osteoporotic bone tissue (Li and Aspden, 1997) and others which have observed an increase in the mineral content and a lack of collagen (Dickenson *et al*, 1981; Birkenhager-Frenkel, 1987; Zioupos and Aspden, 2000). Gadeleta *et al* (2000) found that there was a change in the ratio of mineral to matrix in bone due to osteoporosis. Zioupos *et al* (2000) observed that the ratio of the mineral phase to the organic matrix was higher in osteoporotic bone than in normal bone, and that this ratio increased significantly with the porosity of the bone. Such microstructural changes suggest, but do no prove, that a corresponding change in the mechanical behaviour of the bone tissue could occur during osteoporosis. However, to date, the tissue level properties of osteoporotic bone tissue have not been quantified.

Li and Aspden (1997a, 1997b) assessed trabecular bone from the femoral head and neck region of patients who experienced an osteoporotic fracture of the femoral neck. They observed that the osteoporotic bone had a lower apparent density, stiffness and strength than trabecular bone from age matched patients with no evidence of disease. They found that the correlation between stiffness and the square of the density was weaker in osteoporotic bone tissue than has been previously reported for

healthy cancellous bone. This would suggest that some fundamental change is occurring with the development of the disease.

The majority of research that has been performed on osteoporotic trabecular bone has been concerned with deriving the structural mechanical behaviour as a function of the architecture and the porosity. It is essential to develop an understanding of the tissue behaviour during osteoporosis to seek to fully address the issues of bone fracture during osteoporosis.

2.4.4 Drug Treatment for osteoporosis

The aim of treating osteoporosis is chiefly to reduce fracture incidence. A variety of different treatments have been formulated which are as follows

- Hormone Replacement Therapy
- Anti-resorptive therapy
  - Bisphosphonates
  - Selective Tissue Estrogenic Activity Regulators (STEARs,Tibolone)
  - Selective Estrogen Receptor Modulators (SERMs)
  - Calcitonins
  - Calcium
  - Vitamin D and Metabolites
- Anabolic Agents
  - Parathyroid Hormone (PtH)

Of these treatments, anti-resorptive therapy is a popular choice of treatment. While drugs of these types have different modes of operation, the common aim of anti-resorptive drugs is to maintain bone mass and architecture by restoring the remodelling imbalance through inhibition of osteoclast activity and reducing bone resorption (Kloosterboer and Ederveen, 2002). A study by Yoshitake *et al.* (1999) examined the architecture of bone after anti-resorptive drug treatment and observed higher bone volume, tissue volume, trabecular number and a lower trabecular separation relative to untreated osteoporotic bone.

The efficacy of anti-resorptive drug treatments has been assessed and it has been found, for example, that treatment with Tibolone (Kasugai *et al*, 1998; Yoshitake *et al*, 1999; Ederveen *et al*, 2001) and other anti-resorptive drugs such as estrogen (Mosekilde *et al*, 1995), Risedronate (Mosekilde *et al*, 1995), Etidronate

(Hirano *et al*, 2000) Alendronate (Hu *et al*, 2002), Pamidronate (Bourrin *et al*, 2002) and Incandronate (Teramura *et al*, 2002) increases the structural or bulk trabecular bone strength (Mosekilde *et al*, 1995; Hu *et al*, 2002; Teramura *et al*, 2002) and the whole bone strength (Kasugai *et al*, 1998; Yoshitake *et al*, 1999; Hirano *et al*, 2000; Ederveen *et al*, 2001, Bourrin *et al*, 2002) by maintaining bone mass and trabecular architecture. However, while these drugs are capable of reducing the propensity to fracture by approximately 50%, even with continuous use of drug treatment fractures still arise (Randell *et al*, 2002). It has been found that treatment with high doses of certain anti-resorptive drugs is associated with an increase in the rate of spontaneous fractures of the thoracic spinous process, ribs and pelvic fractures (Flora *et al*, 1981; Parfitt *et al*, 1996; Hirano *et al*, 2000). While these studies reveal that the structural mechanical behaviour is maintained using anti-resorptive drugs, due to the structure of cancellous bone, the material properties obtained using these test methods are highly dependent on the architecture of the matrix and do not represent the properties of the mineralised tissue itself. The effectiveness of drug treatments for improving the mechanical strength of the trabecular tissue has not been investigated.

It has often been proposed, and it is now generally accepted, that osteoclastic bone resorption activity serves as a repair mechanism to remove aged damaged bone tissue (Burr *et al*, 1985; Carter *et al*, 1987, Prendergast and Huiskes, 1995, 1996) and a concern with some HT drugs is that inhibiting the remodelling process prevents the necessary renewal of bone tissue. This may allow microdamage to accumulate in the bone tissue, so that, although bone mass and architecture are maintained, bone strength at the tissue level may be impaired. In order to assess the efficacy of anti-resorptive drug treatments to improve the mechanical performance of osteoporotic bone it is required to measure the mechanical behaviour of bone tissue during osteoporosis and drug treatment.

2.5 Mechano-regulation of bone remodelling

The process by which bone cells are capable of sensing changes in mechanical stimuli in the bone matrix in order to adapt the trabecular architecture has been a subject of great interest to the biomechanics community throughout the years. Of particular interest are the mechanisms by which bone cells sense these changes in mechanical stimuli and the signals they emit to control the process.

2.5.1 Mechano-sensor cells

It is widely believed that bone cells are sensitive to mechanical signals and that the remodelling process is initiated when the osteoclasts receive a signal that is generated by cells, known as mechano-sensors, to begin resorption (Cowin *et al*, 1991; Lanyon, 1993; Huiskes and Hollister, 1993). A number of different cells have been proposed as the likely candidates and it has been suggested that the mechano-sensors involved in initiating remodelling may be one of osteocytes, bone lining cells or osteoblasts (Cowin *et al*, 1991; Lanyon, 1993; Mullender and Huiskes, 1997). A number of studies have investigated which of these cells; osteocytes, osteoblasts or bone lining cells is the most likely mechano-sensor.

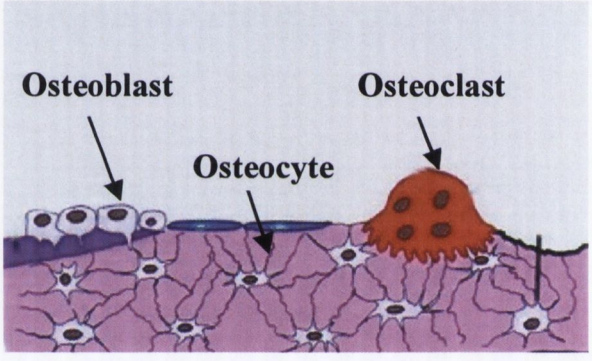

Figure 2.12: *Osteocytes, osteoblasts and osteoclasts network via cell processes*

Trabecular bone remodelling is a surface phenomenon and osteoblasts mature to become bone lining cells and ultimately osteocytes after remodelling is finished. For this reason it has been proposed that bone-lining cells and osteoblasts may be effective mechano-sensors (Mullender and Huiskes, 1997).

However, remodelling in cortical bone occurs by means of a tunnelling motion through the bone tissue and is not restricted to the surface. Osteocytes are distributed throughout the bone matrix in both cortical and trabecular bone, and thus may be ideally placed for strain detection. They are connected by long cell processes, which may sense mechanical stresses in bone and are capable of communicating signals to osteoblasts and osteoclasts, as is illustrated in Figure 2.12. Much of the current knowledge regarding bone cell biology has been derived from *in vitro* experiments. Experimental investigations have shown that osteocytes are responsive to mechanical

loading (el Haj *et al*, 1990; Chambers *et al*, 1999) which activates several cellular processes including energy metabolism, gene activation, growth factor production and matrix synthesis (review by Burger and Klein-Nulend, 1999). It has been found that bone formation under mechanical loading involves early expression of growth factors (c-fos and IGF-1) by osteocytes (Chambers *et al*, 1999). The results of such experiments have shown that strain derived fluid flow activates osteocytes to produce anabolic factors such as prostaglandin's and nitric oxide. Therefore it is generally conceded that osteocytes are indeed the mechano-sensor cells that appraise local mechanical signals and then emit stimuli to recruit osteoblasts or osteoclasts from the bone marrow (Carter *et al* 1985; Cowin *et al*, 1991; Lanyon, 1993; Mullender *et al*, 1994; Mullender and Huiskes, 1995; 1997; Huiskes *et al*, 2000; Smit and Burger, 2000; Burger *et al*, 2003).

However, in developing these *in vitro* systems it is difficult to reproduce the natural environment of bone cells *in vivo*. Many of the experiments concentrate on developing 2D monolayer cultures whereas *in vivo* osteocytes are organized in a 3D matrix. *In vitro*, matrix production is often deficient or the matrix produced is poorly mineralised. Therefore, it is unclear whether the results of such experiments represent the situation *in vivo* or whether they correspond to cellular responses to a foreign environment. While these experiments may be useful tools for preliminary investigations, ultimately they cannot provide a complete picture of the *in vivo* situation due to limitations in the reproduction of the cellular environment.

While important progress has been made in understanding how bone cells may sense the effect of mechanical loading, and how mechanical signals are transduced into cellular signals, many details of the biological process whereby bone tissue responds to loading are still obscure. Firstly, it is yet to be determined definitively whether osteoclasts and osteoblasts are indeed governed by mechanical signals, or whether they also function to maintain mineral homeostasis in the bone tissue or to transport ions. Secondly, if the cells are indeed governed by mechanical stimuli then it is unclear exactly what the molecular signalling cascade is between bone mechanics and adaptive responses.

2.5.2 Mechanical stimuli for bone remodelling

A number of researchers have investigated the process of bone remodelling and have proposed different stimuli for activation, propagation and termination of this process. Two different theories are widely accepted for the mechanism of bone remodelling; namely that bone adaptation is regulated by strain (adaptive elasticity) or it is regulated by microdamage.

The adaptive elasticity theory (Cowin and Hegedus, 1975) refers to the manner in which bone reshapes itself when the loading situation alters. This is commonly observed during bone atrophy, due to lack of use. It is generally accepted that this process tends to optimise the architecture of cancellous bone so that there is minimum stress in the bone tissue relative to its weight. The body removes excess bone that is not required to support loads, to keep bone mass minimal. Experimental evidence has demonstrated that, at low strains, net bone resorption occurs and that, at elevated strains, net bone formation occurs (Carter, 1984). It has thus been hypothesised that bone-remodelling cells are capable of appraising local deformations and adapt bone mass accordingly in order that it is adequate for the loads that it bears. It has been postulated that the manifestation of such a strain stimulus may be deformation of the osteocyte lacuna, strain energy density in the bone tissue (Mullender *et al.*, 1994; Huiskes *et al.*, 2000) or strain-derived fluid flow in the osteocyte canalicular channels (Cowin *et al.*, 1995, Burger *et al.*, 2003).

However it is known that *in vivo* microdamage accumulates in trabecular bone throughout our lifetime, from the cyclic loading situations created by everyday activities such as walking, running etc. *In vivo* microdamage has been identified in bone by a number of researchers, for example by Lee *et al.* (2002) and Vashishth *et al.* (2000). *In vitro* studies have revealed that microdamage is generated in bone under everyday physiological loading conditions, for example by Wenzel *et al* (1996) who observed microdamage both in the central portion and near surfaces of human vertebral trabeculae. Burr *et al* (1998) observed that microcrack accumulation impairs the mechanical properties of bone by reducing its elastic modulus. The ability of bone to renew may thus be vital to remove this microdamage and maintain strength. Therefore, it has been proposed that bone remodelling may be targeted to maintain bone strength by resorbing mature bone and replacing it with new bone thereby preventing accumulation of damage (Prendergast and Taylor, 1994; Carter *et al.*,

1987; Frost, 1986; Martin and Burr, 1989; Prendergast and Huiskes, 1996; Martin, 2002).

It is interesting that experimental evidence has shown that resorption cavities occur preferentially in regions of microdamage in cortical bone (Burr et. al, 1985; Mori and Burr, 1993), which would suggest that resorption cavities might indeed be initiated in sites where microdamage is present. Lee *et al* (1998, 2000a; 2000b) observed microcracks in human ribs, which were all oriented along the long axis of the ribs, parallel to osteons. The microcracks were approximately elliptical in shape, with mean length 404 μm, width 97 μm and thickness 9 μm. They hypothesised that the uniformity in measured crack dimensions is due to a balance between remodelling and crack growth, which may serve to keep cracks below a critical length. A later study by Lee *et al* (2002) observed that microcracks, resorption cavities and osteon formation sites were all located near the periosteal surface of the original cortex, but they found that no microcracks were found in the new fibrolamellar bone laid down at periosteal or endosteal surfaces. They observed that the average microcrack length was 49 μm; this was consistent between sites and across species, and this supported the idea of a repair mechanism triggered beyond a critical crack length.

The experimental evidence in support of both strain (Carter, 1984) and damage (Burr *et al*, 1985; Lee *et al*, 2002) as mechano-regulatory stimuli for bone remodelling suggest that bone remodelling may be, in fact, regulated by a combination of signals due to both strain and microdamage (Prendergast and Huiskes, 1995). A number of hypotheses have been developed regarding the mechano-regulation of bone remodelling; some models have proposed the stimuli for resorption to be strain, others that it is damage.

2.5.3 Computational analyses of BMU activity

The mechanism of mechanical signal appraisal and subsequent stimulation of activity of a BMU in volumes of trabecular bone is have been investigated through the use of computational analyses of mechanical signals local to BMUs.

Smit and Burger (2000) developed finite element models of resorption lacunae in both cortical and cancellous bone. They represented the geometry of a Howship's lacuna on a trabecular surface as semi-cylindrical and loaded the trabecula by 1000 microstrains in the longitudinal direction. They predicted increased strains at the

bottom of the lacuna and perpendicular to the direction of loading, where resorption is stopped and osteoblasts are recruited to fill the gap, and lower strains in the direction of loading, where osteoclast resorption activity continues. Based on these observations they proposed that BMU activity is regulated by strain, and that low strains drive osteoclast resorption whereas increased strains inhibit osteoclasts and activate osteoblasts to refill.

Van der Linden *et al.* (2001) constructed finite element models of cancellous bone at 28-μm resolution and resorption cavities were created by removing 28 x 28 x 28 μm volumes from the trabecular structures. They observed that the presence of resorption lacunae resulted in increased strain at the base of the resorption cavity and decreased strain along the tip. However, given that resorption lacunae are typically 40 – 60 μm in depth, these resolutions did not give a detailed description of the consequences of resorption cavities on the strain distribution in bone tissue. For such an analysis solid models of the geometry of real trabeculae and active resorption lacunae at high resolutions are required.

Burger *et al* (2003) carried out a computational analysis of the fluid flow around a cutting cone in cortical bone in order to develop an understanding of the mechanisms that drive the continuing activity of osteoclasts to resorb through the bone matrix. They hypothesised that strain-induced fluid flow in the caniliculi of osteocytes around the cutting cone induces production of Nitric Oxide (NO) at elevated magnitudes of fluid flow. The NO produced at the base of the resorption cavity, due to high fluid flow, had a protective effect on the osteocytes, whereas at the tip of the cone the lack of NO production caused apoptosis of osteocytes. The osteoclasts had a phagocytic purpose and act to resorb the dead osteocytes. This theory does not address the mechanisms that control the apparent coupling of the osteoclasts and osteoblasts, nor does it address the mechanisms that determine the direction of travel of a BMU or the mechanism by which the resorption process is terminated.

2.5.4 Mechano-regulatory hypotheses for bone remodelling

If bone remodelling is indeed governed by any of the proposed mechanical stimuli (i.e. strain or microdamage) then a mechano-regulatory rule based on such a stimulus should predict realistic remodelling of trabecular bone. A number of researchers have

developed mechano-regulatory rules based on these stimuli and applied these to models of trabecular structures in order to predict trabecular bone adaptation. Simulations of bone remodelling according to proposed mechano-regulatory rules have been performed.

2.5.4.1 Strain as a mechano-regulatory stimulus

The theory of adaptive elasticity, first developed by Cowin and Hegedus (1976), has been used in several computational simulations of bone remodelling. This theory proposes that bone has the capacity to adapt its architecture to attain a remodelling equilibrium strain state.

The basis of this method is that, based on physiological loading, bone material properties and boundary conditions, an equilibrium (homeostatic) strain state can be defined. By altering loading conditions of the bone, a new strain state is achieved. In order to return to the equilibrium strain state, the density of the material is adapted which causes a change in the overall stiffness and/or the mass and shape of the bone is altered. Cowin and Van Buskirk (1979) proposed an equation that is capable of predicting net surface remodelling of bone according to adaptive elasticity theory. This equation describes the change in position of an external bone surface at over time $S(Q)$ and is given by

$$S(Q) = [\mathrm{B}]\{E - E^0\} \tag{2.1}$$

where $[\mathrm{B}]$ is a vector of constants governing the remodelling rate, E^0 is the remodelling equilibrium strain tensor and E is the strain tensor.

A number of researchers have applied this theory to predict adaptive behaviour of bone remodelling for example Huiskes *et al* (1987), Cater *et al* (1989), Weinans *et al* (1992) and Beaupre *et al* (1990a, 1990b). Predictions of change of density of trabecular bone under multiple loading conditions have been made (Carter *et al*, 1989, Beaupre *et al*, 1990b), see Figure 2.13. It has been found that it is possible to predict bone resorption in response to stress shielding of prosthetic implants (Huiskes *et al*, 1987, McNamara *et al*, 1997). Van der Linden *et al* (2004) applied this theory to investigate the consequences of changes in bone tissue properties on the trabecular architecture evolved using an adaptive elasticity model.

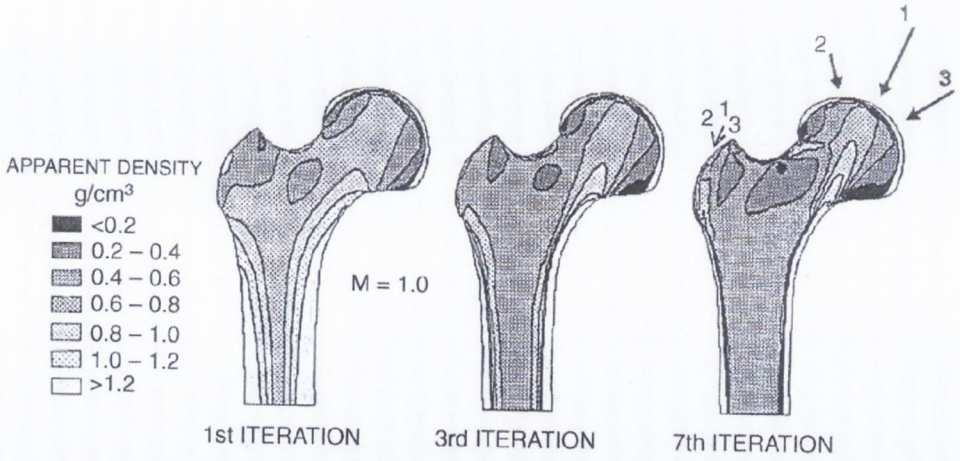

Figure 2.13: *Predicted distribution of trabecular density in the femoral head using multiple loads (Carter et al, 1989*

This theory has also been used to test the hypothesis that the osteocyte network has a mechano-sensory function and is capable of signalling bone cells to adapt trabecular architecture. Mullender *et al* (1994) and Mullender and Huiskes (1997) proposed that osteocyte mediated remodelling of trabecular bone could simulate bone remodelling as a self-organisational process. The adaptive elasticity theory was applied to a model of a volume of trabecular bone, which had a distribution of osteocytes throughout the volume, each of which sensed mechanical signals by appraising the strain energy density at its location. The osteocyte emitted a stimulus to local osteoblasts and osteoclasts to deposit bone or resorb bone from surfaces. The remodelling stimulus was calculated from the change in strain energy density S_j from homeostatic levels and the distance between the cells.

$$F(x,t) = \sum_{i=1}^{N} f_i(x)\{S_i(t) - S_{ref}\} \qquad (2.2)$$

where the strain energy density (S_j) is calculated according to the relationship from Weinans *et al* (1989, 1992)

$$S_i(t) = \frac{E_i \varepsilon_i^{\,2}}{2\rho_i} \qquad (2.3)$$

and E_j is the elastic modulus (MPa) of the material, ε_i is the calculated strain and ρ_i is the density of the material (gcm^{-3}) and the units of $S_i(t)$ are MPa $(gcm^{-3})^{-1}=Jg^{-1}$. The reference strain energy density (S_{ref}) was calculated at an assumed homeostatic stress level.

The spatial influence function $f_i(x)$ accounted for the diminishing behaviour of the remodelling stimulus with increasing distance between sensor cell and actor cells. This assumption was made that osteocytes local to the actor cell would have more of an influence on its activity than more remote osteocytes. Thus the magnitude of the stimulus was assumed to decrease exponentially with increasing distance from the actor cells and determined the regulation of bone density between zero and maximal density. The spatial influence function $f_i(j)$ was calculated by

$$f_i(j) = e^{-d(i,j)/D} \qquad (2.4)$$

where d(i,j) is the distance (μm) between the actor cell i and the sensor cell j. The parameter D represents the distance (μm) from an osteocyte at which location its effect has reduced to e^{-1}; i.e., 36.8%.

They found that trabecular morphology is dependent on the relationship between local load, sensor density and distance of actor cells from the sensor cells. The actor cells received signals from any local sensor cells and their activity was dependant on the sum of these signals. The relative density of bone was altered with time depending on the stimulation received from the sensor cells. They later (Mullender and Huiskes, 1997) used this model to investigate which cells were optimal candidates for mechano-sensors. They developed two different models, with osteocytes and bone-lining cells acting as the mechano-sensors in either model. It was found that the hypothesis that osteocytes are sensor cells is more effective than that of surface cells, with less change in architecture observed upon the application of external loads.

Huiskes *et al* (2000) simulated the remodelling process, using the method described above, in a volume of bone, to confirm that the coupled relationship between the osteoblasts and osteoclasts is due to mechanical forces. They assumed that remodelling was regulated by external forces or by strains generated due to the presence of resorption cavities. The signal appraised was the strain energy density rate in the tissue; and the mechanosensors, osteocytes, emitted a signal that was related to this. They investigated two possible means of osteoclast activation: either presence of microdamage or low strain concentrations (disuse). A regular grid represented the trabecular bone volume, and was subjected to a cyclic 2 MPa external stress at 1 Hz. A homeostatic architecture was generated, which is one in which bone remodelling continues without further changing the architecture, for both situations. The trabecular

orientations were found to line up with the direction of the applied load. Strain-controlled resorption reached homeostasis much quicker than the microdamage initiated remodelling, so they proposed that these results favour the idea that strain is the mechanism of control of bone remodelling.

2.5.4.2 Damage as a mechano-regulatory stimulus

Prendergast and Taylor (1994) developed a damage-adaptive law for bone remodelling. They hypothesised that, even at remodelling equilibrium, there exists a homeostatic burden of microdamage in the form of microcracks within bone tissue. If the amount of damage changed from this equilibrium amount then a stimulus for bone remodelling was generated. The repair rate for bone remodelling was determined from the homeostatic stress. The rate of change of mass (m) of the bone in response to damage was thus given by the following relationship

$$\frac{\mathrm{d}m}{\mathrm{d}t} = C\int_0^t \dot{\omega} - \dot{\omega}_{\mathrm{RE}} \qquad (2.7)$$

where $\dot{\omega}$ is the damage formation rate and $\dot{\omega}_{RE}$ is the damage repair rate. Application of the theory was capable of giving physically reasonable predictions of the adaptive response of a bone diaphysis under a change in torsional load.

Taylor (2004) later developed this theory to predict the probability of failure of bone specimens in the presence of repair.

2.5.4.3 *Strain-adaptive and damage-adaptive combined*

Prendergast (2002) proposed a mechano-regulation model that combined the principles of strain-adaptive and damage-adaptive remodelling to recognize the fact that bone may remodel in response to strain and damage simultaneously. This hypothesis proposed that bone remodelling in response to damage accumulation can only occur if the damage exceed a critical value. Thus

$$\frac{\mathrm{d}m}{\mathrm{d}t} = C\left(\varepsilon - \varepsilon_{ref}\right) + x.C_1\left(\Delta\omega\right) \qquad (2.8)$$

where ε is the calculated strain, ε_{ref} is the homeostatic strain, C, C_1 are remodelling constants, x =1 if $\Delta\omega$ is positive, else x =0 and $\Delta\omega$ is the change in damage from the equilibrium level, which is given by the difference between the damage formation rate $\dot{\omega}$ and the repair rate $\dot{\omega}_{RE}$, given by

$$\Delta\omega(t) = \dot{\omega} - \dot{\omega}_{RE} \qquad (2.9)$$

It was proposed that this rule would be capable of predicting bone atrophy at low strain magnitudes, bone hypertrophy at high strain rates as well as bone atrophy at pathologically high strain rates as is shown in Figure 2.14, however the predictive capacity for bone remodelling of this rule has not been tested.

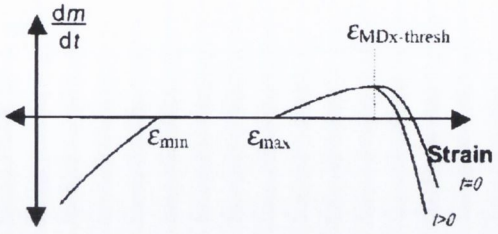

Figure 2.14: *Proposed remodelling behaviour (Prendergast, 2002)*

Many different mathematical bone-remodelling descriptions of the regulation of bone remodelling have been formulated and the application of these models to finite element models produces simulations of bone formation and resorption that are qualitatively reasonable and fit with experimentally reported results (Hart, 2001). However limitations of this approach exist, which may undermine their ability to act as a tool for deriving information about the bone remodelling process.

Firstly, these models are all based on the principle that bone remodelling is induced by a local mechanical signal, which activates the regulating cells. The stimuli chosen in the simulations and the assumption of the existence of mechano-sensor cells are purely hypothetical. Both strain and damage are physical quantities for which it is possible to conceive mechanisms for their sensation by bone cells. Strain energy has been widely used as the remodelling stimulus based on the fact that it is an easily interpretable physical scalar, which is related to both stress and strain. Damage may be sensed by fracture of the osteocyte processes due to the shearing motion between crack faces (Taylor *et al*, 2003), by unloading of the osteocyte lacuna local to the crack (Prendergast and Huiskes, 1996), or by causing apoptosis of the osteocyte (Noble, 2003). However, the existence of strain energy or damage sensors has never been documented in experiments and it is still unclear how bone cells might sense mechanical signals.. Therefore, the possibility that other stimuli or mechano-sensory systems would work equally well cannot be discarded.

Secondly, the remodelling rules chosen in the simulations are also purely hypothetical and the possibility that other remodelling rules would work equally well

cannot be discarded. In fact each of the models is capable of predicting some experimentally observed bone changes, which means that it is difficult to determine which model is the most realistic. It has been shown that any description of the mechanical situation can be successfully used to drive a satisfactory adaptation response. However, many of the parameters that have been used in adaptation simulation models are highly correlated with one another, which mean that it is difficult to interpret the differences between the models.

While the similarities of these predictions to reality are reasonably good, the FE approach is limited due to the number of assumptions and simplifications required to make simulations computationally efficient. Many of these models have been tested on simplified 2D geometries that are chosen to represent bone but which are only schematic representations of the true bone structure. However, if bone remodelling were indeed a mechano-regulated phenomenon then the geometry of the bone would certainly play a role in dictating the remodelling behaviour. Also, physiologically the osteocyte sensory system is a 3D network. For that reason, to fully determine the potential of models to accurately simulate bone remodelling it is required to test them on 3D representative models and observe the predicted remodelling behaviour. The mesh density of the finite element model also limits the predictive powers of the adaptive simulation models. The bone tissue is invariably modelled as linear elastic with isotropic material properties. In reality, bone tissue is a composite material and therefore if this material behaviour were to be included in these models then it would certainly affect the predicted behaviour. Nonetheless, the results obtained are satisfactory and the approach serves well to illustrate the potential applicability of mechano-regulation rules to model bone remodelling. The possible relevance of certain parameters such loading conditions, remodelling rates and osteocyte sensory capacity can also be investigated by removing the complexity due to geometric non-linearity. Previous models have only been tested under a limited number of loading cases. It is yet to be determined the ability of these models to predict realistic bone remodelling behaviour under a variety of loading conditions.

Theoretical models are useful tools for framing experimental questions, testing the consequences of different starting assumptions, and for the predictions of outcomes. They should be used as a tool to help focus *in vivo* experiments on quantification of assumed parameters. These algorithms help to further understand bone as a mechanical structure, but do not provide useful information about the

physiological process of adaptation. In order for these models to provide more insight into be more useful the modelling assumptions should be more tightly coupled to biological parameters that can be histologically measured and manipulated.

2.5.5 Research questions arising regarding BMU regulation

Even though different stimuli have been investigated and simulations of trabecular adaptation have been performed, the exact mechanisms that drive a BMU through bone tissue are not understood. If BMU activity is regulated by local mechanical signals, then the signal should not only activate a Bone Multicellular Unit (BMU) in terms of signal osteoclast activation, it should also govern the depth of resorption cavity or volume of resorbed bone, and the initiation of refilling by osteoblasts, see Figure 2.15. Furthermore, this signal should also cause the BMU to traverse a trabeculum, as is seen *in vivo*. However, to date the nature of such a stimulus that can regulate BMU activity has not been identified.

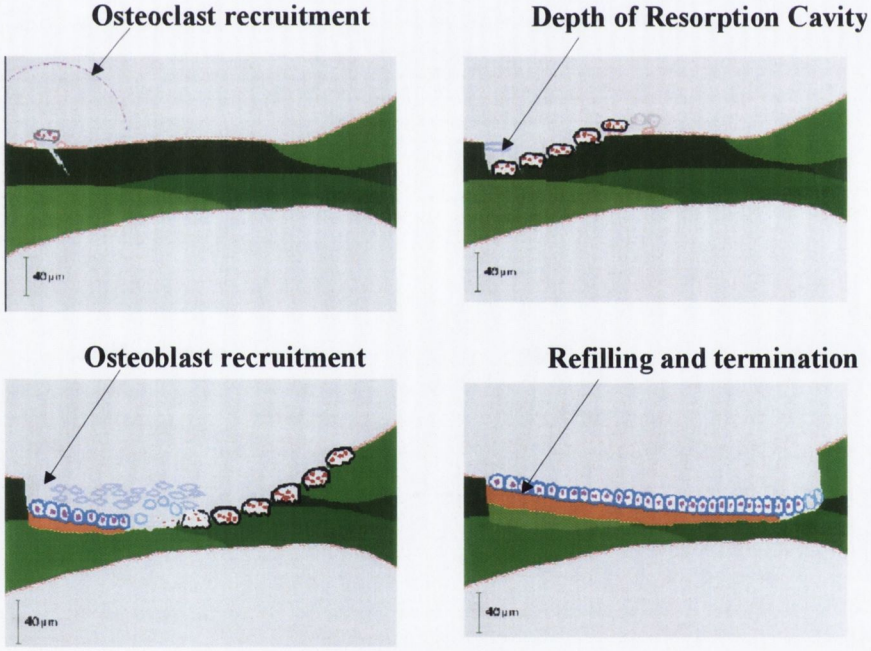

Figure 2.15: *BMU activity along bone trabecular surfaces*

2.6 Conclusion

The problems of osteoporotic fractures are currently attributed to changes in the bone remodelling activity, and consequently the architecture, of the trabecular bone. The effects of osteoporosis and drug treatments that suppress bone turnover on the material constituting cancellous bone trabeculae remain to be discovered. If the contention of this thesis is to be investigated, i.e. that there is a pathological change in bone tissue material properties during osteoporosis, a reliable method for determining the mechanical behaviour of single bone trabeculae is required. This method is also essential for assessing the efficacy of anti-resorptive drug treatments in improving the mechanical performance of osteoporotic bone.

In order to investigate the possibility that changes in material behaviour during osteoporosis may subsequently drive the adaptation of trabecular architecture, the mechanisms that drive the normal bone remodelling process must first be understood. Many different theories have been put forward regarding mechano-regulated bone remodelling; some models have proposed that the stimulus for bone remodelling is strain, others that it is damage. It would be a significant step forward if the regulatory mechanisms governing the cellular activity at the level of the BMU were better understood in order to address the imbalance in the cellular coupling associated with osteoporosis. To develop such an understanding, the mechanical stimuli in the neighbourhood of existing resorption cavities must be examined to confirm whether strain or microdamage may play a role in BMU development.

Previous models have been applied to simulate the adaptation of trabecular architecture under various loading conditions, but the regulation of the activity of BMU at the trabecular-level has not yet been addressed. Given that bone remodelling has been reported to be associated with both of these stimuli, a mechano-regulatory rule is required that encompasses both strain and damage as stimuli to initiate and drive bone multi-cellular units (BMUs). Bone remodelling is a complicated process, involving communication between a network of mechano-sensor cells and actor cells that carry out bone resorption and bone formation. Only by incorporating these aspects of bone cell behaviour into a model of bone remodelling can bone turnover be accurately simulated. If that succeeds, the methodology could be used to evaluate the differences in bone remodelling that occur during osteoporosis.

3. Materials and methods

3.1 Introduction

This chapter presents the details of the methods used to investigate the hypotheses presented at the end of Chapter 1. Finite element models of trabeculae were developed, using both serial sectioning at micro-resolutions and micro-CT scanning. These finite element models are used to analyse the stress distribution local to resorption lacunae within trabeculae and to examine whether these stresses are high enough to generate damage.

An apparatus to measure the mechanical properties of single bone trabeculae is developed, and used to determine the mechanical properties of bone tissue during osteoporosis and drug-treatment.

While there is evidence to suggest that bone adapts in response to both strain and microdamage, previous computational models of bone adaptation have never included both of these aspects. In this chapter, a theoretical model of bone remodelling is proposed which incorporates both strain and microdamage as remodelling stimuli. This model will be used to simulate the activity of a bone multi-cellular unit, where the mechanical stimuli are determined by finite element modelling. If successful in simulating this aspect of bone remodelling, the mechano-regulation model can then be used to explore the changes in bone remodelling activity during osteoporosis.

3.2 Specimen preparation

In order to develop solid models and test single bone trabeculae in a satisfactory manner, a consistent method of removing single bone trabeculae from trabecular bone is required. In developing such a method, it is essential to eliminate errors due to damage or drying out of specimens. There exists a protocol for preparation of trabeculae that has been applied by a number of research groups who have performed mechanical testing of single bone trabeculae (Townsend and Rose, 1975; Runkle and Pugh, 1975; Mente and Lewis, 1989; Ryan and Williams, 1989; Choi *et al.*, 1990; Rho *et al.*, 1993, Samelin *et al.*, 1996). In the work of this thesis, this method has been adapted to include a protocol for removing single trabeculae from the trabecular bone of Wistar rats and minimises damage.

3.2.1 Protocol for extracting single bone trabeculae

Right tibiae from Wistar rats were stored frozen at -20°C. The bone specimen was thawed for 24 hours at –4 °C. All remaining soft tissue was removed using a scalpel blade and forceps. The tibia was bisected along the long axis of the bone using a scalpel blade. The bone section was cleaned of bone marrow using a water jet. A dissecting microscope was used to locate trabecular rods, which were removed from the distal tibia region using a scalpel blade and forceps. Excised specimens were placed in vials of normal saline and stored at –4°C.

3.3 Solid modelling

A technique has been developed that allows for three-dimensional reconstruction of the geometry of individual trabeculae. Solid models of the micro-specimens were generated using either serial sectioning and imaging at micro resolutions, following the technique of Van der Linden *et al.* (2002), or micro-CT scanning (Skyscan 1072 MicroCT, Antwerp, Belgium).

3.3.1 Serial sectioning

A protocol developed by O'Brien *et al.* (2000) for preparation of bone samples for serial sectioning was adapted for use with microspecimens of bone and involved staining trabeculae and then embedding them in methylmethacrylate (MMA) to create samples suitable for serial sectioning. This allows for support of the specimen and this support prevents cracking of the specimen when it is cut with the microtome knife. Methylmethacrylate (MMA) was used as the embedding medium and its properties were optimised through the use of a softener and a catalyst. The times for dehydration and infiltration were adjusted according to the size of specimen. The times were optimised through trial and error to avoid poor infiltration and bubble formation at the onset of polymerisation.

3.3.1.1 Staining

An ultraviolet microscope and camera assembly were used during serial sectioning. Bone epifluoresces under ultraviolet light and it was thus required to stain the specimens in ink so that the boundaries of the bone cross-section could be

distinguished. The procedure for staining the specimens of bone was adapted from previous studies of microdamage accumulation in bone (Huja *et al*, 1999; Lee *et al*; 1998; Lee *et al*, 2000). The individual trabeculae were dehydrated in alcohol and stained in Indian ink using the following procedure.

1. Solutions of 80%, 90%, and 100% ethanol were prepared.
2. Specimens were completely immersed in petri dishes containing the alcohol solutions for 10 minutes each in order to dehydrate them for staining and embedding.
3. Trabeculae were stained with black Indian ink by placing them in petri dishes of the ink.
4. Specimens were then dehydrated for a further 10 mins in each of the solutions of 80%, 90%, and 100% ethanol after staining. This was performed to facilitate uniform polymerisation of the resin during the following embedding procedure.

3.3.1.2 Infiltration

Infiltration of the trabecular specimens with MMA was required to allow the solution to fully penetrate the specimen prior to embedding. The polymer solution used for infiltration consisted of methyl methacrylate, a softener, di-butyl phthalate, and a hardener, benzoyl peroxide. The softener was required to prevent the MMA being too brittle and the hardener acted as a catalyst and induced polymerisation of the polymer at the correct temperature.

The embedding medium was prepared by dissolving 7.0g of Benzoyl peroxide in a solution of 200 cc methyl methacrylate and 50 cc di-butyl phthalate on a magnetic stirrer under a fume hood. The benzoyl peroxide was thoroughly dissolved and the solution was filtered, this allowed it to be stored at 4-6°C for long periods. A base of MMA was prepared in glass vials of approximately 2 cm diameter in order that the specimen could not come into contact with the surfaces of the vial. Bases of MMA were prepared under vacuum at 40 mm Hg. The bases consisted of approximately 5 mls of MMA solution, which was allowed to harden at 55°C in an oven. Once the base was sufficiently hardened, the sample was placed on top of it in the vial and 1-2 mls of the embedding medium was poured completely immersing the trabeculae in the solution. To allow the specimen to be properly infiltrated the vials containing the

base; specimen and solution were placed in a vacuum dessicator, at a pressure of 40 mg Hg, for 1 hour.

3.3.1.3 Embedding

Infiltrated specimens were completely immersed in MMA solution in the glass vial for embedding. The glass vials were placed in a vacuum dessicator for about 2 hours so as to remove any air from the solution. The vials were then capped tightly and placed into an oven at 55°C for 1 day.

3.3.1.4 Sectioning

Serial sectioning of the embedded samples was carried out at the Orthopaedic Research Laboratory at Erasmus University Rotterdam. The apparatus used for obtaining images of serially sectioned bone surfaces consisted of a microtome, a camera, a motorised transversing table, and a computer control interface. The apparatus was fully automated using Labview software for control of the positioning of the table and the timing of the acquisition of images. The system had the capacity to serially section at resolutions from 1-20 μm. The samples were removed from the glass vials and the excess MMA was cut to provide a sharp edge to meet the blade of the microtome. The sample was prepared by filing and cutting of MMA. A hole of diameter 0.3 mm was drilled into the MMA (Figure 3.1) which acted as a reference to facilitate accurate realignment of the images obtained during reconstruction, due to the fact that repositioning of the specimen under the camera showed some slight variability, within a couple of micrometers.

The prepared blocks were mounted in the custom made holder of a microtome and slices of 10 μm were made until the specimen was exposed at the surface of the block and in view under the microscope. The exposed surface was focused in the microscope and the camera properties were optimised for focus. The serial sectioning was carried out at a resolution of 5μm and cutting speed was optimised to allow time for accurate focusing of camera and to allow the software to obtain images of the exposed surface after each slice was made. The slices were removed from the blade using a soft artists brush and no attempt was made to retain the slices. Images of the cross-section were obtained under microscopy after each slice was made, see Figure 3.1.

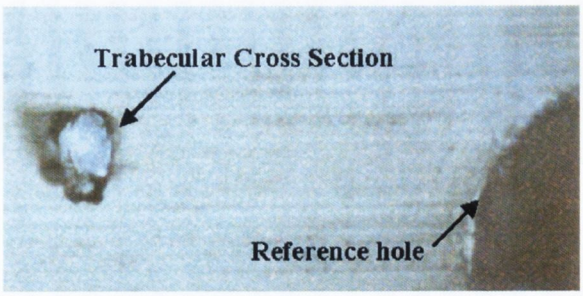

Figure 3.1: *Image of trabecular cross-section obtained during serial sectioning with reference hole*

3.3.2 Micro-CT scanning

For micro-CT scanning, specimens were placed in vials of saline prior to scanning to prevent drying out of the specimens in the scanner and also to facilitate positioning of the micro-specimens in the scanner. Specimens were scanned using a micro-CT scanner (Skyscan 1072 MicroCT, Antwerp, Belgium) at 3.22μm resolution. The datasets obtained were segmented to obtain a thresholded image of the trabecular cross sections, see Figure 3.2. The co-ordinates of the cross-sectional boundaries were recorded using MATLAB software.

Figure 3.2: *Segmented image of trabecular cross-section obtained from CT scanning*

3.3.3 Solid model generation

The images of the sections were imported into the data digitizer package Windig (Lovy, Switzerland) and the co-ordinates for the contours of each bone section were manually recorded from the images using this package. Using these values, a data set of the co-ordinates for the contours were generated in Microsoft Excel and imported in AutoCAD 2000. Splines were fitted to each data set to represent the slices in a solid model, see Figure 3.3. A spline is a smooth curve

passing through a given set of points and is useful for creating irregular-shaped curves. AutoCAD uses a particular type of spline known as a nonuniform rational B-spline (NURBS) curve, which produces a smooth curve between through a set of specified fit points.

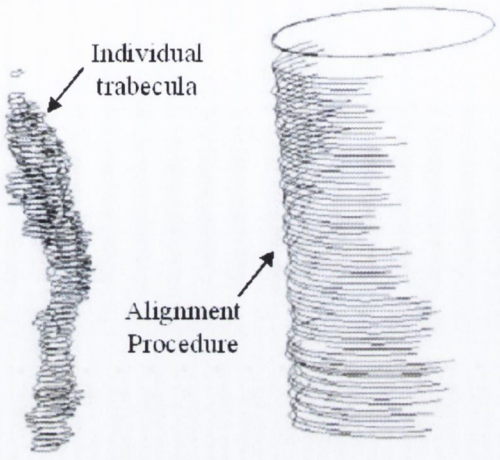

Figure 3.3: *Reconstruction of slice co-ordinates using alignment hole reference*

Volumes were created between each slice using ANSYS to produce solid models of individual trabeculae. The solid models were used as the geometric input for finite element analyses of the distribution of stress within trabeculae, see Figure 3.4.

Figure 3.4: *Solid model of bone trabeculum*

3.4 *Finite element analyses*

The finite element mesh generation and analyses were carried out using ANSYS.

3.4.1 General concepts of Finite Element Analysis

To formulate a finite element approximation for a given problem the domain (geometry of object) of interest is divided into a number of smaller sub-regions by the process of domain discretization. An individual sub region in a discretized domain is known as a finite element and collectively the finite elements provide a finite element mesh. The nodes of the elements are a set of discrete points within the solid body, which represent the sampling points in an element where the numerical values of the unknowns are to be calculated. The main advantage of the discretization of a problem into finite elements is that within each element, unknown functions can be approximated using interpolation procedures.

In a well-defined finite element the variations of a real valued continuous function can be defined over an element in terms of appropriate geometrical functions, known as shape functions. If the values of the function are known at the locations of the nodes then in any other point in the element an approximate value for the function can be defined using the interpolation method. Using a simple interpolation procedure, variations of a continuous function along the element can be calculated.

A common objective of a finite element analyses is to determine the distribution of stress within a solid. This is done by computing the displacements at each node and using the element interpolation functions to determine the displacement at arbitrary points within each element. The displacement field can be differentiated to determine the strains. Once the strains are known, the stress—strain relations for the element are used to compute the stresses.

While this procedure can be used to determine the stress at any point within an element, in reality there exist special points within an element where stresses are computed most accurately and these are known as integration points. Stresses are sampled at these points in the finite element program to evaluate certain volume and area integrals, hence they are known as integration points. The number of integration points of an element increases with the increasing number of nodes an element has. For example a 3-noded triangle element has one integration point, whereas an 8-noded quadrilateral has nine integration points.

The general form of the governing equation for each element in a finite element mesh is

$$\{F\}=[k]\{x\}$$

where $\{F\}$ is the vector of the applied nodal forces that generate a vector of nodal displacement $\{x\}$ and the stiffness matrix $[k]$ governs the amount of displacement occurring in the element in response to the applied force.

3.4.2 Mesh generation

For the finite element discretization of the problem presented in the work of this thesis, the element type chosen is a 3-D 20-Node Structural Solid (Figure 3.5). This element type was chosen as it can tolerate irregular shapes without much loss of accuracy as it has compatible displacement shapes, which are well suited to model curved boundaries. The element is defined by 20 nodes having three degrees of freedom per node: translations in the nodal *x*, *y*, and *z* directions.

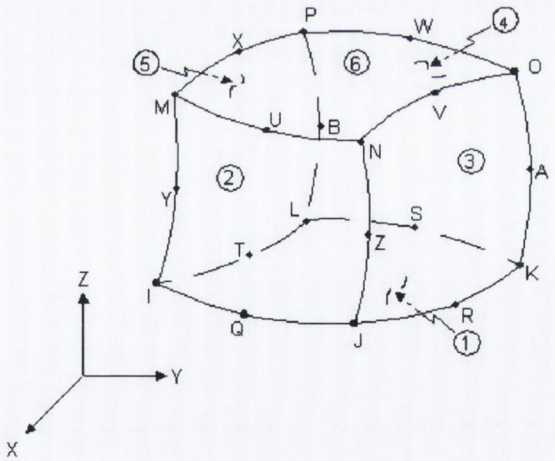

Figure 3.5: *3-D 20-Node Structural Solid*

3.4.3 Material properties and boundary conditions

The trabeculae were modelled as homogenous, linear isotropic materials with a Poisson's ratio of 0.3 and Young's modulus of 2.2 GPa. A load was applied to each trabecula to generate an apparent strain of 3000 με across its entire length. This would

correspond to a stress of 6.6 MPa in a cylindrical trabecula with the chosen elastic modulus.

The force to be carried by each trabecula was calculated from this value using the average cross sectional area of each trabecula. A loading axis was determined as the line connecting the centres of area of each of the loaded faces. This ensured that the specimens were loaded in tension and minimized the effects of bending, see Figure 3.6.The nodes at the base of the specimens were constrained in the loading direction and the node at the centre of area was constrained in all directions.

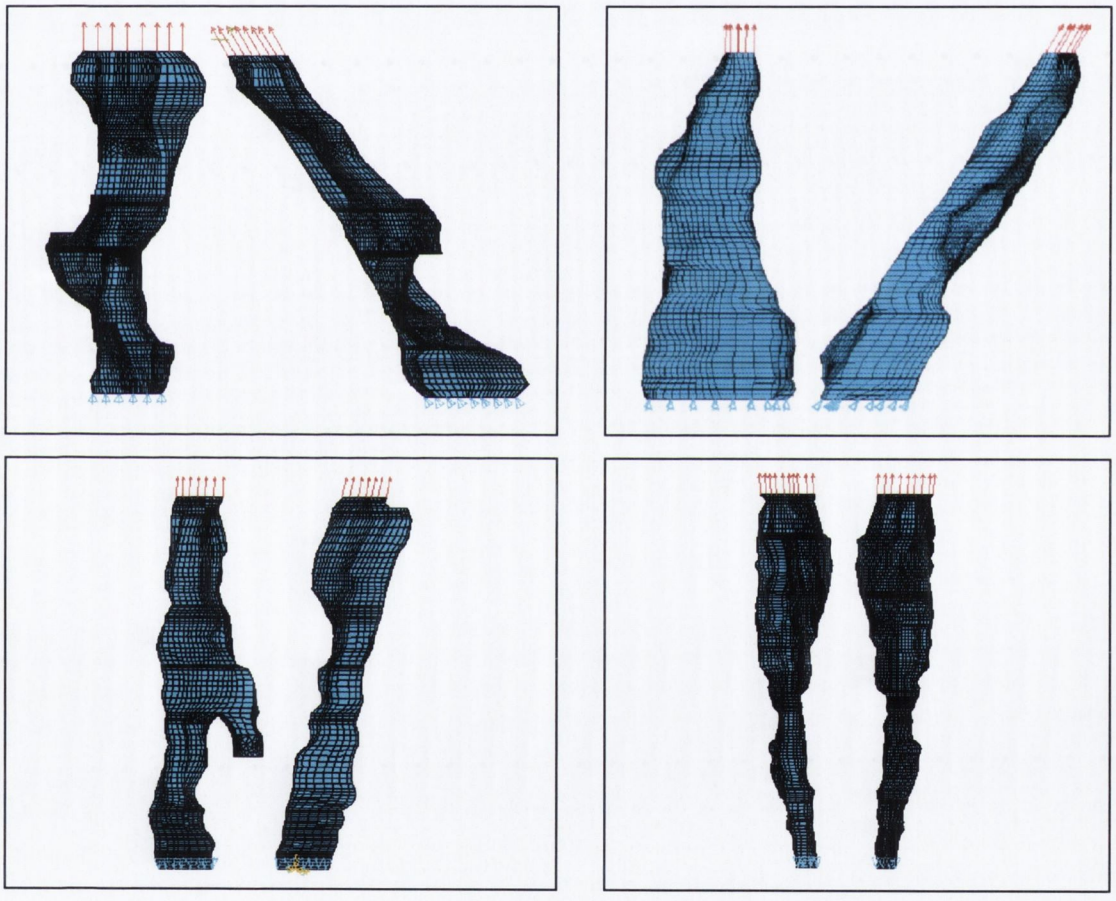

Figure 3.6: *Loading conditions, specimens were loaded by applying a prescribed force along the axis between the centroids of each loaded face images. Each picture shows views from two orthogonal directions*

The idealised model of Smit and Burger (2000) was recreated for comparison; see Figure 3.7, in order to compare the stress distribution in an idealised trabecula containing a lacuna to the actual distributions that were observed in these analyses. In this model the trabecula is modelled as a solid cylinder with a diameter of 200 μm, containing a spherically shaped lacuna with a depth of 60 μm. The same loading conditions were applied

Figure 3.7: *Idealised Model recreated according to Smit and Burger (2000)*

3.5 Animal Experimentation

Three groups of 44 week old female Wistar rats were treated as follows: 1) a control group which was sham operated and treated with vehicle, 2) a group which was ovariectomized (OVX) as a model of osteoporosis and treated with vehicle and 3) an OVX group that was treated orally with the HT drug tibolone (2 mg/kg, d). All treatment was carried out for 54 weeks, i.e. from the 44th week to the 98th week of life.

Bones were harvested after 0, 4, 14, 34 and 54 weeks of treatment. Sections of cancellous bone were cut from below the growth plate of the right proximal tibia (n=3 / group / time point) of each animal. The sections were cleaned of marrow using a water jet. Using a scalpel blade and forceps individual rod-like trabeculae (n~3 per tibia) were excised under a stereomicroscope and stored in saline before testing. The excised specimens were examined under 30X stereomicroscopy and samples with microdamage evident from preparation were eliminated from the test group.

3.6 *Micro-mechanical Testing*

Tensile testing of individual trabeculae required the use of special micro-testing equipment capable of applying low loads and dealing with small samples. The test system used was an MTS Tytron 250 testing machine (MTS Systems Corporation, Minneapolis, USA), which operates using a linear DC servomotor, and is capable of applying loads at a resolution of 0.001 N, see Figure 3.8. This system was modified by customizing a microscope assembly and a grip system, Figures 3.9-3.11.

3.6.1 Gripping micro-specimens

The main problem faced in testing of individual trabeculae is that of gripping the specimens during testing. The procedure for gripping trabeculae (diameter ~ 100 μm) used the shafts of hypodermic needles (inner diameter = 0.3 mm) as grip rods. A close tolerance fit between an alignment sleeve and the grip rods ensured co-axiality of the grip rods. One end of the trabecula was inserted into the grip rod assembled in the fixed platen of the machine, and affixed using a cyanoacrylate adhesive (302, Locktite), see Figure 3.11. The actuator of the machine was used to manipulate the position of the second needle so that the free length of the specimen was maximised. The specimen was aligned under 30X magnification; using a graticule lens as a reference for alignment, see Figure 3.11. A constant displacement rate of 1 μm/sec was applied until failure of the trabecula. The cross-sectional dimensions at the point of fracture were taken under microscopy.

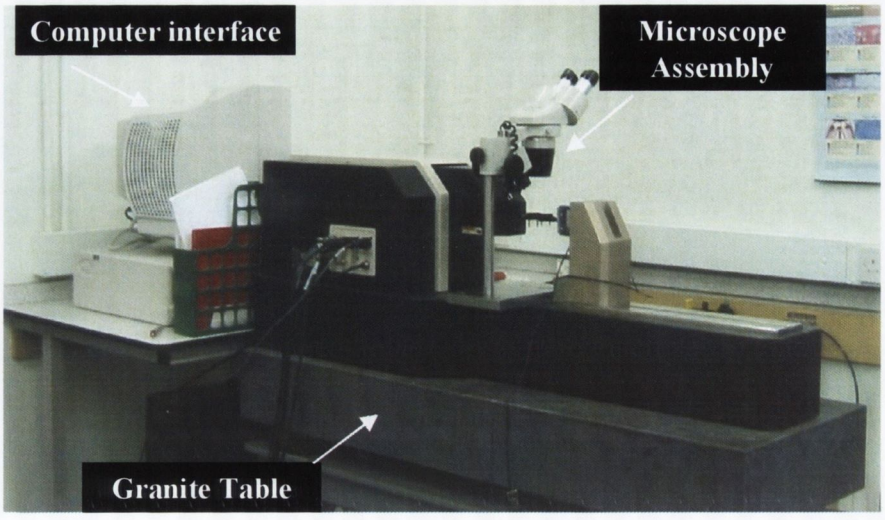

Figure 3.8: *MTS Tytron 250 micro testing machine*

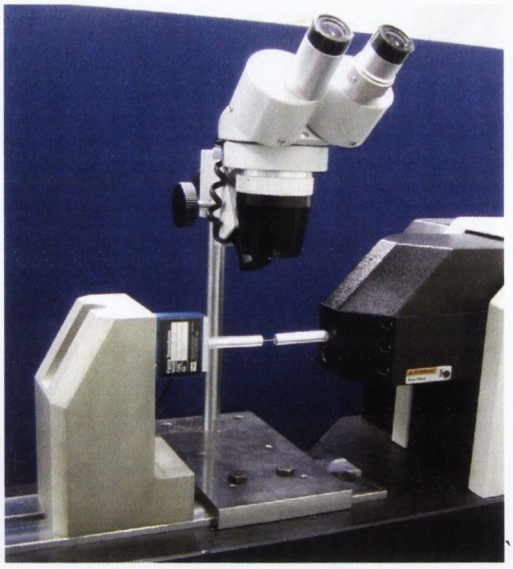

Figure 3.9: *Microscope assembly for use during micro-testing*

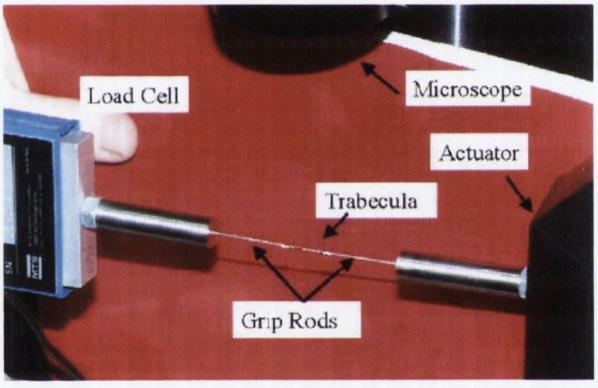

Figure 3.10: *Grip assembly for use during micro-testing*

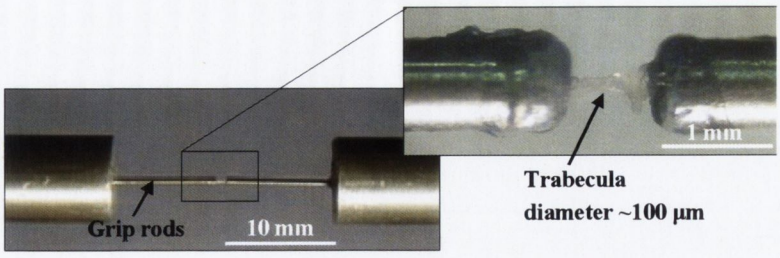

Figure 3.11: *Gripping of micro-specimens during testing*

3.6.2 Correction factor estimation

The displacement recorded during testing was that of the actuator and thus it represented a combination of the displacement of the bone specimen and the glue. Therefore it was necessary to develop a method to compensate for the presence of the glue in order to obtain a measurement of strain in the bone specimen for calculations of Young's modulus. This was performed using finite element analyses, which simulated the mechanical test, including the test specimen, grip rods and the glue layer; see Figure 3.12.

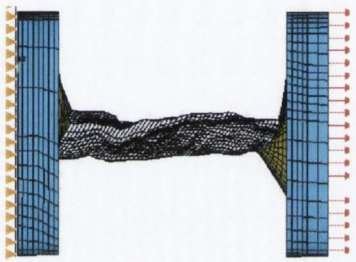

Figure 3.12: *Finite element model of tensile tests including bone specimen, grip rods and glue layer*

For these analyses, solid models of the micro-specimens were generated using the two different methods, (1) serial sectioning and imaging at micro resolutions and (2) micro-CT scanning as described above. The finite element mesh generation and analyses were carried out using ANSYS. The trabecula was modelled as a homogenous, linear isotropic material with a Poisson's ratio of 0.3 and Young's Modulus of 2.2 GPa. The glue was modelled as linear elastic (E=0.3 GPa) with a Poisson's ratio of 0.25. The grip rods were modelled as linear elastic (E=200 GPa) with a Poisson's ratio of 0.29. A displacement that corresponded to 2% strain (approximately the yield strain of a trabecula) between grips was applied to the model. The strain along the bone specimen was calculated and compared to the strain calculated based on the displacement of the grip rods in order to develop a correction factor.

The correction factor was calculated using $\varepsilon_w = k\varepsilon_{wo}$, where ε_w is the applied strain, and ε_{wo} was the strain experienced by the bone specimen. Based on this value ($k = 0.575$) corrections for the data recorded from each experiment were made.

3.6.3 Data Processing and statistical analyses

The stress-strain relationships for samples of trabecular tissue were generated for each of the groups (control, OVX, drug-treated) at each time point (0, 4, 14, 34 and 54 weeks). The 0.2% offset yield strength was calculated, for each group (n~9) at each time point, from the stress-strain curves of the data by constructing a line parallel to the elastic portion of the stress-strain curve but offset from the origin by 0.002 (0.2% strain), see Figure 3.13. The intersection of the stress-strain curve and the offset line gave a value for 0.2% yield strength.

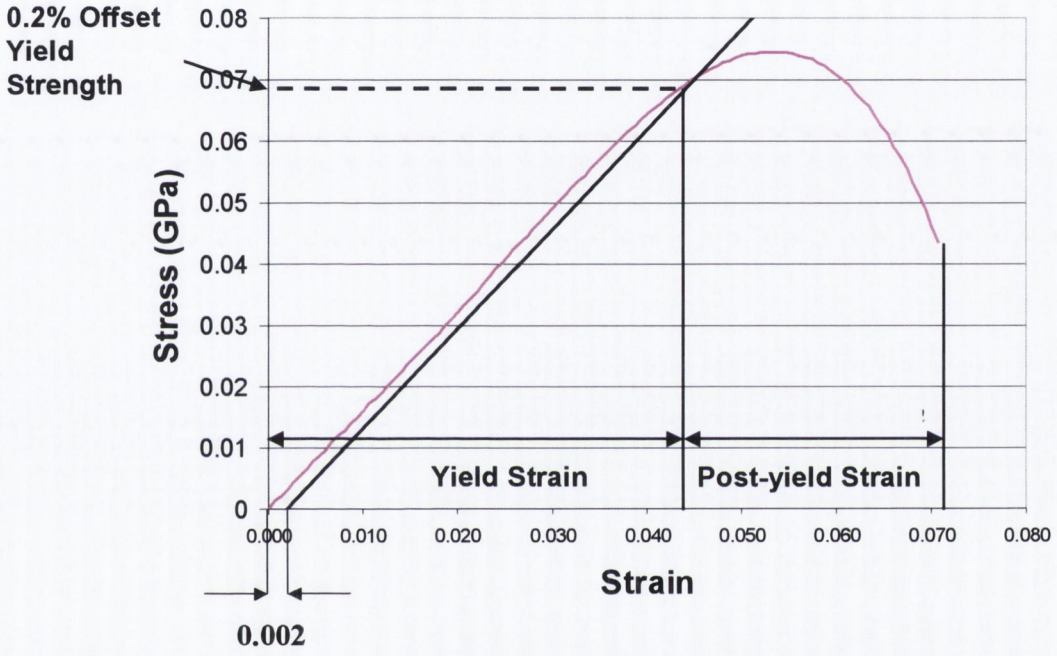

Figure 3.13: *Calculation of 0.2% Offset Yield Strength*

Statistical analyses (ANOVA, Student's t-test) were performed to analyse the effect of the treatments (ageing, osteoporosis and drug treatment) on the yield strength and elastic modulus of the bone tissue.

3.7 Computational modelling of bone remodelling

The aim is to investigate the hypothesis that a change in the material properties of bone during osteoporosis drives the adaptation of the architecture and results in the loss of bone. To achieve this aim, a mechano-regulation rule for normal bone remodelling, which relates the changes in mechanical stimuli to the change in bone mass, is required. In this thesis four, mechano-regulation rules are developed based on two component stimuli, strain and microdamage. The theoretical formulation and application to prediction of bone remodelling along a trabecular surface is described.

3.7.1 Formulation of a mechano-regulation model of bone remodelling

Bone remodelling in trabecular bone is a surface phenomenon. Accordingly, in this model, the assumption is made that the surface cells are actor cells (representing osteoclasts and osteoblasts) and changes in bone mass are restricted to the locations of the actor cells.

It is also assumed that mechano-sensor cells are present in the bone tissue, which are capable of sensing local changes in mechanical stimuli. At these locations, mechanical signals (changes in strain and damage) are evaluated and two separate stimuli are generated. The total remodelling stimulus emitted by a sensor cell is calculated as a function of these two component stimuli. In the work of this thesis, two different mechano-sensor cells are considered, namely surface cells (osteoblasts and bone lining cells) and osteocyte cells evenly distributed throughout the tissue volume. For surface based remodelling, the stimulus is appraised at the actor cell location, whereas for osteocyte based adaptation the total remodelling stimulus received by an actor cell is a sum of the stimuli from all the sensor cells in the model.

3.7.1.1 Strain component of remodelling stimulus

The strain component of the remodelling stimulus is calculated from the change in strain energy density S_j from homeostatic levels where the strain energy density is calculated according to the following relationship (Fyhrie and Carter 1990; Weinans *et al* 1992),

$$S_j = \frac{E_j \varepsilon_j^{\,2}}{2\rho_j} \tag{3.1}$$

and E_j is the elastic modulus (MPa) of the material, ε_j is the calculated strain and ρ_j is the density of the material (gcm^{-3}) and the units of S_j are MPa $(gcm^{-3})^{-1} = Jg^{-1}$.

a. For surface based remodelling, the strain component of the bone remodelling stimulus is calculated from the difference between the strain energy density (S_j) and a homeostatic value (S_{ref})

$$F_{strain}(i) = \{S_i(t) - S_{ref}\} \tag{3.2}$$

b. For osteocyte mediated remodelling, the stimulus received by the actor cell from the sensor cell is a function of the change in strain energy density at the sensor cell and the distance between the cells, which is accounted for by the corresponding spatial influence function $f_i(j)$. The spatial influence function is calculated following the methods of Mullender and Huiskes (1997). It is assumed that osteocytes local to the actor cell will have more of an influence on its activity than more remote osteocytes. Thus the amount of stimulus received by an actor cell (i) from a mechano-sensor cell (j) will diminish with increasing distance between the cells. The diminishing behaviour of the stimulus is calculated using the spatial influence function given by

$$f_i(j) = e^{-d(i,j)/D} \tag{3.3}$$

where d(i,j) is the distance (μm) between the actor cell i and the sensor cell j. The parameter D represents the distance (μm) from an osteocyte at which location its effect has reduced to e^{-1}; i.e., 36.8%. Thus the stimulus F^j_{strain} at a time t received by the actor cell (i) from the sensor cell (j) is given by

$$F^j_{strain}(t) = f_i(j)\{S_j(t) - S_{ref}\} \tag{3.4}$$

where S_{ref} is the reference strain energy density calculated as

$$S_{ref} = \frac{E\varepsilon_{ref}^{\,2}}{2\rho} \tag{3.5}$$

E and ρ are the elastic modulus (MPa) and density of bone (g/cm^3).

The total strain component of the bone-remodelling stimulus received by an actor cell is a sum of the stimuli generated by each sensor cell in the model

$$F_{\text{strain}}(i) = \sum_{j=1}^{N} f_i(j)\{S_j(t) - S_{\text{ref}}\} \tag{3.6}$$

where N is the total number of osteocytes in the tissue domain considered.

3.7.1.2 Damage component of remodelling stimulus

Following the methods of Prendergast and Taylor (1994), it is assumed that, even at remodelling equilibrium, there exists a certain amount of microdamage within the bone tissue. Remodelling in response to damage accumulation occurs only when the amount of damage changes from homeostatic levels, i.e. $\Delta\omega > 0$ where

$$\Delta\omega = \omega - \omega_{RE} \tag{3.7}$$

and ω is the damage and ω_{RE} is the remodelling equilibrium damage burden. The rate of change of damage is given by

$$\frac{\mathrm{d}(\Delta\omega)}{\mathrm{d}t} = \int_0^t \frac{\mathrm{d}\omega}{\mathrm{d}t} - \frac{\mathrm{d}\omega_{\text{RE}}}{\mathrm{d}t} = \dot{\omega} - \dot{\omega}_{\text{RE}} \tag{3.8}$$

where $\dot{\omega}$ is the damage formation rate and $\dot{\omega}_{\text{RE}}$ is the damage repair rate, which is assumed to be equal to the rate of production of damage at remodelling equilibrium, calculated from a homeostatic stress.

Damage (ω) is calculated using the remaining life approach, which quantifies damage formation rate using Miner's rule for cumulative damage under repetitive loading and is calculated as follows

$$\dot{\omega} = \frac{1}{N_f} \tag{3.9}$$

where N_f is the number of cycles to failure of the material at a given stress and is calculated from the empirical relationship of Carter *et al* (1976)

$$\log(N_f) = H\log(\sigma_j) + JT + K\rho_j + M \tag{3.10}$$

where σ_j is the cyclic stress (MPa), T is the temperature (°C) and ρ_j is the density of the material (g/cm^3) . H, J, K, and M are empirical constants.

In the development of the theory to be used in this thesis, it is assumed that remodelling in response to damage accumulation only occurs if the damage exceeds a critical value.

a. Therefore, for surface based remodelling, the damage component of the bone-remodelling stimulus is calculated and the change in damage from homeostatic levels $\Delta\omega(i)$ and is given by

$$F_{\text{damage}}(i) = x\Delta\omega(i) \tag{3.11}$$

where x =1 if damage accumulation is positive (i.e. $\Delta\omega$ >0), else x =0

b. For osteocyte mediated remodelling the stimulus generated by a sensor cell due to damage is then given by

$$F^{j}_{\text{damage}}(t) = xf_i(j)\Delta\omega(j) \tag{3.12}$$

where $f_i(j)$ is the spatial influence function described in section 3.7.1.1 above. The total damage component of the bone-remodelling stimulus received by an actor cell is a sum of the stimuli generated by each sensor cell in the model

$$F_{\text{damage}}(i) = \sum_{j=1}^{N} xf_i(j)\Delta\omega(j) \tag{3.13}$$

All unrepaired damage is allowed to accumulate in the model and damage accumulation is predicted using Euler integration

$$\Delta\omega^{i+1} = \Delta\omega^{i} + (\dot{\omega} - \dot{\omega}_{RE})\Delta t \tag{3.14}$$

3.7.1.3 Mechano-regulation rules for bone remodelling

Four different mechano-regulation rules are developed as follows **(i-iv)** to investigate the two stimuli described above as components of the remodelling stimulus

i. Damage regulation

This rule considers damage adaptive mechano-regulation where the rate of change of density predicted from the following equation

$$\frac{d\rho_i}{dt} = C_2 F_{damage}(i) \qquad (3.15)$$

where C_2 is a constant governing the rate of remodelling in response to the damage stimulus and $F_{damage}(i)$ is calculated according to equation 3.11 as described above. It is intended that the use of such a remodelling law would predict damage based bone resorption as shown in Figure 3.14 (i).

ii. Strain regulation

The rate of change of density according to strain adaptive mechano-regulation is given by

$$\frac{d\rho_i}{dt} = C_1 F_{strain}(i) \qquad (3.16)$$

where C_1 is a constant governing the rate of remodelling in response to the strain stimulus and $F_{strain}(i)$ is calculated according to 3.4 as described above. The use of such a remodelling law would predict strain based bone resorption and bone formation as shown in Figure 3.14 (ii). The reference strain, ε_{ref} for calculation is defined from known loading histories (Carter *et al*, 1987) that define net bone resorption, the dead zone, and net bone formation, as is illustrated in Figure 3.14(ii). Thus

$0 < \varepsilon_j < 1000\ \mu\varepsilon$ $\qquad$ $\varepsilon_{ref} = 1000\ \mu\varepsilon$

$1000\ \mu\varepsilon < \varepsilon_j < 2000\ \mu\varepsilon$ $\qquad$ $\varepsilon_{ref} = 0$

$2000\ \mu\varepsilon < \varepsilon_j < 3500\ \mu\varepsilon$ $\qquad$ $\varepsilon_{ref} = 2000\ \mu\varepsilon$

iii. Combined strain and damage regulation

For this rule the assumption is made that the rate of change of density is given by a combination of the strain and damage stimuli

$$\frac{\mathrm{d}\rho_{\mathrm{i}}}{\mathrm{d}t} = C_1 F_{\mathrm{strain}}(i) + C_2 F_{\mathrm{damage}}(i) \qquad (3.17)$$

It is intended that the use of such a remodelling law would predict not only the strain based bone formation and resorption but also bone resorption that has been observed at pathological strain rates as shown in Figure 3.14(iii).

iv. Either strain or damage regulation where damage was prioritised

For this mechano-regulatory rule it is assumed that remodelling is governed by *either* strain or damage, but not a combination of the two, see Figure 3.14(iv). The assumption is made that if the damage burden is greater than a predefined critical amount then remodelling in response to microdamage is prioritised over strain based remodelling. According to this rule the rate of change of density is given by

$$\omega > \omega_{\mathrm{crit}} \qquad \frac{\mathrm{d}\rho_{\mathrm{i}}}{\mathrm{d}t} = C_2 F_{\mathrm{damage}}(i)$$

$$\omega < \omega_{\mathrm{crit}} \qquad \frac{\mathrm{d}\rho_{\mathrm{i}}}{\mathrm{d}t} = C_1 F_{\mathrm{strain}}(i) \qquad (3.18)$$

where ω is the accumulated damage, ω_{crit} is the predefined critical damage, C_1 is a constant governing the rate of remodelling in response to the strain stimulus and C_2 is a constant governing the rate of remodelling in response to the damage stimulus.

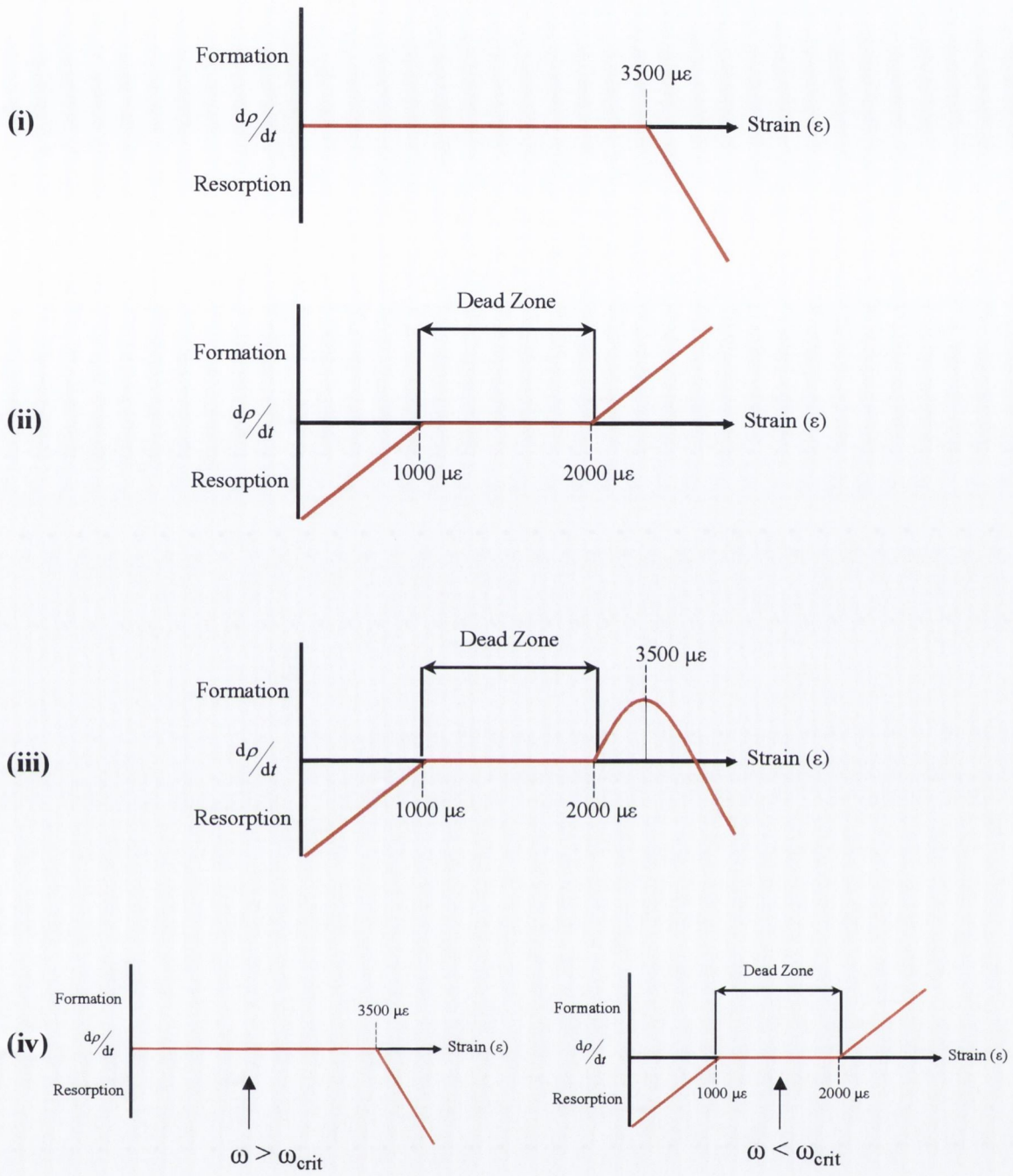

Figure 3.14: *Bone adaptation according to the four mechano-regulation rules*

3.7.1.4 Prediction of bone adaptation

For all four mechano-regulation rules the density of the adapted volume of bone tissue is given by

$$\rho_{i+1} = \rho_i + \Delta\rho(t) \tag{3.19}$$

Using the predicted density the local elastic properties are calculated according to the relationship of Currey *et al*, 1988

$$E_{i+1} = C_e \rho_{i+1}^{\ 3} \tag{3.20}$$

where C_e (MPa) is a constant governing the relationship between elastic modulus (E) and density (ρ).

3.7.2 Implementation of mechano-regulation rule

Implementing this theory required certain assumptions to be made. These assumptions will be outlined below before explaining how the theory was written into an algorithm.

3.7.2.1 Simulation of resorption and formation

Resorption is simulated by assuming that resorbed tissue is converted into marrow, and conversely formation occurs by the changing of marrow to bone tissue. Thus as the cells resorb, or form bone, the material properties of the bone tissue will change.

3.7.2.2 Remodelling rates

In the absence of experimentally determined values for remodelling rates, it was necessary to estimate the constants (C_1, C_2) governing the rate of remodelling in response to the strain and damage stimuli. It was required to calculate two separate rates for C_1, one governing the rate of remodelling in the net resorption region (< 1000 με) and a separate rate to govern remodelling activity in the net formation region (> 2000). The rate of remodelling in response to microdamage (C_2) is calculated similarly to C_1 in the resorption region, as in this model it is assumed to be purely a resorptive response.

To calculate a value for C_1 (in the resorption region) and C_2 (damage rate), a volume of bone thickness y undergoing resorption Δy was considered. The adapted tissue is a mixture of bone and marrow consisting of $y - \Delta y$ bone and Δy marrow, see Figure 3.15.

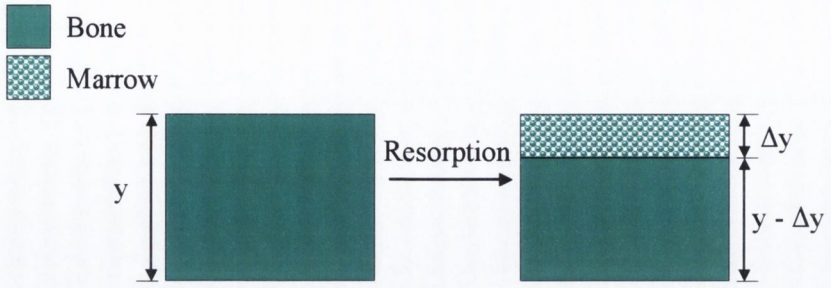

Figure 3.15: *Schematic of element mixture during resorption*

If this volume represented a single element (i) in a finite element model of bone tissue, the Young's modulus of any element undergoing bone *resorption* within a finite element model can be calculated according to mixture theory where the elastic modulus of the element is a mixture of bone and marrow and is given by

$$E_{j+1} = \frac{\Delta y}{y} E_{marrow} + \frac{y - \Delta y}{y} E_{bone} \qquad (3.21)$$

where E_{marrow} is the elastic modulus of bone marrow and E_{bone} is the elastic modulus of bone tissue.

Similarly, C_1 is calculated for the *formation* region. If a volume of marrow of thickness y undergoes formation Δy (see Figure 3.16) then the adapted material consists of $y - \Delta y$ marrow and Δy bone and its elastic modulus is

$$E_{i+1} = \frac{\Delta y}{y} E_{bone} + \frac{y - \Delta y}{y} E_{marrow} \qquad (3.22)$$

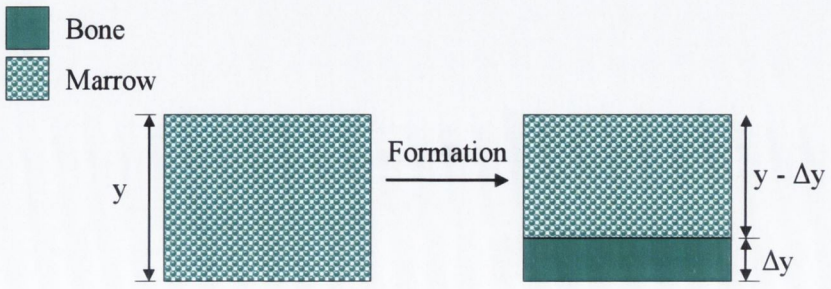

Figure 3.16: *Schematic of element mixture during formation*

Both C_1 and C_2 are estimated using the defined relationships (equations 3.15-3.18) between these rates and the change in density of the adapted tissue, equation 3.17 is given here for example

$$\Delta\rho_i = C_1 F_{\text{strain}}(i) + C_2 F_{\text{damage}}(i)$$

By rearranging equation 3.19 the change of density of a resorbing *bone* element (i.e. $\rho_i = \rho_{\text{bone}}$) is given by

$$\Delta\rho_i = \rho_{i+1} - \rho_{\text{bone}} \tag{3.23}$$

Using equation 3.20 ρ_{i+1} can be substituted and it is then possible to calculate $\Delta\rho_i$ in terms of the new elastic modulus (E_{i+1}) of the element

$$\Delta\rho_i = \sqrt[3]{\frac{E_{i+1}}{C_e}} - \rho_{\text{bone}} \tag{3.24}$$

To calculate C_1 and C_2, each rate is considered separately, i.e. to solve for C_1 the effect of damage is assumed negligible ($F_{\text{damage}}(i)=0$) and to solve for C_2 the effect of strain is assumed to be negligible ($F_{\text{strain}}(i)=0$). So an expression for the rates C_1 and C_2 in terms of the adapted elastic modulus (E_{i+1}) and the initial material properties (ρ_{bone}) is derived

$$C_1 = \frac{\sqrt[3]{\frac{E_{i+1}}{C_e}} - \rho_{\text{bone}}}{F_{\text{strain}}(i)}$$

$$C_2 = \frac{\sqrt[3]{\frac{E_{i+1}}{C_e}} - \rho_{\text{bone}}}{F_{\text{damage}}(i)} \tag{3.25}$$

To solve for C_1, an analysis of a 2D cylinder is carried out under loading conditions known to correspond to disuse resorption (ε=500 $\mu\varepsilon$) and bone formation (ε=2500 $\mu\varepsilon$) from Carter *et al* (1984). It has been observed that the osteoclasts typically resorb bone at a rate of 1 μm/day (Eriksen and Kassem, 1992). The change in thickness Δy is thus assumed to be 1μm/day and according to equation 3.18 a new value for E_{i+1} can be calculated. The stimuli F_{strain} are calculated for each sensor element in the

model and then a value for C_1 can be estimated. This method is applied considering osteocytes and surface cells separately as the sensor cells and the following values are estimated

a. Surface sensors

$\varepsilon_j < 1000$ με $\quad C_1 = 3.87 \times 10^1$

2000 με $[\varepsilon_j \quad C_1 = 1.98 \times 10^2$

b. Osteocyte sensors

$\varepsilon_j < 1000$ με $\quad C_1 = 1.55 \times 10^1$

2000 με $[\ \varepsilon_j \quad C_1 = 4.54 \times 10^1$

To calculate C_2, an analysis is carried out under loading conditions that correspond to overuse resorption (ε=3400 $\mu\varepsilon$) and the following values are estimated

a. Surface sensors

$$C_2 = 7.21 \times 10^8$$

b. Osteocyte sensors

$$C_2 = 2.82 \times 10^8$$

3.7.2.3 Numerical formulation

In order to implement this theory, a number of material constants are assumed based on reported values from literature. These constants are listed in Table 3.1 below. It is important to note that the density of the material was calculated according to the relationship $E = C_e \rho^3$ (Currey *et al*, 1988). Elastic modulus for trabecular bone tissue from mechanical testing (results to be presented in chapter 4) was used to estimate the density of trabecular bone tissue.

Parameter	Value
Density ρ (g/cm^3)	0.67[a]
Temperature T (°C)	37
H	-7.789[b]
J	-0.0206[b]
K	2.364[b]
M	15.470[b]
C_e (MPa)	6000[c]
D (μm)	25[c]

[a] Calculated according to Currey *et al*, 1988

[b] Carter *et al* (1976), [c] Mullender *et al* (1997)

Table 3.1 *Assumed constants for numerical formulation.*

3.7.2.4 Calculation of material properties

Using the calculated elastic moduli from equation 3.20, the remaining material properties of a volume of tissue are calculated. Consider a volume of tissue of elastic modulus E_i and Poisson's ratio ν_i undergoing adaptation to have a new elastic modulus E_{i+1}, see Figure 3.17.

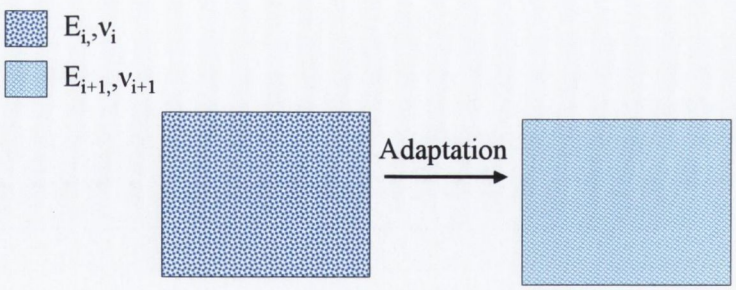

Figure 3.17: *Schematic of change in material properties during remodelling*

If it is assumed that the elastic modulus is proportional to the Poisson's ratio then

$$\left(\frac{E_{i+1}}{E_i}\right)=\left(\frac{\nu_{i+1}}{\nu_i}\right) \tag{3.26}$$

If this volume of tissue represented a single element in a finite element model of a bone trabeculum, the new Poisson's ratio of any element within a finite element model can be calculated as follows

$$\nu_{i+1} = \left(\frac{E_{i+1}}{E_i} \right) \times (\nu_i) \tag{3.27}$$

Similar equations are used to determine the permeability, porosity and compressive moduli.

3.7.2.5 Algorithm

A graphical summary of the final algorithm that was developed to include each of the aspects above is presented in Figure 3.18. It should be noted that the algorithm depicted in this figure is generic and each separate mechano-regulation rule (i-iv) is used to calculate the new material properties. A finite element mesh is first generated and used as an initial condition. The mechanical signal is calculated at each sensor location in the tissue by running a poroelastic structural finite element analysis. The overall stimulus received by each surface element is calculated from the sum of the products of the stimuli from each sensor cell and their influence function as described in equation 3.14. Based on the magnitudes of these stimuli, the change in density of the element is calculated and consequently a new elastic modulus is determined for each surface element within the model. Based on the volume fraction of the elastic modulus within any one element, the remaining material properties for the next iteration are determined. Any sensor element that undergoes resorption is deactivated from the sensory network and there also exists sensor elements within the marrow tissue that can be activated if formation occurs at this location. This algorithm is iterated until convergence is achieved.

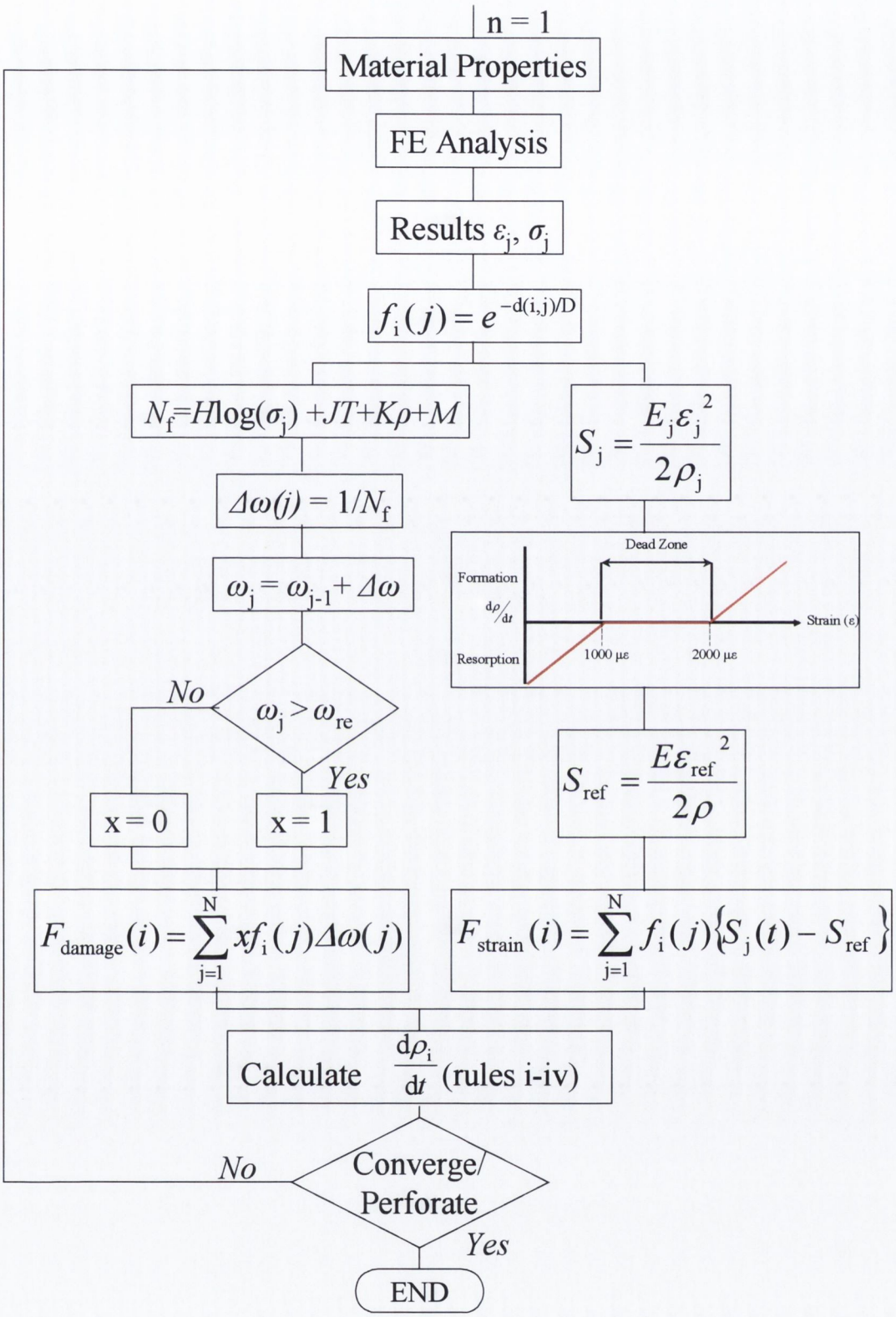

Figure 3.18: *Flow chart diagram of computational algorithm to model bone remodelling*

3.7.2.6 Application of algorithm to Finite element models

The finite element method is used to determine the mechanical stimuli local to an active resorption lacuna. A poroelastic analysis is carried out as *in vivo* bone is a porous material and it has been proposed that lacunar-canilicular porosity of bone has an important role in the mechano-regulation of bone remodelling. A poroelastic element is available within the commercial finite element package DIANA (TNO, Delft, The Netherlands), which can be used to solve the poroelastic equations for complex geometries and loadings. Constitutive equations similar to those developed by Biot are used to relate the stress to the strain.

i. Region of damage

A 2D finite element model of a bone trabeculum with a region of damaged tissue was developed. The mesh is generated using four-node quadrilateral isoparametric plane strain elements, see Figure 3.18. The trabecula was modelled as a 2D block of length 800 μm, and diameter 100 μm, and a region of damaged tissue was generated as indicated by the box in Figure 3.19.

ii. Existing resorption cavity

Using similar methods, a 2D finite element model of a bone trabecula with an active resorption lacuna was also developed, see Figure 3.20. A resorption cavity was introduced into the strut of varying depth, as described in section 3.7.3.1.

3.7.2.7 Application of algorithm to Finite element models

There are two different materials in both models; bone tissue or marrow, see Figure 3.19 and Figure 3.20. The material properties for the different tissue types used in this model are given in Table 3.2. Both tissues were modelled as poroelastic, compressible isotropic materials therefore six parameters are required to completely describe the mechanical behaviour - the Young's modulus, the permeability, the Poissons's ratio and the porosity, the solid bulk modulus, and the fluid bulk modulus. These values have been reported in the literature for the lacunar-canilicular porosity of bone (Cowin, 2002) and are used in this analysis. In this study, the differences for remodelling of normal and osteoporotic bone are investigated using the elastic moduli obtained from mechanical testing of normal and osteoporotic bone trabeculae, see section 3.7.3.4.

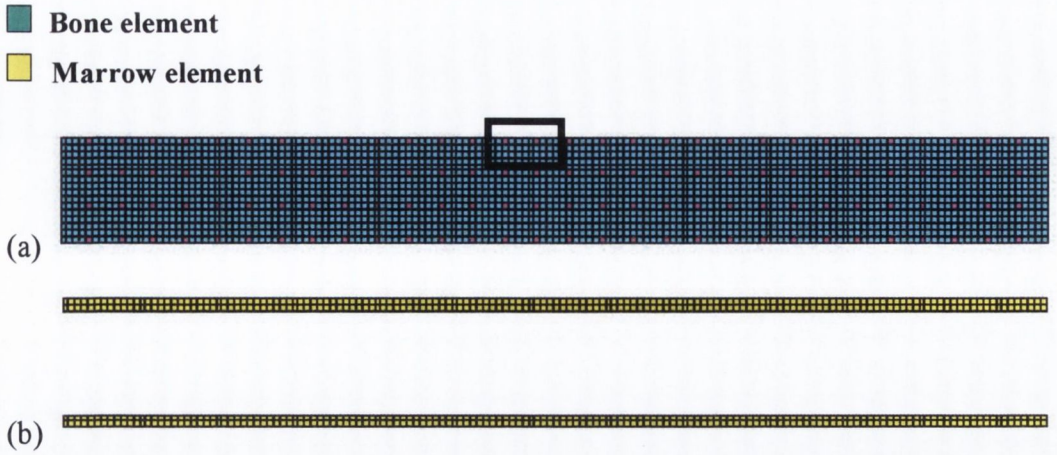

Figure 3.19: *Finite element model of bone trabeculum with damaged region showing (a) bone elements and (b) marrow elements. Elements in pink are the sensor cells that represent osteocytes in the model*

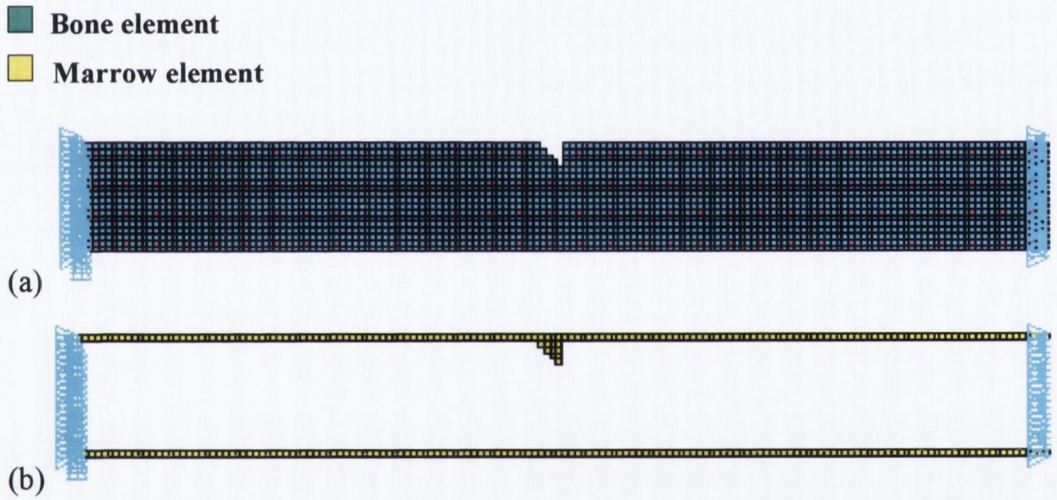

Figure 3.20: *Finite element model of bone trabeculum with resorption cavity showing (a) bone elements and (b) marrow elements. Elements in pink are the sensor cells that represent osteocytes in the model*

	Normal Bone	Osteoporotic Bone	Marrow
Young's modulus (MPa)	1800	4000	2
Poisson's ratio	0.3	0.3	0.167
Permeability (m^4/N.s)	1.47e-17	1.47e-17	1 e-14
Porosity	0.023	0.023	0.8
Solid bulk modulus (MPa)	1800	4000	2300
Fluid bulk modulus (MPa)	2300	2300	2300

Table 3.2 *Material properties of tissue.*

It has been observed that, *in vivo* trabeculae are aligned along stress trajectories and as such bear mainly compressive/ tensile loads. Therefore, in this model, nodes were constrained in the loading direction and a displacement was applied along the longitudinal direction to simulate this behaviour. An axial displacement of 1.2 μm was applied over 0.5 seconds. This value corresponds to a strain of 1500 με, which is within reported physiological loading ranges for homeostatic bone turnover. The pore fluid pressure was set to zero at the surface of the resorption cavity (Figure 3.20).

The outputs from this analysis, including strain and stress in each of the elements, are inputted into the algorithm. When a mechanical signal is detected according to the above criteria, a stimulus is emitted to initiate remodelling.

3.7.3 Parameter variation study

Parameter variation studies were carried out to analyse the effect of the assumed parameters in the model. A number of different mechano-regulatory rules were first compared (as described in section 3.7.1.3 above). The use of osteocytes and surface cells as sensors was also compared. The size of the cavity was varied to analyse the effect on the bone remodelling behaviour.

3.7.3.1 Effect of choice of mechano-sensor cells

To investigate whether the osteocyte sensors or surface cells were capable of more accurately simulating BMU, behaviour analyses were performed in which the mechano-sensor cells in the model were

(a) Surface elements

(b) Osteocyte representative elements

3.7.3.2 Depth of resorption cavity

To investigate whether there is a critical size of resorption cavity above which the proposed remodelling process is incapable of refilling, a parameter variation study was done on the size of the resorption cavity. The depth of the cavity was varied (10 μm, 15 μm, 25 μm, 70 μm) and the effects of the resorption cavity size were analyzed.

3.7.3.3 Normal remodelling vs. Osteoporotic Remodelling

To determine whether or not a change in the material behaviour during osteoporosis would lead to a difference in the remodelling behaviour of a bone trabecula, analyses were carried out using elastic moduli obtained from mechanical testing of single bone trabeculae from normal and osteoporotic bone.

3.8 Summary

To investigate the hypothesis that osteoporosis initiates with a pathological change in material properties that subsequently drives the adaptation of the trabecular architecture, a combination of (a) mechanical testing (b) finite element analyses and (c) computational simulations are employed.

Firstly, to ascertain whether in fact there exists a difference in the mechanical behaviour of bone tissue during osteoporosis, a method for mechanical testing of single bone trabeculae is developed. The method is used to determine the properties of trabecular bone tissue during osteoporosis and also to assess the efficacy of a drug treatment for osteoporosis at the level of the bone tissue.

To investigate the possibility that changes in material behaviour may subsequently drive the adaptation of trabecular architecture, it is first required to

develop an understanding of the mechanisms that drive normal bone remodelling Therefore, stress analyses of the mechanical environment local to resorption cavities are developed. Solid models of bone trabeculae with active resorption lacunae are developed using serial sectioning and imaging at micro-resolutions, and also micro-CT scanning. Using finite element analyses, the mechanical environment local to resorption cavities is analysed to investigate the possible mechanical stimuli that govern BMU activity at the trabecular level.

So as to further investigate the driving mechanisms for bone remodelling mechano-regulatory rules are developed to simulate the normal bone remodelling process. Four mechano-regulatory rules are developed to investigate the effects of encompassing both strain and damage as stimuli to initiate and drive bone multi-cellular units (BMUs). To test this theory, finite element models of a bone trabecula with a damaged region and an existing resorption cavity are created and these rules are applied to simulate the bone remodelling activity of a bone multi-cellular unit along the surface of a bone trabecula. The effects of the use of osteocyte sensors vs. surface sensors are analysed. The effect of varying the size of the cavity on the bone remodelling process in investigated. Accurate simulation of BMU activity under these different conditions would verify the mechano-regulation model proposed.

Finally, the developed mechano-regulation theory is applied in combination with material properties from mechanical testing of osteoporotic bone tissue and the effect on the remodelling activity of a BMU during osteoporosis is analysed. The results of each of these analyses are presented in chapter 4

4. Results

4.1 Introduction

The following chapter details the results obtained from each of the methods described in Chapter 3. These methods have been used to test the hypothesis that osteoporosis is a disease that originates with a pathological change in the material properties and that this change subsequently drives the adaptation of the trabecular architecture.

To test this hypothesis, the change in bone tissue material behaviour occurring during osteoporosis was determined. As part of this study tests were performed to assess whether a drug treatment for osteoporosis is capable of maintaining bone strength at the level of the bone tissue. In this chapter, the results of the tensile testing of single bone trabeculae from normal, osteoporotic and drug treated bone are compared over the course of 54 weeks treatment. The mechanical behaviour is reported in terms of yield strength, elastic modulus, yield strain and post-yield strain and graphs of each of these properties are presented in this chapter.

Finite element analyses of the bone trabeculae with resorption lacunae were performed to investigate whether a combination of local strain and damage within bone trabeculae may act as stimuli to initiate and drive bone multi-cellular units (BMUs) during normal bone remodelling. The distributions of stress and strain within trabecular volumes are presented along with contour plots of these stress and strain distributions.

In order to further investigate the stimuli for normal bone remodelling, a mechano-regulation rule for bone remodelling was developed. The results of four different stimuli considered for regulation of bone remodelling along a bone trabeculum are compared; (1) strain, (2) damage, (3) combined strain and damage and (4) a damage priority combined rule. The use of surface cells or osteocyte cells as sensors are also compared to investigate the regulatory mechanisms of BMU activity.

Finally, the results of the application of the developed mechano-regulation rule to material properties obtained from testing of osteoporotic bone trabeculae are presented and remodelling behaviour during osteoporosis is predicted.

4.2 Mechanical behaviour of bone tissue

In this section, the results from the tensile tests of single bone trabeculae described in Section 3.6 of the methods chapter will be presented. The material behaviour of single trabeculae from normal, osteoporotic and drug treated bone tissue after 0, 4, 14, 34, and 54 weeks will be compared. The mechanical behaviour will be compared in terms of yield strength, elastic modulus, yield strain and post-yield strain, see Fig. 3.13.

4.2.1 Yield strength

There was no significant change in the yield strength of control specimens over the course of ageing (ANOVA, p=0.35), see Table 4.1.

Ovariectomy caused a significant increase in the yield strength of bone tissue relative to the control over the course of 54 weeks (p=0.0003, ANOVA). Compared to the control, the yield strength of OVX bone tissue was significantly higher at 34 weeks [50.8 MPa ± 19.9 MPa vs. 23.2 MPa ± 16.9 MPa; p = 0.014] and also at 54 weeks [81.7 MPa ± 43.4 MPa vs. 34.1 MPa ± 15.9 MPa; p = 0.013], see Fig. 4.1.

The yield strength of OVX bone tissue was significantly higher than the drug-treated group at 14 weeks [51.1 MPa ± 25.0 MPa vs. 19.2 MPa ± 19.6 MPa; p = 0.008], at 34 weeks [50.8 MPa ± 19.9 MPa vs. 27.9 MPa ± 13.4 MPa; p = 0.005] and also at 54 weeks [81.7 MPa ± 43.4 MPa vs. 21.6 MPa ± 11.0 MPa; p = 0.004], see Fig. 4.1. The yield strength of the drug-treated tissue was lower than the control tissue after 14 weeks [19.2 MPa ± 19.6 MPa vs. 50.7 MPa ± 44.3 MPa; p = 0.062] and 54 weeks treatment [21.6 MPa ± 11.0 MPa vs. 34.1 MPa ± 15.9 MPa; p = 0.058] (Fig. 4.1).

	Time					*p*
Test Group	0 Weeks	4 Weeks	14 Weeks	34 weeks	54 weeks	value
Control	27.0 ± 15.	33.9 ± 23.3	50.7 ± 44.3	23.2 ± 16.9	34.1 ± 15.9	0.35
OVX	-	31.9 ± 21.0	51.1 ± 25.0	50.8 ± 19.9	81.7 ± 43.4	0.01
OVX; drug treated	-	33.3 ± 35.8	19.2 ± 19.6	27.9 ± 13.4	21.6 ± 11.1	0.29

Table 4.1. *Effect of Ageing on yield strength (MPa) of all groups (ANOVA)*

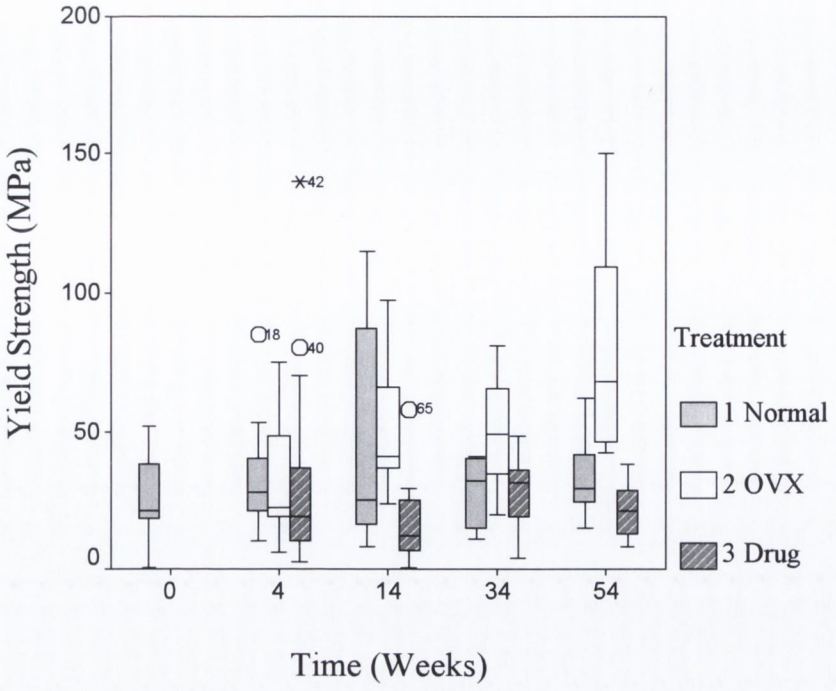

Figure 4.1: *Yield strength (MPa) of control, OVX and drug treated bone tissue over the course of ageing*

Note: Data is presented using box plot format. The box stretches from the 25th percentile to the 75th percentile of the data and therefore contains the middle half of the data in the distribution. The median is shown as a line across the box. The lines from the box stretch from 1.5 times the box length. Outliars (O) are by extreme values (*) are indicated

4.2.2 Elastic Modulus

There was no significant difference found between the elastic moduli of control specimens between 0, 4, 14, 34 and 54 weeks (ANOVA, p = 0.98), see Table 4.2. No significant difference was found between the elastic moduli of control specimen at 0 weeks and the OVX specimens at 4, 14, 34 and 54 weeks (p = 0.46).

	Time					*p*
Test Group	0 Weeks	4 Weeks	14 Weeks	34 weeks	54 weeks	value
Control	2.65 ± 1.94	2.31 ± 1.24	2.43 ± 1.62	2.61 ± 0.79	2.81 ± 2.09	0.98
OVX	-	3.11 ± 2.13	5.11 ± 3.89	3.77 ± 1.86	4.23 ± 2.86	0.46
OVX; drug treated	-	2.59 ± 2.23	1.72 ± 1.23	2.59 ± 1.53	1.98 ± 1.68	0.09

Table 4.2. *Effect of Ageing on elastic modulus (GPa) of all groups (ANOVA)*

However, the stiffness of OVX tissue was higher than the control bone tissue at 14 weeks (5.11 GPa ± 3.89 GPa vs. 2.43 GPa ± 1.62 GPa; $p = 0.05$) and 34 weeks (3.77 GPa ± 1.86 GPa vs. 2.61 GPa ± 0.79 GPa; $p = 0.05$). The elastic modulus of OVX was higher than the drug-treated bone tissue at 14 weeks (5.11 GPa ± 3.89 GPa. vs. 1.72 GPa ± 1.23 GPa; $p = 0.02$) and at 54 weeks treatment (4.23 GPa ± 2.86 GPa vs. 1.98 GPa ± 1.69 GPa; $p = 0.05$); this result indicates that the drug treatment reduces the bone tissue stiffness relative to osteoporotic bone tissue, see Table 4.2. There was no difference found between the stiffness of the control and drug-treated bone tissue over the course of 54 weeks.

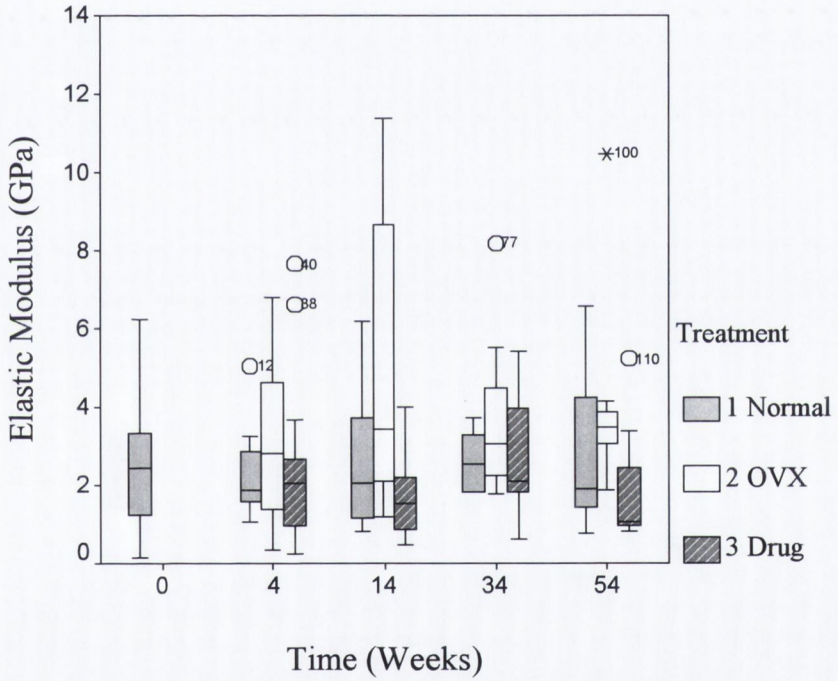

Figure 4.2: *Elastic moduli of normal, ovariectomized and drug treated bone tissue over the course of ageing*

4.2.3 Cross sectional area at point of fracture

There was no significant difference found between the cross sectional area at the point of fracture of control specimens between 0, 4, 14, 34 and 54 weeks (ANOVA, $p = 0.91$), see Table 4.3. At 34 weeks treatment the control group were significantly smaller than both the OVX ($p = 0.008$) and the drug treated ($p = 0.01$), however no difference was found between the OVX and the drug treated trabecular cross sections.

Test Group	Time					*p* value
	0 Weeks	4 Weeks	14 Weeks	34 weeks	54 weeks	
Control	0.012 ± 0.019	0.010 ± 0.005	0.012 ± 0.011	0.006 ± 0.002	0.010 ± 0.006	0.91
OVX	-	0.012 ± 0.015	0.009 ± 0.008	0.010 ± 0.005	0.011 ± 0.008	0.98
OVX; drug treated	-	0.007 ± 0.004	0.014 ± 0.012	0.010 ± 0.005	0.016 ± 0.012	0.43

Table 4.3. *Effect of Ageing on Cross Sectional Area (mm^2) of all groups (ANOVA)*

4.2.4 Yield Strain

There was no significant difference between the yield strain of control specimens from 0, 4, 14, 34 and 54 weeks (ANOVA, p=0.29), see Table 4.4. The yield strain of the OVX bone tissue was significantly higher than the control bone tissue at 34 weeks (1.80 % ± 0.84 % vs. 1.17 % ± 0.25 %; p = 0.023) and at 54 weeks (2.45 % ± 1.89 % vs. 1.55 % ± 1.05 %; p = 0.047). There was a significant difference found between the yield strain of the OVX and drug-treated bone tissue at 54 weeks (2.45 % ± 1.89 %; vs. 1.48 % ± 0.83 %; p = 0.02), see Fig. 4.3. There was no significant difference found between the yield strain of the control and the drug-treated bone tissue over the course of 54 weeks.

Test Group	Time					*p* value
	0 Weeks	4 Weeks	14 Weeks	34 weeks	54 weeks	
Control	1.34 ± 1.04	0.96 ± 0.31	1.86 ± 0.95	1.17 ± 0.25	1.55 ± 1.05	0.29
OVX	-	1.90 ± 1.90	1.23 ± 0.55	1.80 ± 0.84	2.45 ± 1.89	0.23
OVX; drug treated	-	1.29 ± 0.77	1.14 ± 0.77	1.29 ± 0.70	1.48 ± 0.83	0.92

Table 4.4. Effect of Ageing on Yield Strain (%) of all groups (ANOVA)

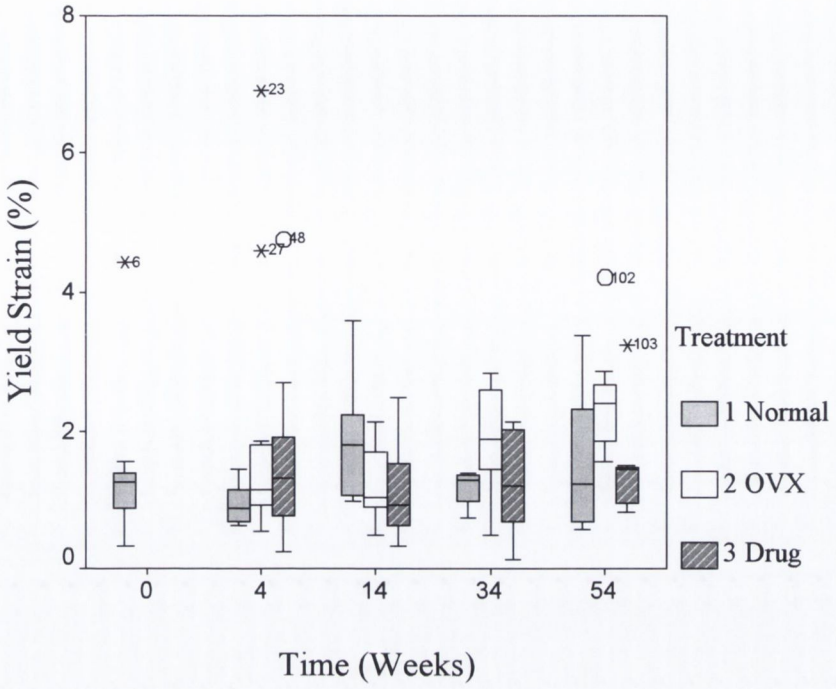

Figure 4.3: *Yield Strain (%) of normal, ovariectomized and drug treated bone tissue over the course of ageing*

4.2.5 Post-yield strain

There was no significant difference found in the post-yield strain to failure of the trabeculae from the different groups, see Fig. 4.4. No significant difference was found between any of the groups at any time point.

	Time					*p*
Test Group	0 Weeks	4 Weeks	14 Weeks	34 weeks	54 weeks	value
Control	5.76 ± 6.99	5.17 ± 5.38	4.88 ± 5.71	4.89 ± 7.17	4.06 ± 5.17	0.98
OVX	-	5.71 ± 6.16	6.70 ± 7.50	4.66 ± 648	2.55 ± 1.79	0.10
OVX; drug treated	-	6.17 ± 8.59	2.94 ± 4.42	3.82 ± 4.89	4.19 ± 8.78	0.58

Table 4.5. Effect of Ageing on Post-Yield Strain (%) of all groups (ANOVA)

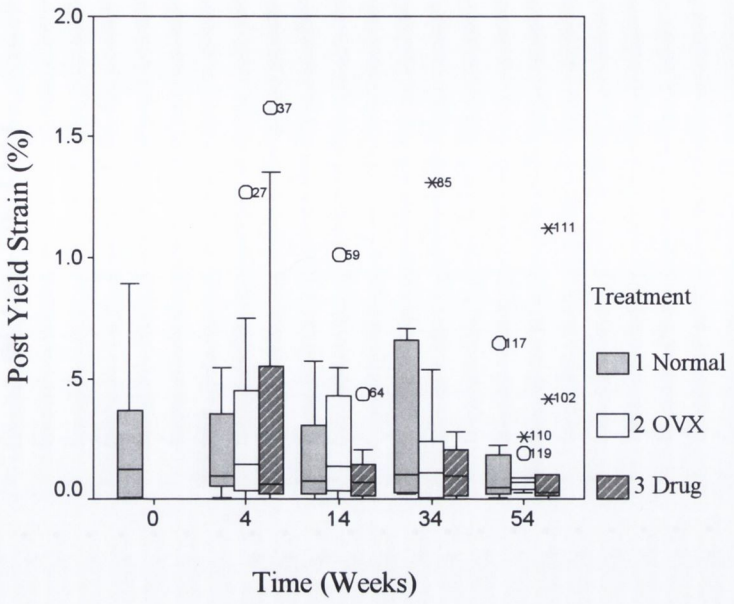

Figure 4.4: *Post-yield Strain (%) of normal, ovariectomized and drug treated bone tissue over the course of ageing*

A comparison of the yield strength and elastic modulus of normal, osteoporotic and drug-treated bone tissue at each time point is detailed in Table 4.6 below.

	Treatment		p	Treatment		p	Treatment		p
Test Group	Control	OVX	value	OVX	Drug-treated	value	Control	Drug-treated	value
4 Weeks									
Yield Strength (MPa)	33.9 ± 23.3	31.9 ± 21.0	0.42	31.9 ± 21.0	33.3 ± 35.8	0.45	33.9 ± 23.3	33.3 ± 35.8	0.45
Elastic Modulus (GPa)	2.31 ± 1.24	3.11 ± 2.13	0.15	3.11 ± 2.13	2.44 ± 2.15	0.21	2.31 ± 1.24	2.44 ± 2.15	0.43
14 Weeks									
Yield Strength (MPa)	50.7 ± 44.3	51.1 ± 25.0	0.49	51.1 ± 25.0	19.2 ± 19.6	0.008	50.7 ± 44.3	19.2 ± 19.6	0.06
Elastic Modulus (GPa)	2.43 ± 1.62	5.11 ± 3.89	0.05	5.11 ± 3.89	1.72 ± 1.23	0.02	2.67 ± 2.05	1.72 ± 1.23	0.16
34 Weeks									
Yield Strength (MPa)	23.2 ± 16.9	50.8 ± 19.9	0.01	50.8 ± 19.9	27.9 ± 13.4	0.005	23.2 ± 16.9	27.9 ± 13.4	0.49
Elastic Modulus (GPa)	2.61 ± 0.79	3.77 ± 1.86	0.05	3.77 ± 1.86	2.59 ± 1.53	0.09	2.61 ± 0.79	2.59 ± 1.53	0.48
54 Weeks									
Yield Strength (MPa)	34.1 ± 15.9	81.7 ± 43.4	0.03	81.7 ± 43.4	21.6 ± 11.1	0.004	34.1 ± 15.9	21.6 ± 11.1	0.06
Elastic Modulus (GPa)	2.81 ± 2.09	4.23 ± 2.86	0.18	4.23 ± 2.86	1.98 ± 1.69	0.05	2.81 ± 2.09	1.98 ± 1.69	0.20

Table 4.6: Effect of Ovariectomy and Drug Treatment. Statistically significant differences are indicated in red

4.3 Mechanical stimuli local to resorption lacunae

The images obtained from serial sectioning and micro-CT scanning, as described in section 3.3, were obtained at a resolution that was adequate for identifying the micro-structural geometry of trabeculae. Geometrical features such as resorption cavities (Fig. 4.5) and side branching were observed in the cross-sectional images of some of the trabeculae.

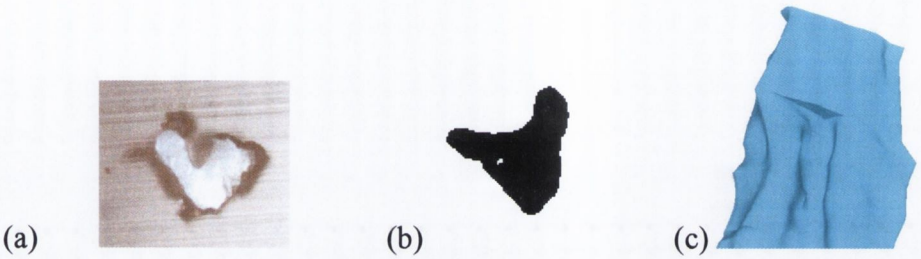

Figure 4.5: *Image of a trabecular cross section with resorption lacuna obtained from (a) serial sectioning and (b) micro-CT scanning (c) solid model of resorption lacuna (from trabecula 4 below)*

4.3.1 Stress distribution in the neighbourhood of resorption cavities

Using the finite element method, it was possible to analyse the distribution of mechanical stimuli in bone trabeculae with and without resorption lacunae. Stress analyses revealed that the distributions of maximum principal stress observed in single bone trabeculae were non-uniform (Fig.4.6). While a large percentage of volume of bone tissue experiences stresses below 10 MPa, there exist regions of tissue that experience very high stresses (Fig. 4.6).

Contour plots of the maximum principal stress demonstrate the mechanical signals within individual trabeculae and the elevation in the stress levels along the cross section of the trabecula (Fig. 4.8). Active resorption lacunae were identified in trabeculae 1,2 and 4, as can be seen in the cross sectional images shown in Fig 4.8 (a) at section 7, Fig 4.8 (c) at section 13 and Fig 4.8 (d) at section 4. The peak stresses observed in trabeculae with active resorption lacunae were 93.4 MPa, 123.1 MPa, and 148.4 MPa, as compared to 72.9 MPa in the trabecula with no resorption lacunae identified (Table 4.7).

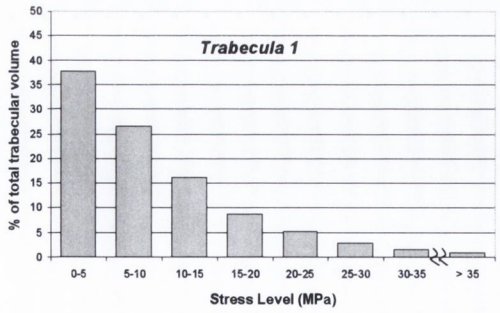

(a)

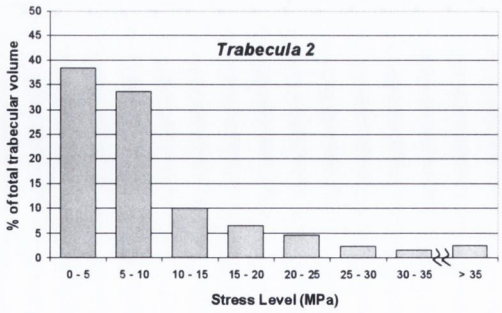

(b)

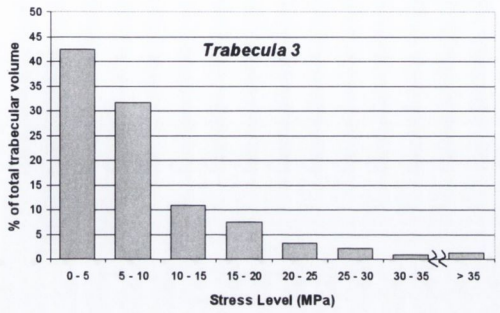

(c)

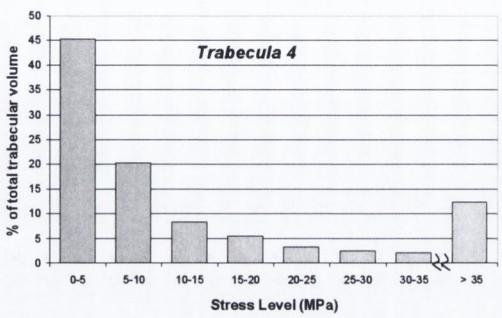

(d)

Figure 4.6: *The maximum principal stress distributions in rat trabeculae. In trabeculae 1, 3, and 4 resorption lacunae were identified*

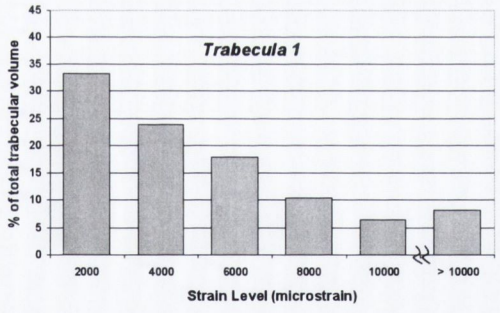

(a)

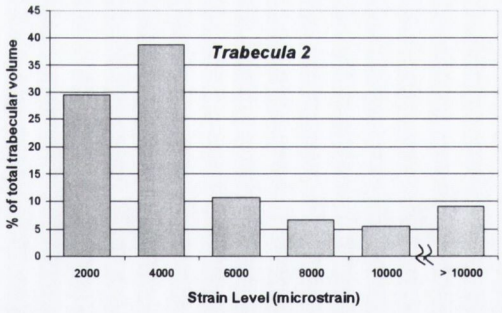

(b)

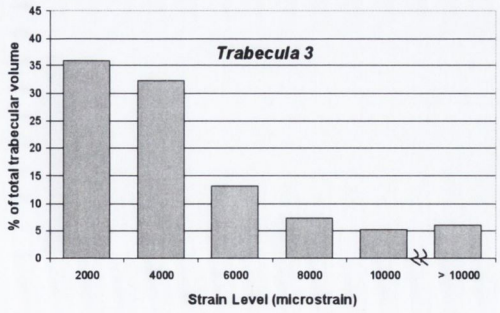

(c)

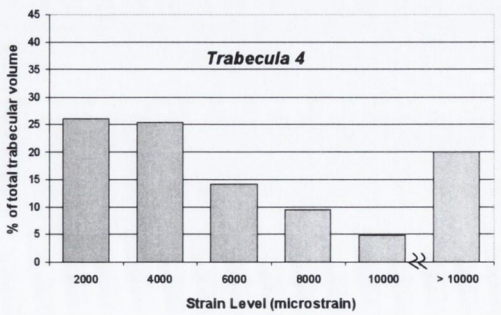

(d)

Figure 4.7: *The maximum principal strain distributions in rat trabeculae. In trabeculae 1, 3, and 4 resorption lacunae were identified*

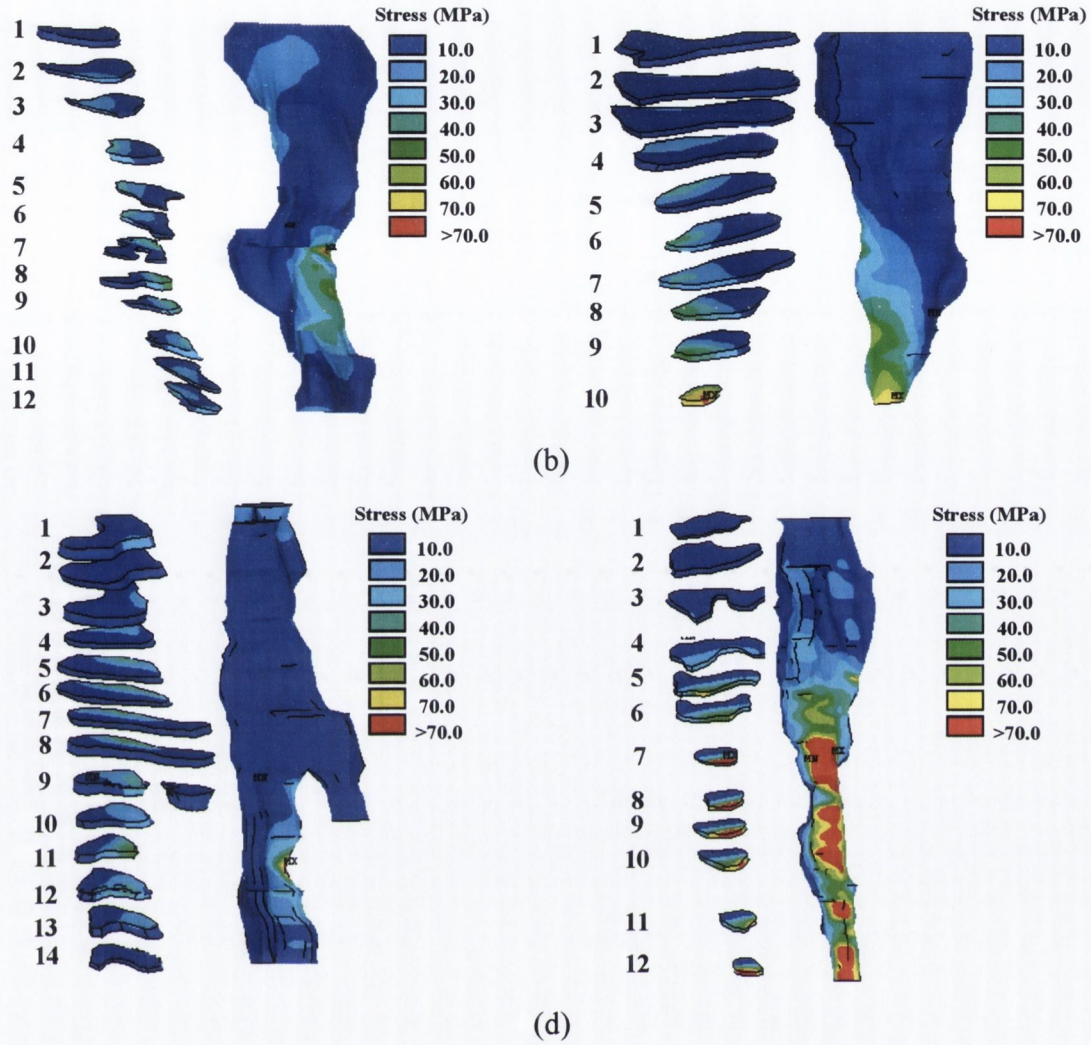

Figure 4.8: *Contour plot of maximum principal stress distribution in (a) trabecula 1, (b) trabecula 2, (c) trabecula 3, (d) trabecula 4*

4.3.2 Strain distribution in the neighbourhood of resorption cavities

While a large percentage of volume of bone tissue experiences strains within the range considered to be physiological (< 4000 με), there exist regions of tissue that experience very high strains (Fig. 4.7).

The peak strains observed in trabeculae with active resorption lacunae were 40,685 με, 53,573 με and 64,179 με, as compared to 31,385 με in the trabecula with no resorption lacunae identified (Table 4.7). The peak strains were mainly located ahead of the resorption cavity in the direction of loading (Fig. 4.9 (a) section 9; Fig. 4.9 (c) section 11; Fig. 4.9 (d) section 6). Elevated strain levels were also observed at the base of the resorption cavity (Fig. 4.9 (a) section 7; Fig. 4.9 (c) section 12; Fig. 4.9 (d) section 4).

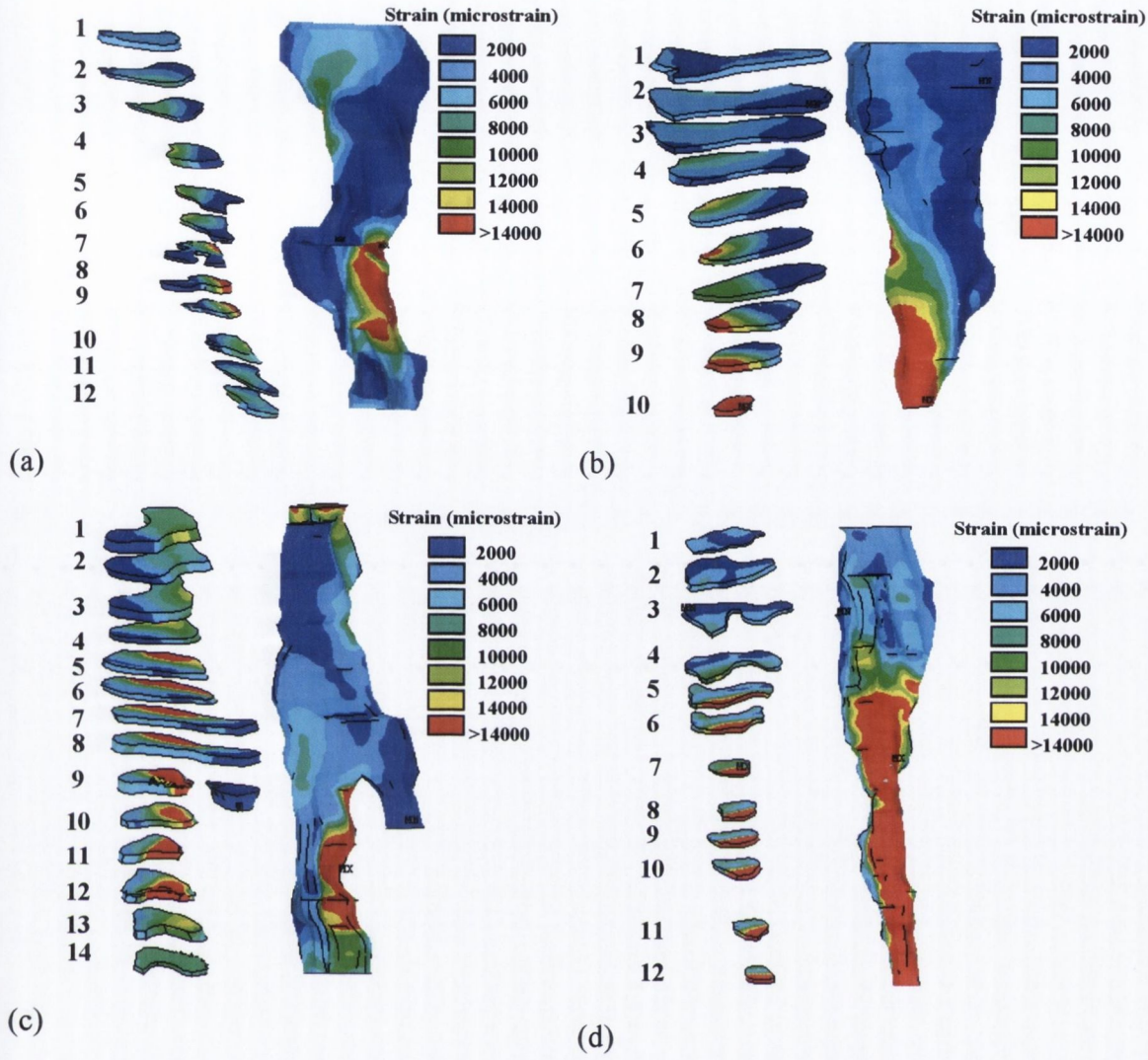

Figure 4.9: *Contour plot of Maximum Principal Strain distribution in (a) Trabecula 1, (b) Trabecula 2, (c) Trabecula 3, (d) Trabecula 4*

It the idealised model representing that of Smit and Burger (2000), the maximum principal stress across the volume was non-uniform (Fig.4.10). The majority (98.7%) of the volume experienced stresses below 10 MPa but there existed regions of elevated stress, not exceeding 16 MPa, within the tissue (Fig. 4.10).

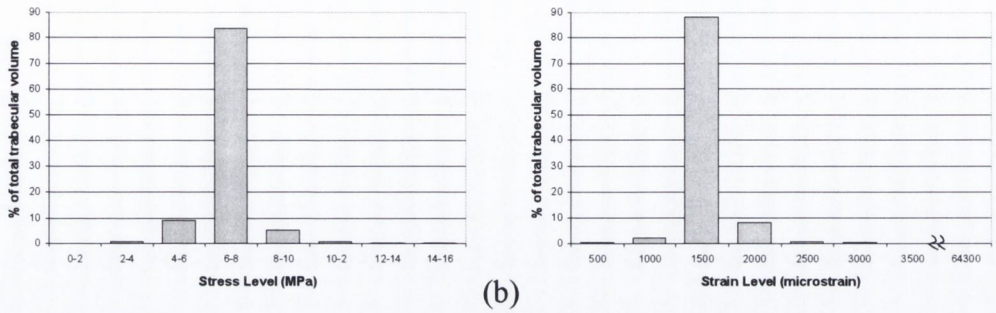

Figure 4.10: **(a)** *The maximum principal stress and (b) maximum principal strain distributions in Smit and Burger model (2000)*

It is interesting to note that in the idealised model representing that of Smit and Burger (2000), the maximum stress observed in the trabecula was 15.8 MPa and the maximum strain was 3072 με, which are approximately 90% lower than the values observed in the models that represented the proper anatomical geometry of bone trabeculae, see Fig. 4.11. For ease of comparison the results of each of the analyses are summarised in Table 4.7 below.

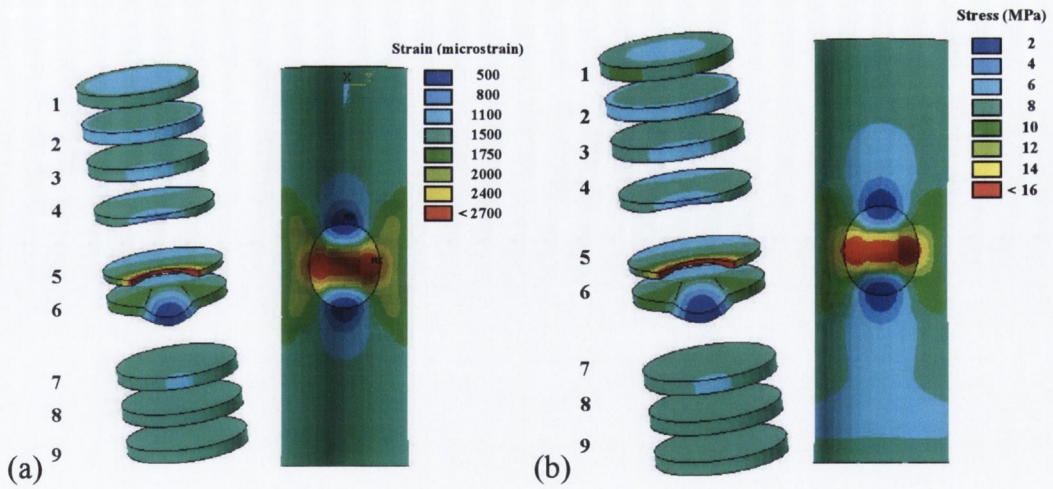

Figure 4.11: *Contour plot of (a) Maximum Principal Strain and (b) Maximum Principal Stress distribution in idealised model of Smit and Burger (2000)*

Model	Trabecula 1	Trabecula 2	Trabecula 3	Trabecula 4	Idealised*
Resorption lacuna	Yes	No	Yes	Yes	Yes
Calculated Load (N)	0.099	0.080	0.011	0.013	0.205
Average CSA (mm^2)	0.0151	0.0121	0.0017	0.0021	0.031
Mean Stress (MPa)	10.4	10.8	8.6	10.8	6.9
Maximum Stress (MPa)	93.4	72.9	123.1	148.4	15.8
Volume < 10MPa	62.6%	72.2%	73.9%	65.6%	98.7%
Volume > 30 MPa	2.4%	4.3%	2.1%	14.6%	-
Mean Strain (με)	4,906.0	5,158.2	4042.0	6054.9	1,366
Maximum Strain (με)	40,685	31,385	53,573	64,179	3,072
Volume < 4000 με	57.1%	68.4%	68.2%	51.2%	100%
Volume > 16000 με	4.3%	5.7%	3.3%	16.6%	-

* recreated according to Smit and Burger (2000)

Table 4.7: *Comparison of mean, maximum and distribution of principal stress and strain within the tissue volume of the trabecular specimens and an idealised trabecular geometry. The loading is generated by prescribing a force to generate an apparent strain of 3000 με.*

4.4 Mechano-regulation of bone turnover

As described in section 3.7.1.3, a rule for mechano-regulation is considered based on the following:

i. Strain,

ii. Damage,

iii. Combined strain and microdamage,

iv. *Either* strain or damage, where removal of microdamage is prioritised over strain.

In each case, results with either osteocytes or bone lining cells as mechano-sensor cells are given. Each of the stimuli is compared according to its ability to respond to a region of damaged tissue in the bone and also in its regulation of an existing 20 μm resorption cavity.

The mechanical stimuli in a bone trabecula with a damaged region of tissue and an existing 20 μm resorption cavity will first be presented. In each case, the figures of the predicted patterns of bone remodelling along a trabecular surface are given. In these figures the strain in elements that are either partially bone or fully bone in composition are plotted at specific time points/iterations of interest during the simulation. The results of each of the above stimuli (i–iv) are then compared by analysing the percentage volume of tissue maintained at homeostatic strain and damage levels. The distributions of two mechanical stimuli (i.e. strain and damage) are presented at specific time points during the simulation.

The following criteria are used to assess the efficiency of each mechano-regulation rule for simulating bone remodelling by considering the patterns of bone remodelling, and the plots of the damage generation and strain levels during the simulation.

i. Initiation of a resorption cavity in response to a region of damaged tissue

ii. Refilling of resorption cavity by new bone tissue,

iii. Removal of accumulating micro-damage in order to maintain microdamage burden below homeostatic levels,

iv. Attaining or maintaining homeostatic strain levels (1500 με).

4.4.1 Mechanical stimuli in bone trabecula with damaged region (Iteration 1)

It should be first noted that damaged was not explicitly modelled in this model. Damage values were assigned to the elements indicated in the region of the box shown in Fig. 3.19; 0.66% of the volume was damaged above critical due to this introduction of damage. The critical damage was calculated at a stress corresponding to 3300 με. The results presented here are thus analogous to an idealised trabecular structure. After the first iteration, the distribution of stress is homogeneous with a mean stress of 2.25 MPa and the maximum stress is 4.78 MPa. The mean strain is 1442 με, and the maximum strain is 4013 με. The distribution of strain was homogeneous with 1% of the volume of bone tissue strained above 2000 με (formation) and 1% is below 1000 με (resorption). The maximum fluid flow was 2.74 nm/sec.

4.4.2 Mechanical stimuli local to 20 μm resorption cavity (Iteration 1)

After the first iteration the mean stress is 2.22 MPa and the maximum stress is 7.27 MPa. The mean strain is 1,538 με, and the maximum strain is 22,830 με, see Fig. 4.12. The distribution of stress is inhomogeneous and 0.03% of the volume is damaged above critical under applied loading conditions. The distribution of strain was inhomogeneous with 4.6% of the volume of bone tissue strained above 2000 με (formation) and 1.6% is below 1000 με (resorption), see Fig. 4.13. The maximum fluid flow was 8.42 nm/sec, see Fig. 4.14.

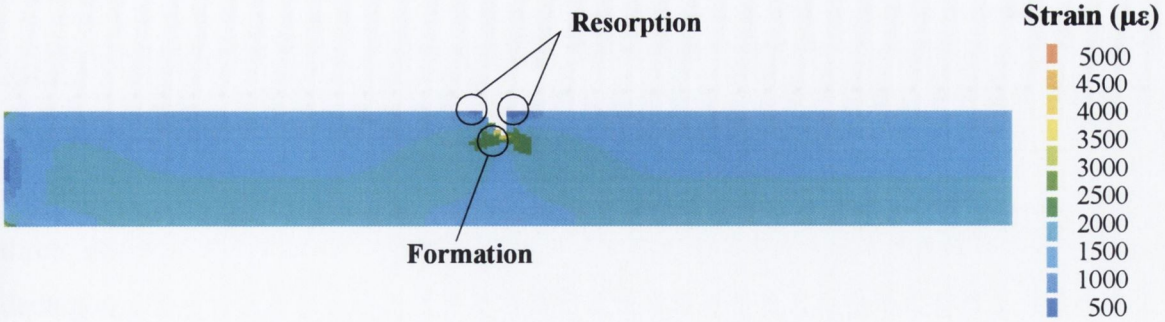

Figure 4.12: *Distribution of strain local to 20 μm resorption cavity*

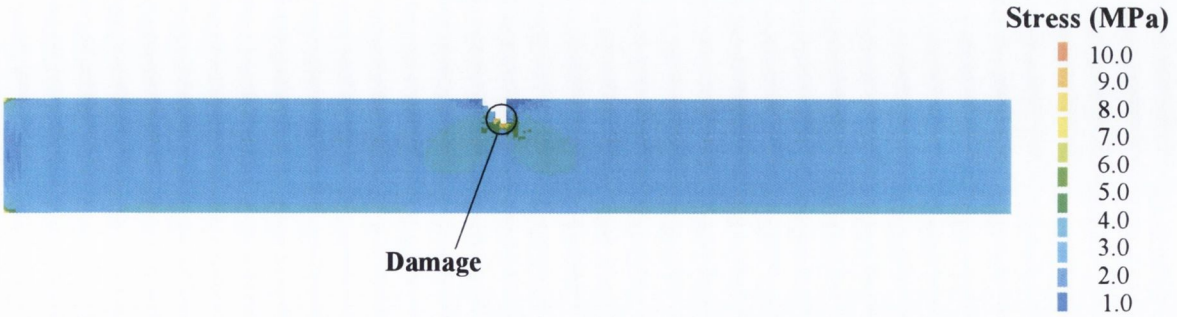

Figure 4.13: *Distribution of stress local to 20 μm resorption cavity*

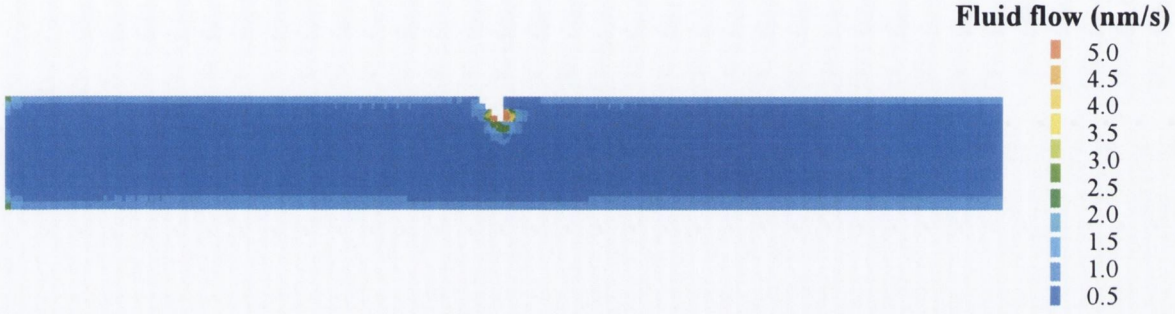

Figure 4.14: *Distribution of fluid-flow local to 20 μm resorption cavity*

4.4.3 Regulation with surface sensors

In this section, the results of the surface sensor appraisal in combination with each of the mechano-regulatory rules (i-iv) are presented. The predictive quality of each model is assessed according to its ability to respond to a damaged region of tissue, refill an existing resorption cavity, and attain/maintain strain and damage levels at homeostatic levels.

4.4.3.1 Response to damaged region of tissue

The results of the predicted patterns of the three different damage responsive mechano-regulatory rules are presented in Fig. 4.15. It is seen by comparison that all three of the mechano-regulatory rules are capable of responding to a region of damaged tissue by initiating a resorption cavity. The strain only regulation model is unresponsive to regions of damaged tissue and therefore is not included in the results of this section.

i. The damage-regulation model (i) forms a cavity that it is incapable of being refilled. As the model iterates, this eventually results in accumulation of microdamage below the cavity causing trabecular perforation, see Fig. 4.15(i). While

it reduces the percentage of damage that is above the critical value to zero after 4 iterations, the resorbed tissue is not refilled and damage accumulates under the applied load, see Fig. 4.16. The strain levels deviate from homeostatic levels and after 30 iterations the percentage volume of bone tissue below homeostatic levels (< 1000 με) is 34.9% and that above homeostatic levels is 6.53%, see Figs.4.17 and 4.18.

iii. In contrast, for mechano-regulation using a combined stimulus (iii) according to equation 3.17, while a resorption cavity is indeed initiated, the model is incapable of completely resorbing the region of damaged tissue, and refilling of the cavity is not achieved, see Fig 4.15(iii). This rule is not capable of reducing the percentage of damaged tissue below critical levels, see Fig. 4.16. However, the strain levels are maintained closer to homeostatic levels with a smaller percentage being in the resorption (Fig. 4.17) and formation regions (Fig. 4.18).

iv. Mechano-regulation where the stimulus is *either* strain or microdamage (iv), according to equation 3.18, is capable of completely resorbing the region of bone tissue and then refilling the resorbed cavity with new bone tissue, see Fig. 4.15(iv). This model reduces the percentage volume of tissue that is damaged above the critical value to 0.12% after 5 iterations, see Fig. 4.16. While the strain levels deviate from homeostatic levels throughout the resorptive phase of the simulation, the model is capable of restoring the strain levels to homeostatic levels, see Figs. 4.17 and 4.18.

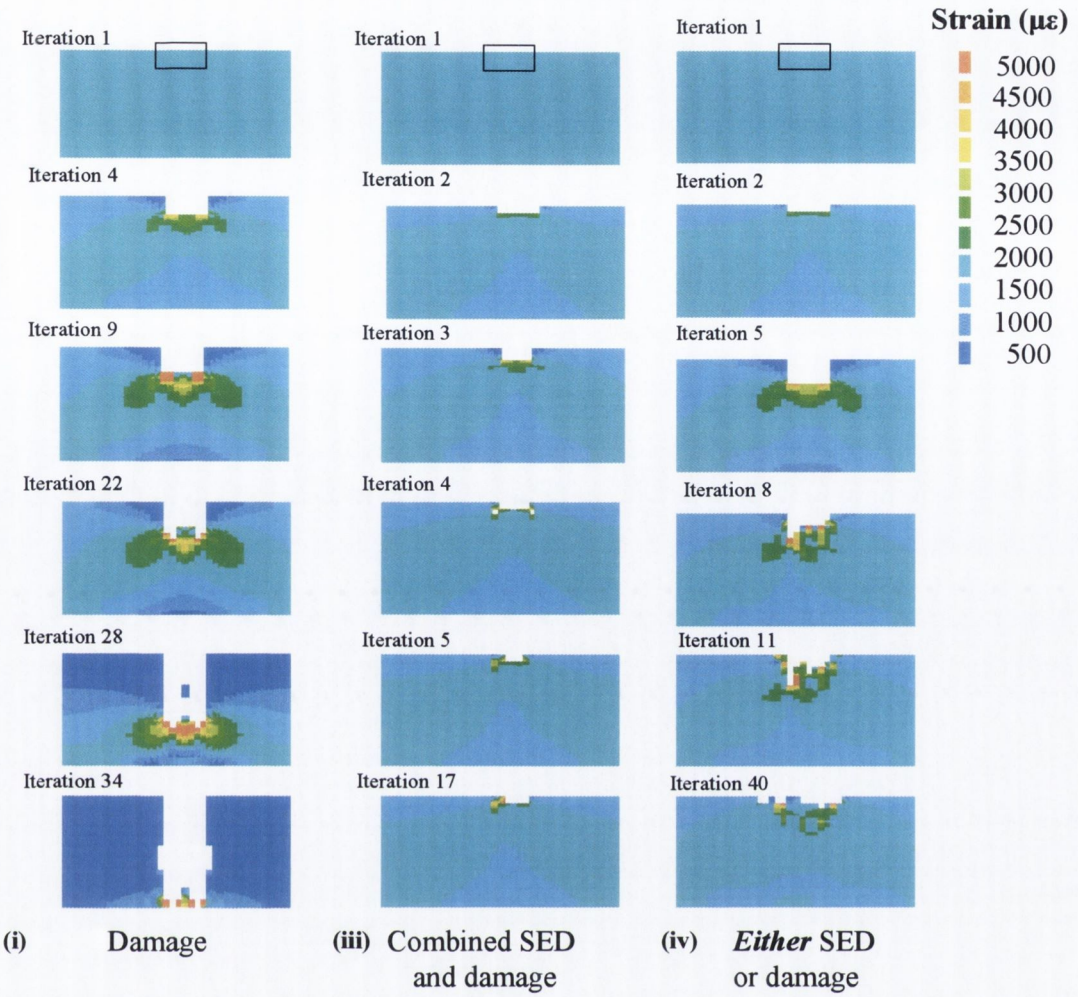

Figure 4.15 *Response of different mechano-regulation rules considered to region of damaged tissue (i) If the stimulus is damage, then bone resorption is predicted forming a cavity which cannot be refilled and leads to trabecular perforation (iii) If the stimulus is a combination of strain and microdamage (Eq. 3.17), then bone resorption is predicted and forming a cavity but the region of damaged tissue is not completely resorbed before refilling is initiated (iv) If the stimulus is* ***either*** *strain or damage (Eq. 3.18: removal of microdamage is prioritised over strain), then complete resorption of the damaged region of bone tissue is predicted followed by refilling of the cavity with new bone tissue*

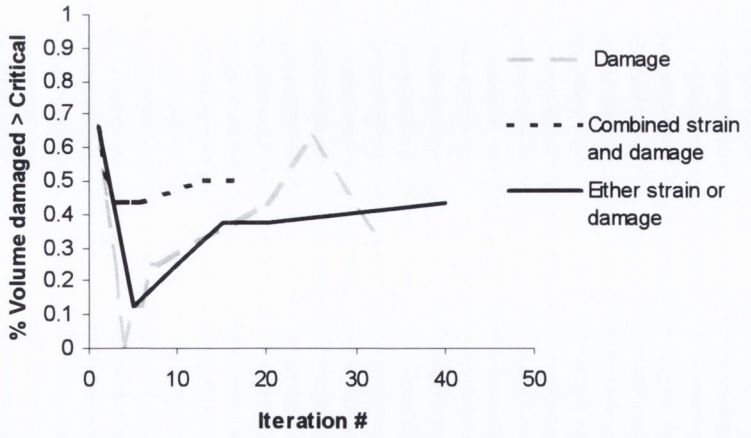

Figure 4.16 *Comparison of % tissue damaged above critical value over the course of the simulation regulated with surface sensors*

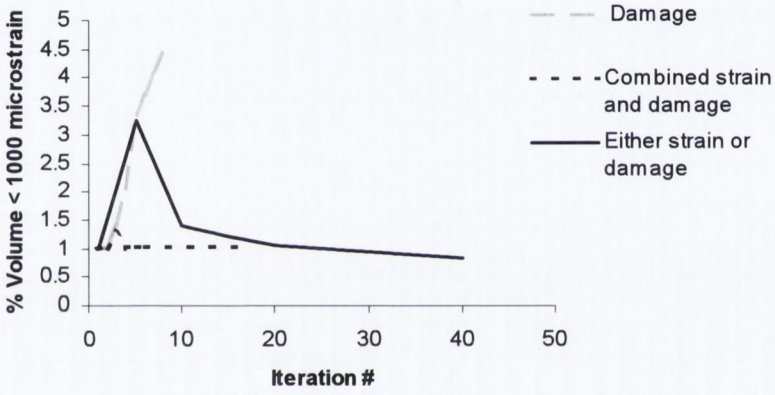

Figure 4.17 *Comparison of % tissue in resorption region (< 1000 με) over the course of the simulation regulated with surface sensors*

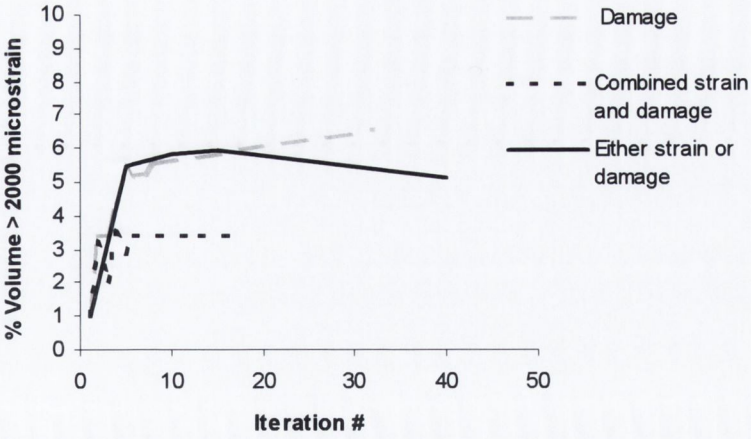

Figure 4.18 *Comparison of % tissue in formation region (> 2000 με) over the course of the simulation regulated with surface sensors*

4.4.3.2 Response to existing resorption cavity

i. The predicted pattern of bone adaptation for damage only regulated remodelling is presented, see Fig. 4.19(i). Complete perforation of the trabecular strut occurs after 23 iterations. After 20 iterations the mean stress was 1.74 MPa, the maximum stress was 19.7 MPa. The distribution of stress was inhomogeneous with 0.3% of the volume being damaged above critical after 23 iterations. The distribution of strain is inhomogeneous after 20 iterations with 7.4% of the volume of bone tissue strained above 2000 με and 40.6% below 1000 με, see Figs. 4.21 and 4.22.

ii. The predicted pattern of bone adaptation for a strain only regulated remodelling is presented in Fig. 4.19(ii). While the cavity was refilled to a depth of 5 μm after 5 iterations, complete refilling of the resorption cavity along the trabecular strut was not achieved after 50 iterations, see Fig. 4.20. The mean stress was 2.11 MPa, the maximum stress is 10.2 MPa, and the amount of damage did not change appreciably over the course of 50 iterations (Fig. 4.20) with 0.03% damaged above critical after 50 iterations. After 50 iterations, 5.15% of the volume of bone tissue is strained above 2000 με and 4.91% is below 1000 με, see Figs. 4.21 and 4.22.

iii. The predicted pattern of bone adaptation for combined strain and damage remodelling regulated according to equation 3.17 is presented, see Fig. 4.19 (iii). While refilling of the cavity to a 5-μm depth occurred after 5 iterations, complete refilling of the trabecular strut was not achieved after 30 iterations. The stress-volume and damage-volume distributions are inhomogeneous with 0.09% of the volume being damaged above critical after 50 iterations, see Figure 4.20. The mean stress is 2.2 MPa, the maximum stress is 4.79 MPa and 2.65 % of the volume of bone tissue is strained above 2000 με after 50 iterations and 1.02% is below 1000 με, see Figs. 4.21 and 4.22.

iv. The predicted pattern of bone adaptation for a damage priority regulated remodelling according to equation 3.18 is presented in Fig. 4.19 (iv). Refilling of the resorption cavity along the trabecular strut occurs after 50 iterations. The mean stress is 2.24 MPa, the maximum stress is 4.7 MPa and 0.03% of the volume was damaged above critical after 50 iterations, see Figure 4.20. The distribution of strain was inhomogeneous after 50 iterations and 4.12% of the volume of bone tissue was strained above 2000 με and 0.87% is below 1000 με, see Fig's 4.21 and 4.22.

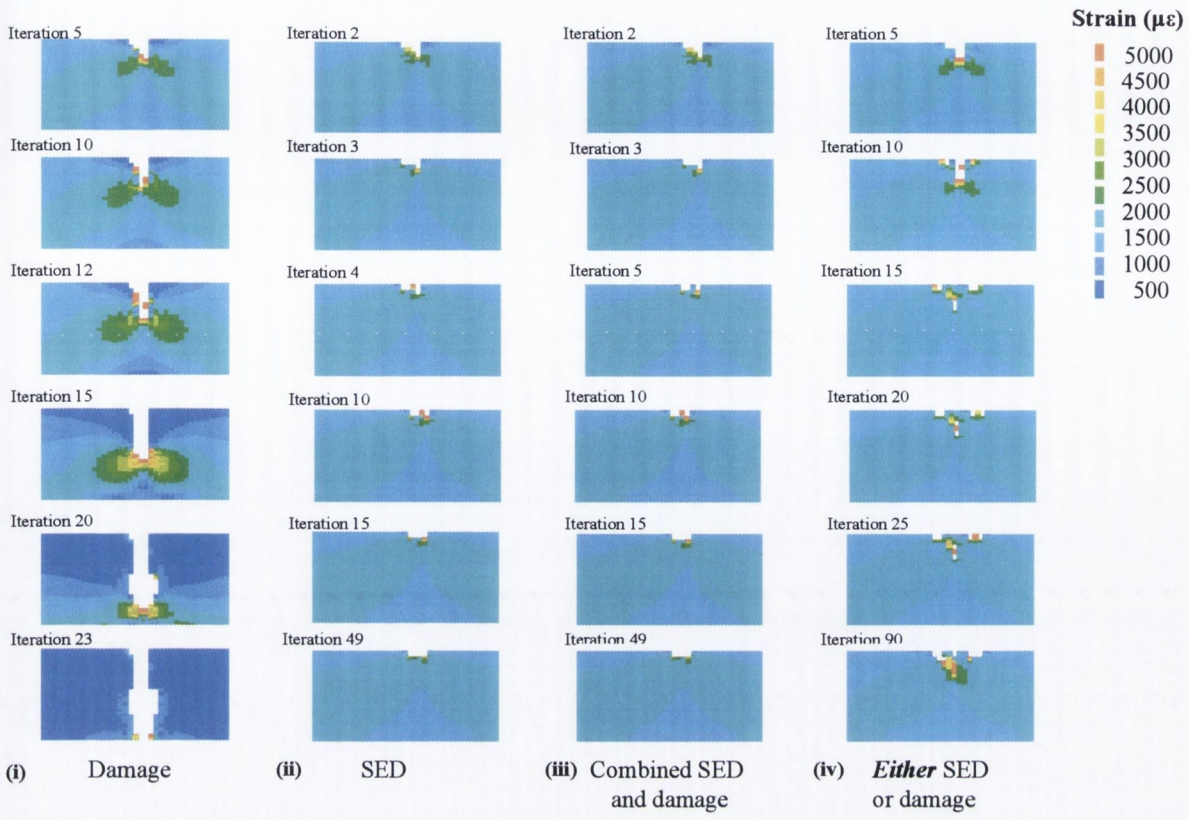

Figure 4.19 *Response of each mechano-regulation rule considered to 20 μm cavity (i) If the stimulus is damage, then bone resorption is predicted leading to complete trabecular perforation (ii) If the stimulus is strain (SED), then refilling of the cavity is predicted to a depth of 5 μm (iii) If the stimulus is a combination of strain (SED) and microdamage (Eq. 3.17), then refilling of the cavity is predicted to a depth of 5 μm (iv) If the stimulus is* ***either*** *strain or damage (Eq. 3.18: removal of microdamage is prioritised over strain), then complete refilling of the resorption cavity is predicted. For each case surface cells act as mechano-sensors*

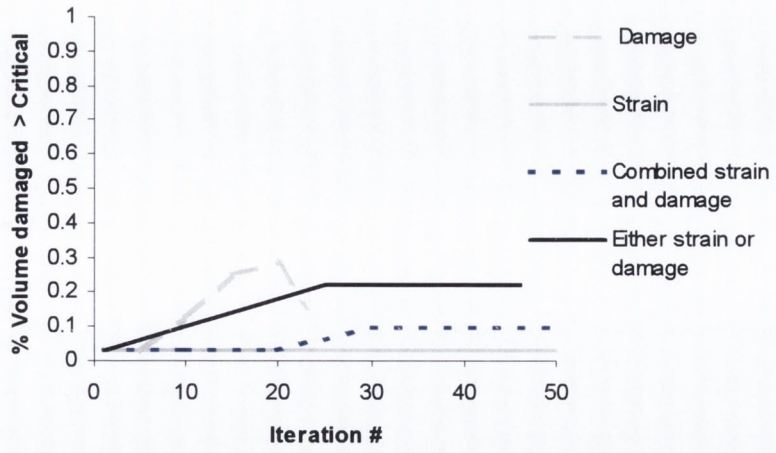

Figure 4.20 *Comparison of % tissue damaged above critical value over the course of the simulation regulated with surface sensors*

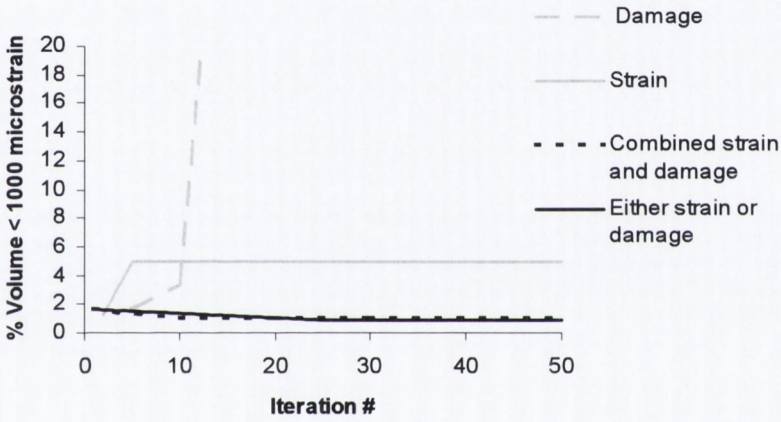

Figure 4.21 *Comparison of % tissue in resorption region (< 1000 με) over the course of the simulation regulated with surface sensors*

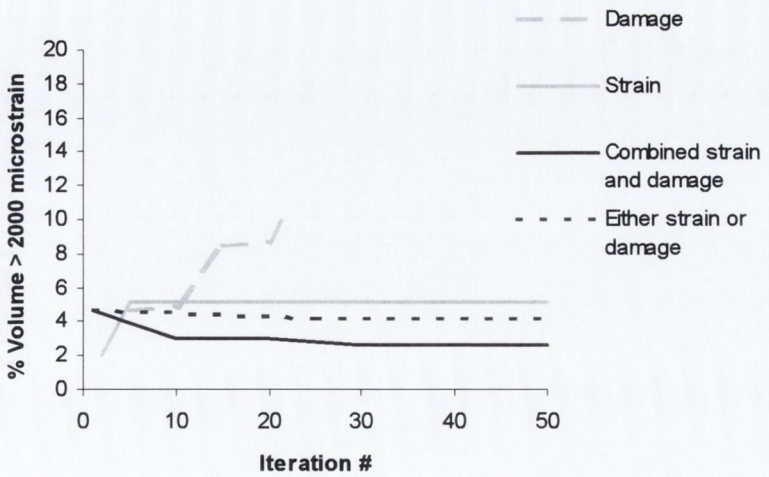

Figure 4.22 *Comparison of % tissue in formation region (> 2000 με) over the course of the simulation regulated with surface sensors*

4.4.4 Regulation with osteocyte sensors

In this section the results of the osteocyte sensor appraisal in combination with each of the mechano-regulatory rules are presented. The predictive quality of each model is assessed according to its ability to respond to a damaged region of tissue, refill an existing resorption cavity and attain/maintain strain and damage levels at homeostatic levels.

4.4.4.1 Response to damaged region of tissue

The results of the predicted patterns of the three different damage responsive mechano-regulatory rules are presented in Fig. 4.23. It is seen by comparison that all three of the mechano-regulatory rules are capable of responding to a region of damaged tissue by initiating a resorption cavity. The strain- only regulated model is unresponsive to regions of damaged tissue therefore it is not included in the results of this section.

i. The damage-regulated model is incapable of completely removing the damaged region of tissue; see Fig. 4.23 (i). While it reduces the percentage of damage that is above the critical value in the first few iterations, the damage removal is stopped and reaches a homeostasis, see Fig. 4.24 (i). The resorbed tissue is not refilled. The strain levels deviate from homeostatic levels throughout the simulation and the percentage of tissue that is overused rises as resorption proceeds but reaches homeostasis when damage removal ceases, see Figs. 4.25 and 4.26.

ii. The predicted remodelling behaviour of the model where there is a combined stimulus according to equation 3.17 is similar to the damage based remodelling described above, see Figure 4.23 (ii) and also Figs. 4.24 – 4.26.

iii. The predicted remodelling behaviour of the model where there the stimulus is *either* strain or damage, and removal of damage is prioritised according to equation 3.18 is similar to the damage based remodelling described above, see Figure 4.25 (b) and also Fig's 4.26 – 4.28.

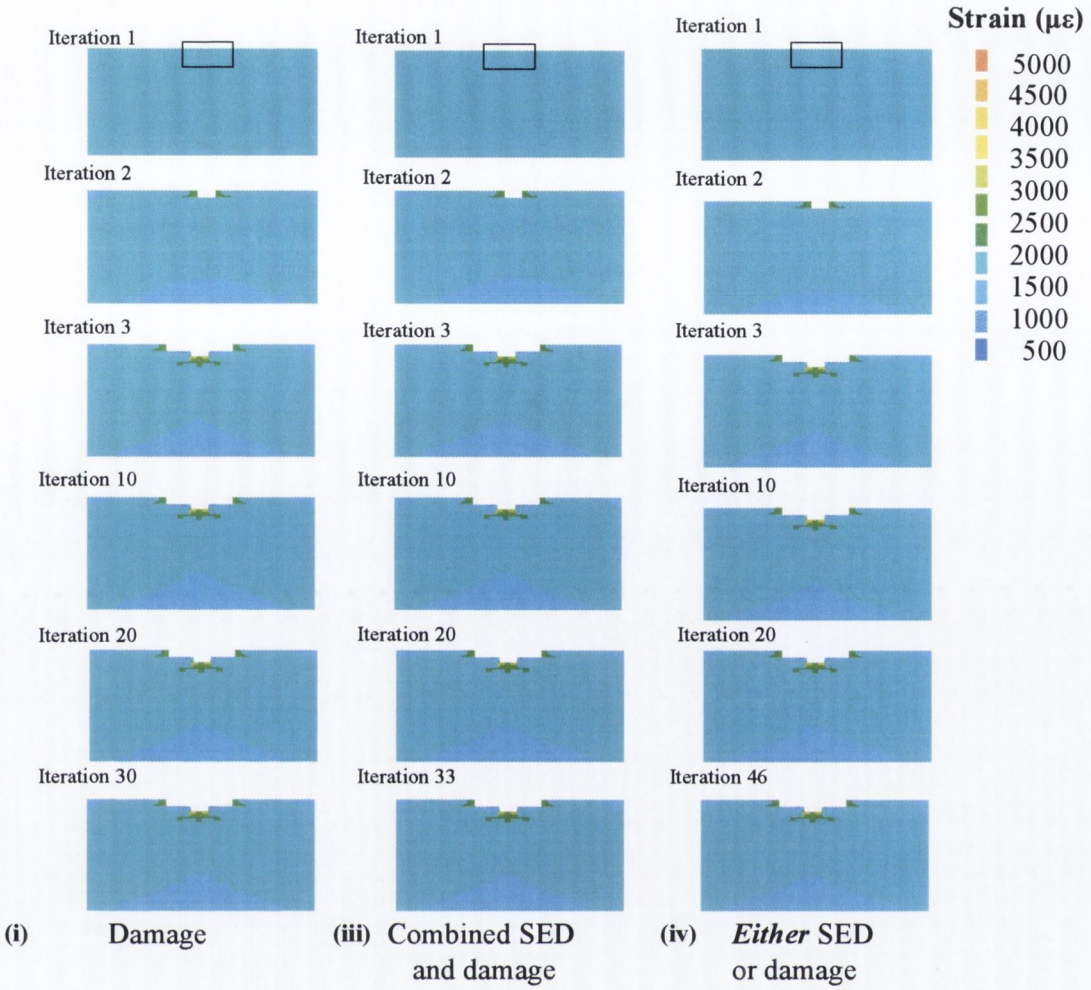

Figure 4.23 *Response of different mechano-regulation rules considered to region of damaged tissue as indicated by box (i) If the stimulus is damage, then complete resorption of the damaged region of tissue is not predicted and the cavity is not refilled (iii) If the stimulus is a combination of strain and microdamage (Eq. 3.17), then the predicted remodelling behaviour is similar to the damage based remodelling described above (iv) If the stimulus is* ***either*** *strain or damage (Eq. 3.18: removal of microdamage is prioritised over strain), then the predicted remodelling behaviour is similar to the damage based remodelling described above. For each case osteocyte cells act as mechano-sensors*

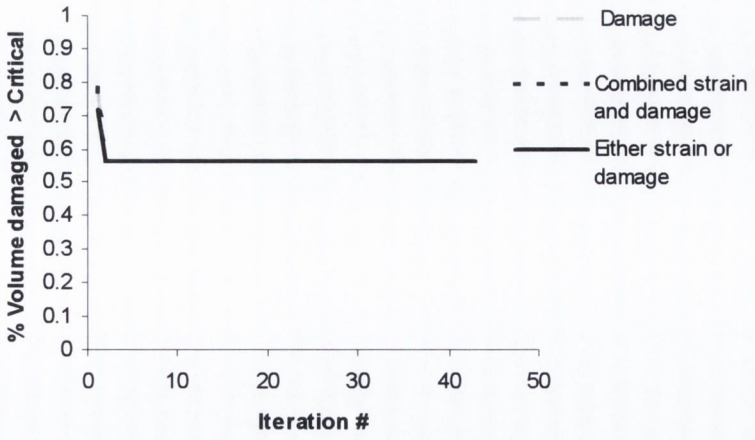

Figure 4.24 *Comparison of % tissue damaged above critical value over the course of the simulation*

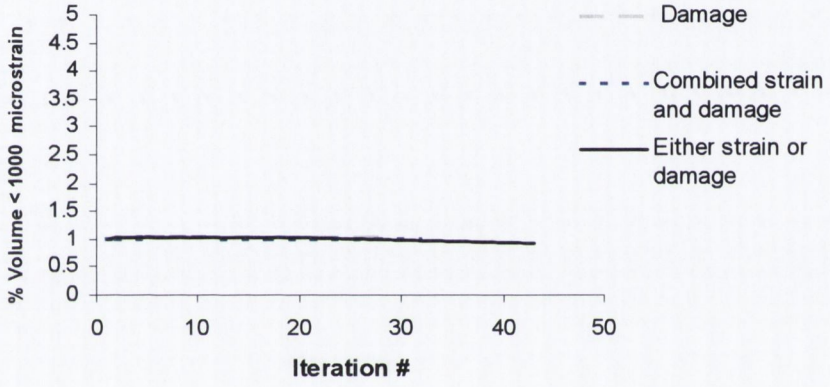

Figure 4.25 *Comparison of % tissue in underuse region (< 1000 με) over the course of the simulation*

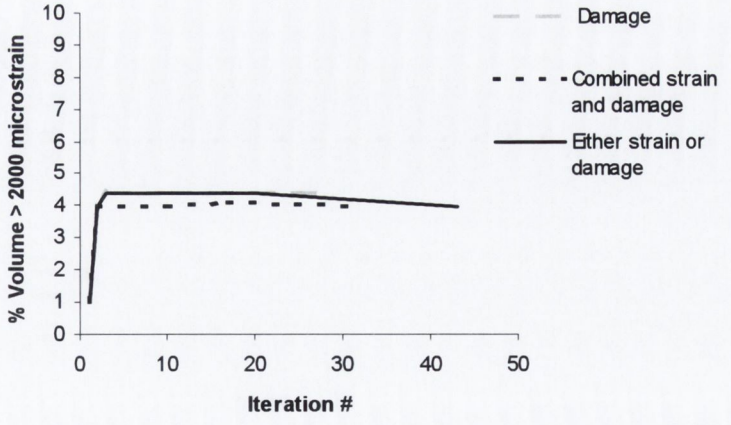

Figure 4.26 *Comparison of % tissue in formation region (> 2000 με) over the course of the simulation*

4.4.4.2 Response to existing resorption cavity

i. The predicted pattern of bone adaptation for damage only regulated remodelling is presented; see Fig. 4.27(i). Complete perforation of the trabecular strut did not occur after 100 iterations. After 100 iterations the mean stress was 2.2 MPa, the maximum stress was 7.3 MPa. The distribution of stress was inhomogeneous with 0.31% of the volume being damaged above critical after 100 iterations. The distribution of strain was inhomogeneous after 100 iterations with 4.6% of the volume of bone tissue strained above 2000 με and 1.62% below 1000 με, see Figs. 4.29 and 4.30.

ii. The predicted pattern of bone adaptation for strain only regulated remodelling is presented in Fig. 4.27(ii). Refilling of the resorption cavity along the trabecular strut was not achieved after 41 iterations; see Figure 4.27(ii). The mean stress was 2.1 MPa, the maximum stress was 5.1 MPa, and the amount of damage did not change appreciably over the course of 41 iterations (Fig. 4.28) with 0.12% damaged above critical after 41 iterations. After 41 iterations, 4.6% of the volume of bone tissue was strained above 2000 με and 1.8% was below 1000 με, see Figs. 4.29 and 4.30.

iii. The predicted pattern of bone adaptation for combined strain and damage remodelling regulated according to equation 3.17 is presented, see Fig. 4.27(iii). No refilling of the resorption cavity was achieved after 35 iterations. The stress-volume and damage-volume distributions are inhomogeneous with 0.12% of the volume being damaged above critical after 35 iterations; see Figure 4.28. The mean stress was 2.1 MPa, the maximum stress was 5.1 MPa and 4.7 % of the volume of bone tissue was strained above 2000 με after 35 iterations and 1.8% was below 1000 με, see Figs. 4.29 and 4.30.

iv. The predicted pattern of bone adaptation for either strain or damage with damage priority (equation 3.18) regulated remodelling with osteocyte sensors is presented, see Fig. 4.27(iv) Complete refilling of the resorption cavity along the trabecular strut was not achieved after 98 iterations. The stress-volume and damage-volume distributions are inhomogeneous with 0.34% of the volume being damaged above critical after 98 iterations and 5.81% of the volume of bone tissue was strained above 2000 με after 98 iterations and 1.97% was below 1000 με

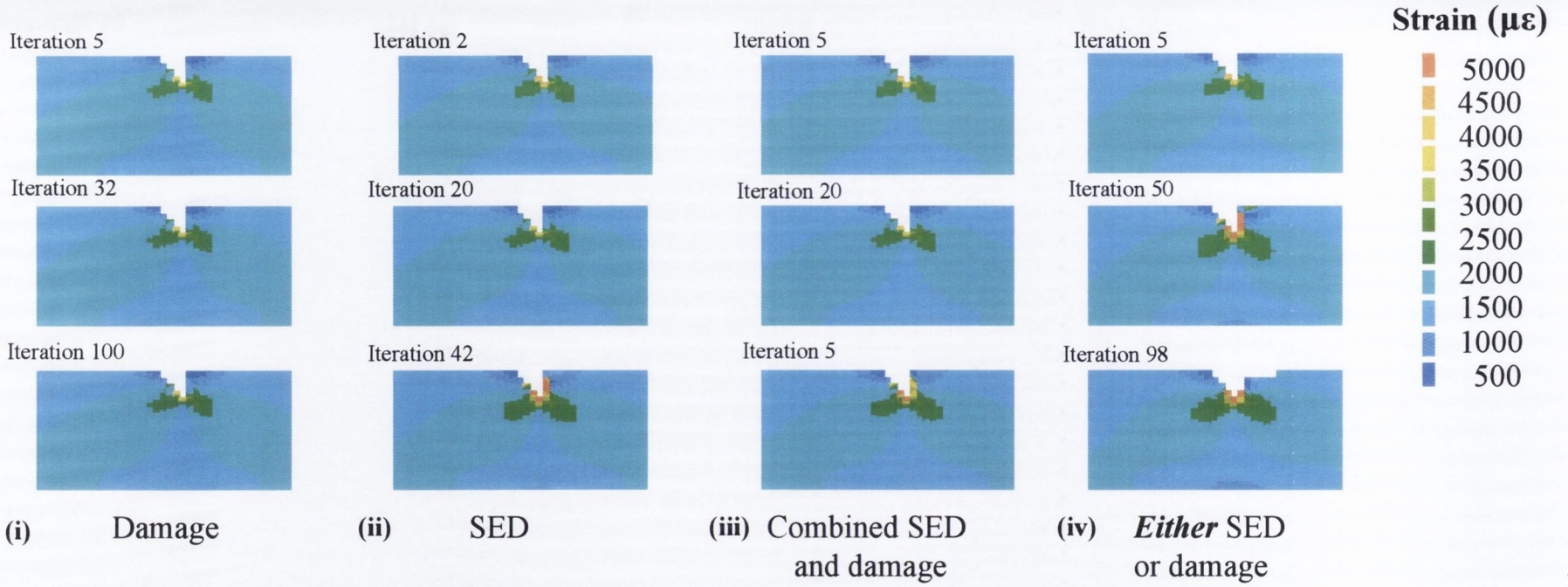

Figure 4.27 *Response of different mechano-regulation rules considered to 20 μm resorption cavity (i) If the stimulus is damage, then complete refilling of the resorption cavity is not predicted (ii) If the stimulus is strain (SED), then refilling of the resorption cavity was not achieved (iii) If the stimulus is a combination of strain and microdamage (Eq. 3.17), then refilling of the resorption cavity was not achieved (iv) If the stimulus is* ***either*** *strain or damage (Eq. 3.18: removal of microdamage is prioritised over strain), then refilling of the resorption cavity was not achieved. For each case surface cells act as mechano-sensors*

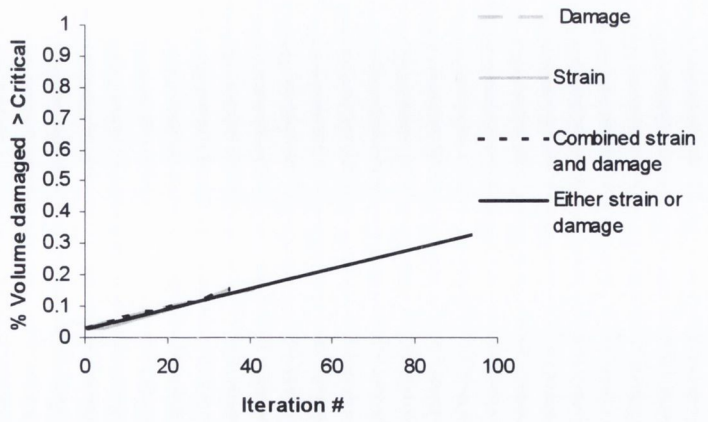

Figure 4.28 *Comparison of % tissue damaged above critical value over the course of the simulation*

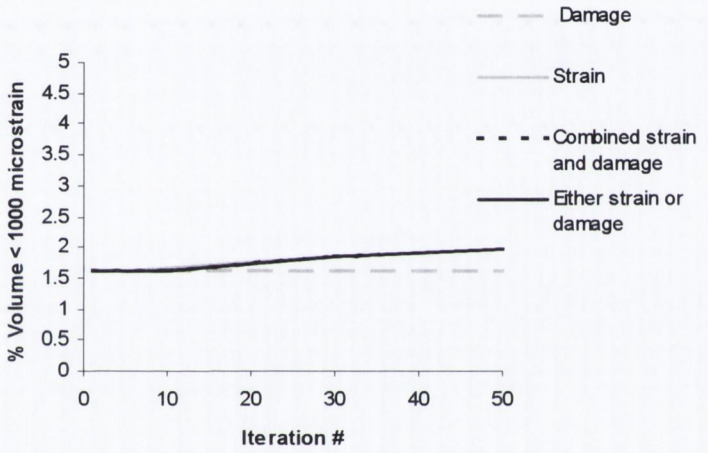

Figure 4.29 *Comparison of % tissue in underuse region (< 1000 με) over the course of the simulation*

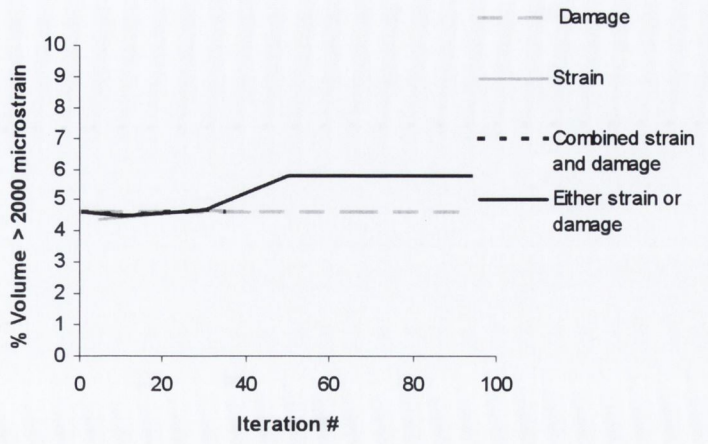

Figure 4.30 *Comparison of % tissue in formation region (> 2000 με) over the course of the simulation*

4.5 Parameter variation study – depth of resorption cavity

In the following section, the results of varying the depth of the resorption cavity on the ability of the separate remodelling rules to refill are presented. The parameter chosen for comparison is number of iterations to perforation of the trabecular strut. Neither strain-regulated remodelling nor combined strain and damage-regulated remodelling lead to perforation. However, their activities in response to variable resorption depths are presented in Figure 4.32, 4.33 and 4.35.

4.5.1 Regulation with surface sensors

The predicted pattern of bone adaptation according to damage-based regulation and also according to regulation by either strain or damage regulated (equation 3.18) with surface sensors is presented; see Fig. 4.31. It can be seen that for both cases, perforation of the trabecular strut occurs only for cavities above a specific resorption depth. At smaller resorption depths damage priority remodelling (equation 3.18) is capable of refilling the cavity but damage based resorption is incapable of refilling the cavity.

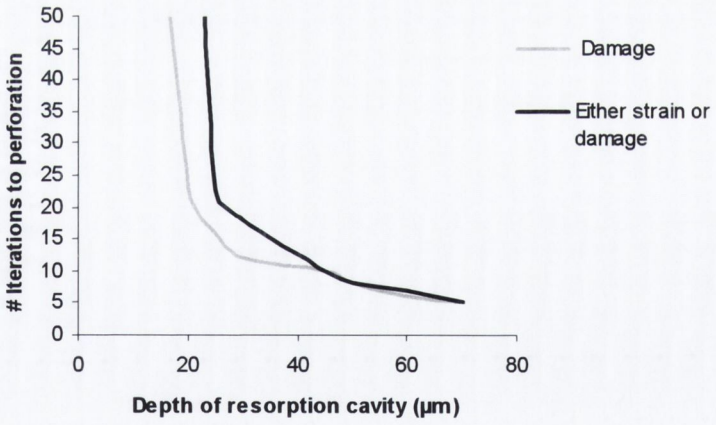

Figure 4.31 *Number of iterations to perforation vs. depth of resorption cavity for mechano-regulation rules (i,iv) with surface sensors*

The results of regulation of a 25 μm cavity and a 70 μm cavity are presented in Figs. 4.32 and 4.33. It can been seen that strain based and combined strain and damage based remodelling (equation 3.17) refill the cavity irrespective of its size. Remodelling according to equation 3.18 has a critical depth of resorption cavity, which it can refill; beyond this perforation occurs.

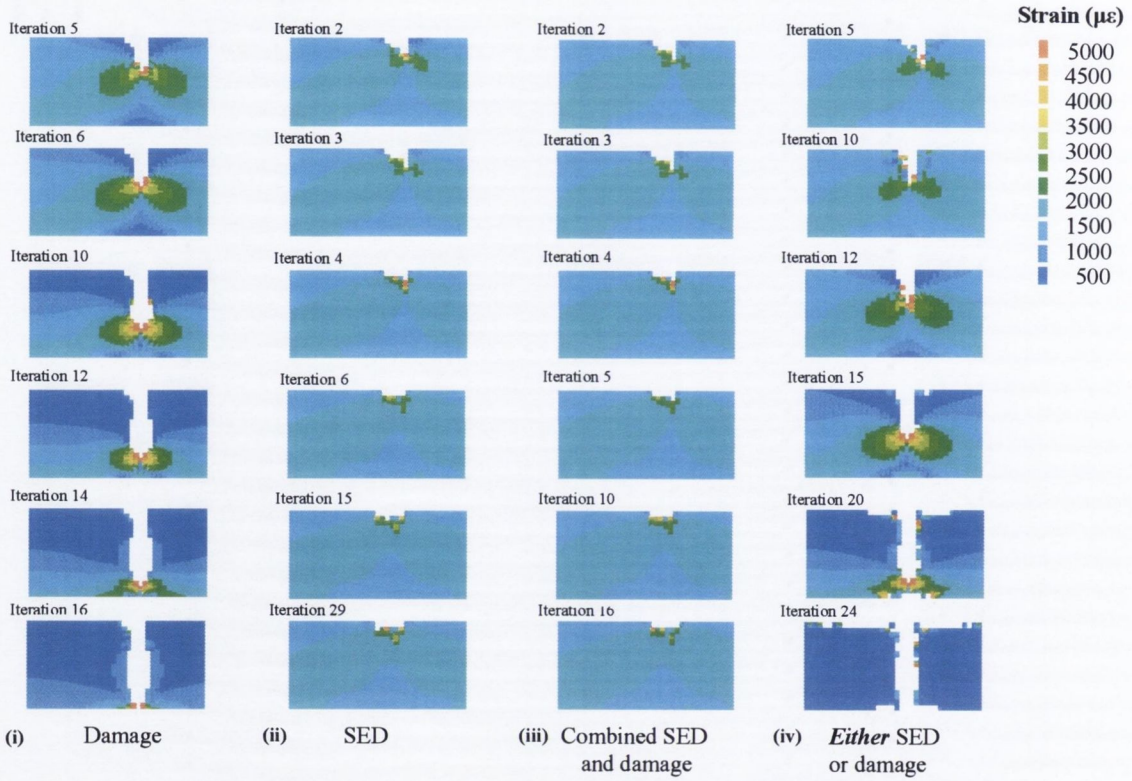

Figure 4.32 *Response of each mechano-regulation rule considered to 25 μm resorption cavity (i) If the stimulus is damage, then perforation of the strut is predicted (ii) If the stimulus is strain (SED), then refilling of the resorption cavity is predicted (iii) If the stimulus is a combination of strain and microdamage (Eq. 3.17), then refilling of the resorption cavity is predicted (iv) If the stimulus is either strain or damage (Eq. 3.18: removal of microdamage is prioritised over strain) then perforation of the strut is predicted due to resorption in response to critically large cavity. For each case surface cells act as mechano-sensors*

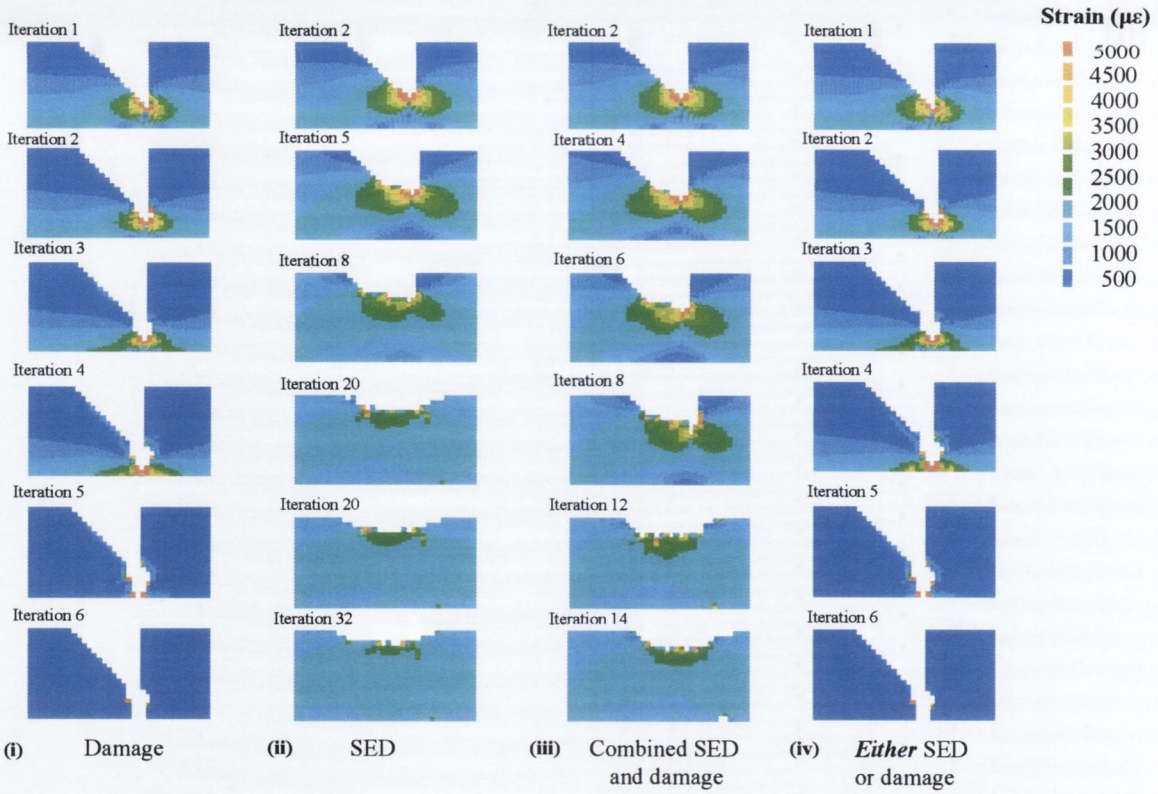

Figure 4.33 *Response of each mechano-regulation rule considered to 70 μm resorption cavity (i) If the stimulus is damage perforation of the strut is predicted (ii) If the stimulus is strain (SED) refilling of the resorption cavity occurs (iii) If the stimulus is a combination of strain and microdamage (Eq. 3.17) refilling of the resorption cavity occurs (iv) If the stimulus is* ***either*** *strain or damage (Eq. 3.18: removal of microdamage is prioritised over strain) perforation of the strut is predicted due to resorption in response to critcally large cavity resulting in damage. For each case surface cells act as mechano-sensors*

4.5.2 Regulation with osteocyte sensors

The predicted pattern of bone adaptation according to damage based regulation and also according to regulation by either strain or damage-regulation (equation 3.18) with osteocyte sensors is presented; see Fig. 4.34. It can be seen that for both cases perforation of the trabecular strut occurs only after a specific resorption depth. At smaller resorption depths, damage priority remodelling (equation 3.18) is capable of refilling the cavity but damage based resorption is incapable of refilling the cavity.

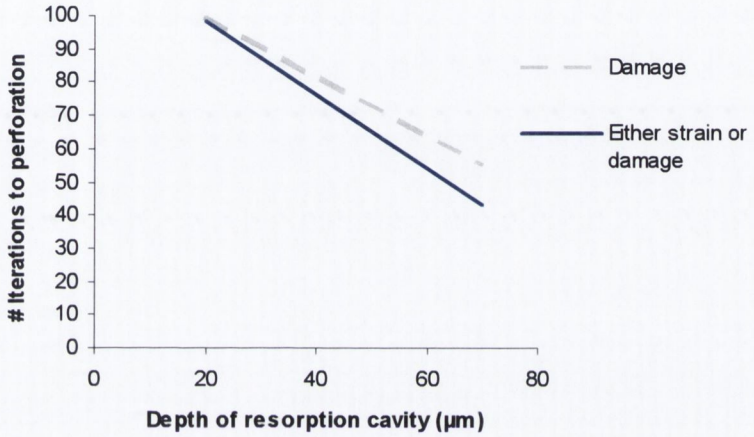

Figure 4.34 *Comparison of the number of iterations to perforation vs. depth of resorption cavity for applied mechano-regulation rules with osteocyte sensors*

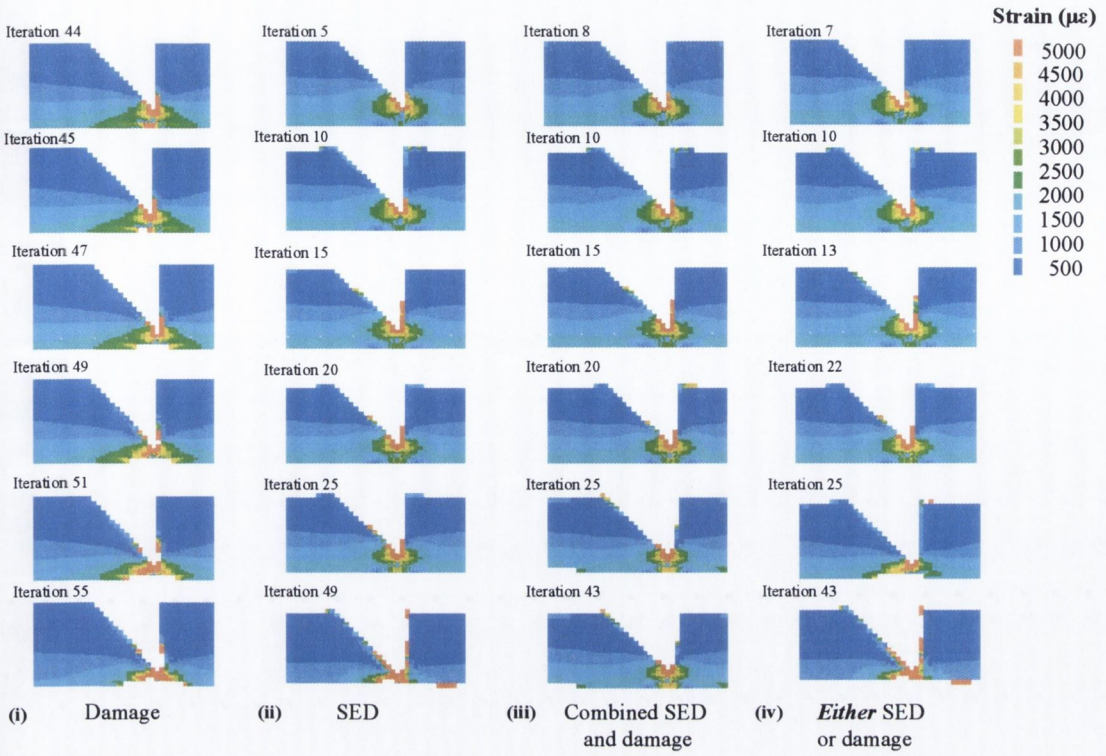

Figure 4.35 *Response of each mechano-regulation rule considered to 70 μm resorption cavity (i) If the stimulus is damage, then refilling of the cavity is not achieved (ii) If the stimulus is strain (SED), then refilling of the cavity is not achieved (iii) If the stimulus is a combination of strain and microdamage (Eq. 3.17), then refilling of the cavity is not achieved (iv) If the stimulus is* ***either*** *strain or damage (Eq. 3.18: removal of microdamage is prioritised over strain), then refilling of the cavity is not achieved. For each case osteocyte cells act as mechano-sensors*

4.6 Mechano-regulation during osteoporosis

This section compares the mechano-regulation using osteoporotic material properties. The mechano-regulation of a 20 μm cavity using the normal elastic modulus is compared to mechano-regulation using an osteoporotic elastic modulus. The mechano-regulation rule that is used is a rule that governs remodelling according to either strain or damage, where damage is prioritized (equation 3.18). The results of the application of this rule to a surface sensor model and an osteocyte sensor model are compared.

4.6.1 Surface cells as mechano-sensors

The predicted pattern of bone adaptation for a damage priority regulated remodelling applied to a model with elastic properties from osteoporotic bone tissue (from results detailed in Figure 4.2) is compared to the model applied to elastic properties from normal bone tissue (from results detailed in Figure 4.2); see Fig. 4.36. In the case presented in this figure the mechano-sensor cells are surface cells.

Complete perforation of the trabecular strut occurs after 14 iterations, and this was followed by further resorption of the strut. The stress-volume and damage-volume distributions are inhomogeneous with 1% of the volume being damaged above critical after 12 iterations, see Figure 4.37. The mean stress is 1.99 MPa, the maximum stress is 38.1 MPa and 10.16% of the volume of bone tissue is strained above 2000 με after 12 iterations and 56.15% is below 1000 με, see Figure 4.38 and Figure 4.39.

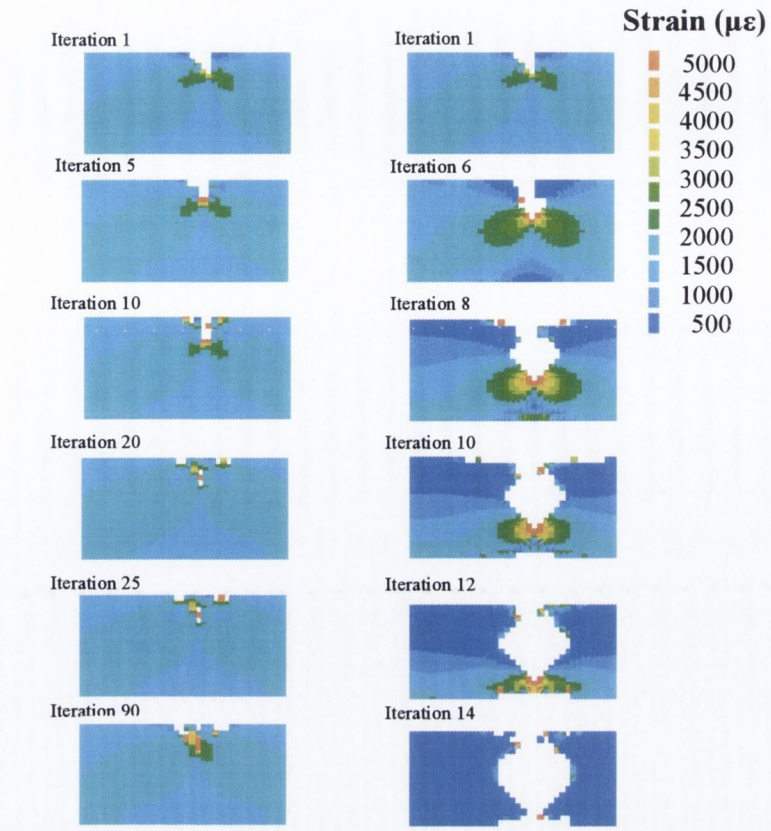

(a) Normal (E = 2.2 GPa) (b) Osteoporotic (E = 4 GPa)

Figure 4.36 *Comparison of predicted remodelling of 20 μm resorption cavity with surface sensor cells according to mechano-regulation rule where the stimulus is* ***either*** *strain or damage (Eq. 3.18: removal of microdamage is prioritised over strain) applied to (a) normal bone tissue (E = 2.2 GPa) and (b) osteoporotic bone (E = 4.0 GPa). The values for normal and osteoporotic bone tissue are determined from Figure 4.1, Pg. 7. for these simulations the sensor cells were surface cells.*

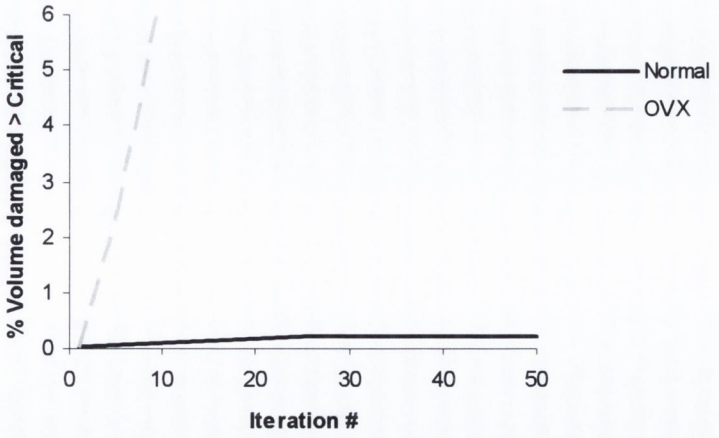

Figure 4.37 *Comparison of % tissue damaged above critical value over the course of the simulation*

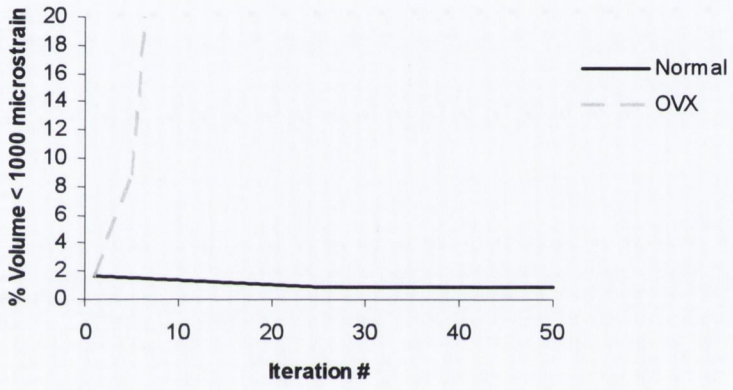

Figure. 4.38 *Comparison of % tissue in underuse region (< 1000 με) over the course of the simulation*

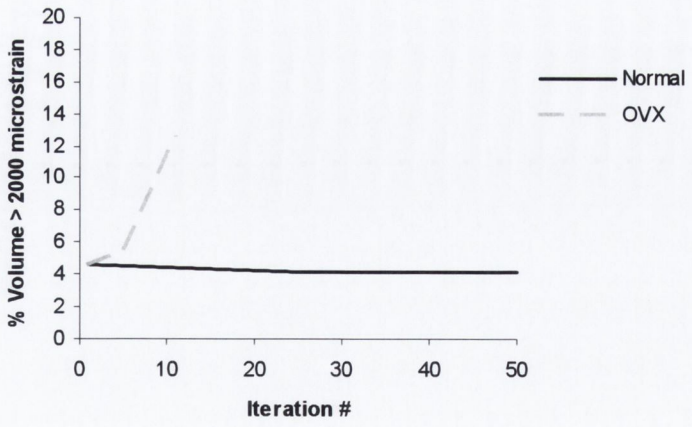

Figure. 4.39 *Comparison of % tissue in formation region (> 2000 με) over the course of the simulation*

4.6.2 Osteocytes appraisal

The predicted pattern of bone adaptation for a damage priority regulated remodelling applied to a model with elastic properties from osteoporotic bone tissue (from results detailed in Figure 4.2) is compared to the model applied to elastic properties from normal bone tissue (from results detailed in Figure 4.2); see Fig. 4.40. In the case presented in this figure the mechano-sensor cells are osteocyte cells.

Complete perforation of the trabecular strut occurs after 16 iterations, and this was followed by further resorption of the strut (see iteration 20). The strain distribution is inhomogeneous and 5.4% of the volume is damaged above critical value after 15 iterations, Fig. 4.40. It was found that 16.2% of the volume of bone tissue is strained above 2000 με after 16 iterations and 49% is below 1000 με, see Figs. 4.41, Fig. 4.42.

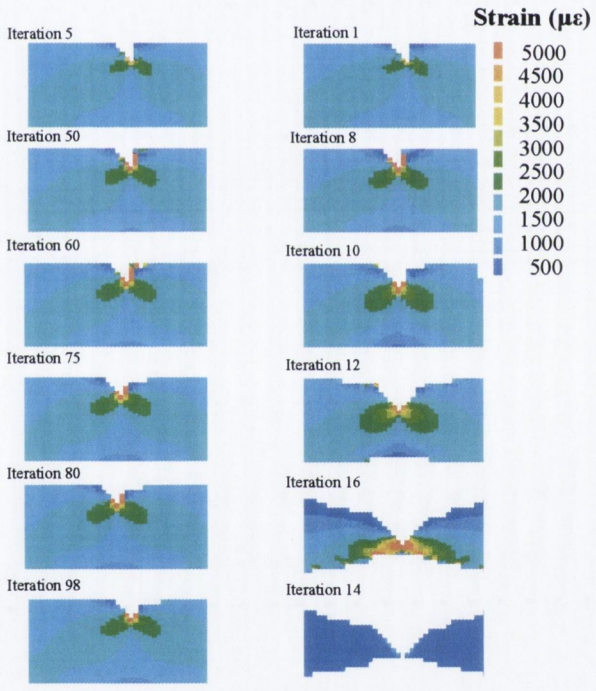

(a) Normal (E = 2.2 GPa) (b) Osteoporotic (E = 4 GPa)

Figure 4.40 *Comparison of predicted remodelling of 20 μm resorption cavity with surface sensor cells according to mechano-regulation rule where the stimulus is either strain or damage (Eq. 3.18: removal of microdamage is prioritised over strain) applied to (a) normal bone tissue (E = 2.2 GPa) and (b) osteoporotic bone (E = 4.0 GPa). The values for normal and osteoporotic bone tissue are determined from Figure 4.1, Pg. 7. for these simulations the sensor cells were osteocyte cells.*

4.7 Conclusion

Mechanical testing of trabeculae from normal, osteoporotic and drug-treated bone was used to determine the effect of osteoporosis and anti-resorptive drug treatment on trabecular bone tissue properties. By measuring the tensile strength of individual trabeculae, it was found that the bone tissue of trabeculae is stiffer and stronger in osteoporotic bone compared to normal. Using Tibolone treatment normalizes the bone tissue properties (stiffness and strength) of single trabeculae on or slightly below normal levels. These findings indicate that in both OVX, and in this specific anti-resorptive treatment, there are subtle processes ongoing that affect bone strength and stiffness that certainly interfere with the changes in mechanical properties as a consequence of BMD changes. During osteoporosis, a pathological change in the material properties of bone tissue (stiffness and strength) occurs. Suppressing bone turnover in drug treated bone results in weaker bone tissue than that of normal and osteoporotic bone.

Through the use of finite element analyses of bone trabeculae, it was shown that the stress/strain distribution within individual trabeculae is highly heterogeneous, even under the simplified loading conditions employed in this analysis. Furthermore it was shown that stress and strain levels within trabeculae are elevated by resorption cavities. In each of the trabeculae the peak stresses were located ahead of the resorption lacunae.

In this study, a mechano-regulation rule has been developed that is capable of initiating a BMU cycle to remove microdamage and refill an existing resorption cavity. By incorporating the two mechanical stimuli, strain and microdamage, simulations of BMU development and activity can be executed successfully. The use of surface based remodelling predicted more physiologically realistic remodelling than the osteocyte based remodelling.

It was found that the application of this mechano-regulation rule to mechanical properties obtained from the tensile testing of single bone trabeculae of osteoporotic bone was capable of predicting BMU activity similar to that observed during osteoporosis (perforation of trabecular struts).

5. Discussion

5.1 Introduction

In this thesis, the author puts forward the idea that a pathological change in bone tissue material properties occurs during osteoporosis, and this alters the mechanical stimuli to bone remodelling cells to drive adaptation of the trabecular architecture. The acceptance for this thesis rests on investigations carried out using finite element analyses, mechanical testing, and computational modelling. The aims of each analysis was to confirm three specific hypotheses; if these can be confirmed then the whole thesis can be inferred.

In the previous chapter the results of each of these analyses were presented. In this chapter the assumptions and limitations of each of methods will first be discussed. To support the author's results, they will be next compared to what has been observed computationally and experimentally by other researchers. The relevance of the results in relation to the central argument of the thesis will then be discussed. Finally, an attempt will be made to use the predictions of the mechano-regulation model to give a biomechanical explanation as to why BMU activity leads to trabecular thinning and loss of bone mass during osteoporosis.

5.2 Assumptions and limitations of this study

In this section the assumptions and limitations associated with each of the methods employed in this study will be discussed separately.

5.2.1 Mechanical testing of bone trabeculae

Firstly, a limitation of this study is that some bias may exist in the choice of test specimens from the cancellous bone sections. Thicker trabeculae were chosen to facilitate gripping and alignment of micro-specimens. Selection of thicker trabeculae minimised the possibility of the specimen sustaining damage on extraction and, at the advanced stages of osteoporosis, only thicker trabeculae remained, as Waarsing *et al* (2004) found using micro-CT scanning. If there were differences in the ratio of new bone lamellae to old bone lamellae in trabeculae of different thickness then this may bias reported results, particularly in view of the fact that the mineral content of bone increases over the course of ageing (Boyde *et al*, 1993) and that increased mineralization is associated with increased stiffness (Compston *et al*, 1989; Homminga *et al*, 1998). In fact a theoretical study by Van der Linden *et al* (2001)

found that the ratio of the highly mineralized interstitial lamella to the less mineralized surface layer of bone tissue does indeed affect the mechanical properties of cancellous bone tissue at the apparent level. This strongly suggests that a difference in mechanical behaviour may also occur at the tissue-level due to different degrees of mineralization.

Secondly, a review by Lucchinetti *et al* (2000) of the different methods of micro-mechanical testing of individual trabeculae previously employed (Runkle and Pugh, 1975; Townsend *et al.*, 1975; Kuhn, J.L. *et al.*, 1989; Mente and Lewis, 1989; Ryan and Williams, 1989; Choi *et al.*, 1990; Rho *et al*, 1993; Samelin *et al*, 1996) postulated on the possible sources of error associated with the different test methods that may explain the range in reported elastic moduli (a range of 0.75 GPa to 20 GPa). They noted that, due to the extremely small and irregular shape of test specimens, reconstruction of sample geometry for calculation of elastic modulus might be a source of error. They noted that resulting uncertainties in reported results has a worse impact on bending tests than on tensile test results. For this reason tensile testing was chosen as the mechanical test method for the present study. Townsend *et al* (1975) describe that removing the marrow mechanically and by chemical defatting has a drying effect on the trabeculae and this in turn affects the mechanical properties of the tissue. This author overcame this difficulty in the present study by keeping the specimens moist prior to, and directly after marrow removal, and also keeping excised specimens moist.

Thirdly, as highlighted by Luchinetti *et al* (2000), the presence of glue in tensile tests might be a source of error if the displacement of the specimen is assumed to be the actuator displacement. Rho *et al* (1993) previously investigated the effect of gluing specimens using an ultrasonic measurement of the elastic modulus before and after the glue was applied. It was found that the glue increased the elastic modulus by 4% but that this was not statistically significant. In this study, the issue of a possible error due to the presence of glue during mechanical testing was addressed by calculating a correction factor to compensate for the displacement of the glue. Although the author would not suggest that this procedure eliminates this source of error entirely, it should reduce it considerably. It should also be noted that the elastic moduli fall within the range of elastic moduli previously reported (Runkle and Pugh, 1975; Townsend *et al.*, 1975; Kuhn, J.L. *et al.*, 1989; Mente and Lewis, 1989; Ryan and Williams, 1989; Choi *et al.*, 1990; Rho *et al*, 1993; Samelin *et al*, 1996).

Finally, another error postulated by Luchinetti *et al* (2000) was that of alignment inaccuracies during tensile testing. This has also been addressed using a graticule lens as a reference for alignment under 30X microscopy.

The whole bone specimens were stored frozen following removal from the animals. Linde and Sorenson (1993) investigated the effects of different storage methods of bone on the elastic properties of trabecular bone. They concluded that storage by freezing, and thawing/refreezing storage methods resulted in no significant change in mechanical stiffness at the apparent level. Refreezing, thawing and retesting on five subsequent occasions did not alter the mechanical properties significantly. Chemical defatting has a drying effect on the trabeculae and this in turn affects the mechanical properties of the tissue, with an observed 30% increase in stiffness. It was noted that keeping the specimens moist prior to and directly after marrow removal and also keeping excised specimens moist might overcome this. In this study specimens were not refrozen following thawing. Excised single trabecular specimens were stored in normal saline prior to testing.

Finite element models were not generated to simulate each test, as both methods used to generate solid models were unsuitable for use with subsequent mechanical assessment. Serial sectioning is a destructive method of obtaining the solid geometry and specimens are not available subsequently for mechanical testing. Micro-CT scanning is a process that results in drying out of the specimens and they are thereafter unsuitable for mechanical testing. However, the use of one correction factor does not explain the variation in elastic properties (Fig. 4.2). There was no significant difference found in the specimen geometry or cross sectional area at the point of fracture between the three groups, see Table 4.3. Therefore it can be inferred that there was no significant difference between the volumes of glue required to affix the specimens from each of the groups and as such the use of one correction factor should not explain the variation in mechanical properties.

5.2.2 Stress analyses of bone trabeculae

A number of assumptions were made in the development of finite element analyses of single bone trabeculae (section 3.4) that require further elaboration.

Firstly, for these analyses the assumption was made that bone tissue material properties were linear elastic and isotropic. Bone tissue material properties are in fact viscoelastic and anisotropic (Gottesman and Hashin. 1980) and as such these

assumptions will effect the observations made in this analysis. However, modelling bone as a linear elastic isotropic material is an approach that has been used by various researchers previously. The elastic modulus chosen was that obtained from the results of micro-mechanical testing of single bone trabeculae (section 4.3.2). Conflicting results are available for the elastic modulus of cancellous bone tissue; some that suggest material properties that are the same as those of cortical bone (Nicholson *et al.*, 1997), and others that determine a lower elastic modulus (Ryan and Williams, 1989; Choi *et al.*, 1990). However, using a higher modulus would result in even higher distributions of stress in the structures and further confirm the observations of this analysis.

Secondly, trabecular bone is lamellar in structure consisting of packets of aged bone, alongside newly formed bone (Birkenhager-Frenkel *et al.*, 1993). It has been shown that the mineral content of bone is increased over the course of ageing (Boyde *et al.*, 1993), and that increased mineralization is associated with increased stiffness (Currey, 1984b; Hodgskinson *et al.*, 1989); therefore the elasticity distribution within the trabeculum is not likely to be homogeneous and the presence of stiffer mature lamellae of bone would also affect the distribution of strain within the tissue.

Thirdly, a tensile load was applied to the trabecula. Since the exact loading conditions to which the four trabeculae used in this study were subjected in vivo are not available, this assumption seems reasonable. This approach has previously been used by Smit and Burger (2000) to simulate in vivo loading conditions on single bone trabeculae.

5.2.3 Mechano-regulation rule for bone remodelling

Section 4.4 presents the results of the four stimuli proposed to regulate remodelling: (i) damage, (ii) strain, (iii) combined strain and damage and (iv) *either* strain or damage, where the removal of microdamage is prioritized. These stimuli are used to predict remodelling of trabeculae, of particular importance is the testing of the hypothesis that a change (increase) in Young's modulus would make it easier for remodelling to result in trabecular perforation. In view of the importance of this for the defence of this thesis, it is necessary to address the assumptions made in the mechano-regulation algorithm.

Firstly, the assumption was made that the mechanical signals that bone cells appraise are strain energy density and damage. While a variety of theories regarding

the regulation of bone remodelling have been formulated (see Chapter 2 for review) it is still unclear how bone cells sense mechanical signals. Both strain and damage are physical quantities for which it is possible to conceive mechanisms for their sensation by bone cells. Following the methods of previous strain-adaptive mechano-regulation models (Huiskes *et al*, 1987; Weinans *et al*, 1992) strain energy density (SED) was chosen as a measure of strain or deformation of the bone tissue. Damage may be sensed by fracture of the osteocyte processes due to the shearing motion between crack faces (Taylor et al, 2003), by unloading of the osteocyte lacuna local to the crack (Prendergast and Huiskes, 1996), or by causing apoptosis of the osteocyte (Noble, 2003). The damage was calculated according to the SN curve for cortical bone (Carter *et al*; 1976); however it would be of interest to develop fatigue failure criterion for trabecular tissue and use this instead to determine the damage accumulation in this model.

In this model the sensors are considered to control the BMU activity by comparing the mechanical signal with reference signals. However it is still unclear whether the remodelling process is controlled by the osteocytes cells or the surface cells (bone lining cells and osteoblasts), and how sensor cells transmit signals to actor cells. This issue was investigated by comparing a model where osteocytes controlled remodelling to a model where the surface cells regulated remodelling.

For osteocyte-regulated remodelling the assumption of a specific distance over which osteocytes have an influence is a limitation of the model. The assumption is made that osteocytes local to actor cells will have a greater influence on their activity but also that osteocytes in the center of the trabecula may be capable of transmitting signals to actor cells at the surface. The assumption was made that at the center of the trabecula the strength of this signal would diminish to 36% of the original signal and thus it was assumed that the influence domain of the osteocytes was of the order of 45 μm (diameter/2). It would be interesting to carry out a parameter variation study to investigate whether this specific choice of distance of influence may have limited the predictive power of an osteocyte-regulated model.

Another assumption made was that there was a uniform sensor distribution throughout the bone matrix; however it has previously been observed that aged bone tissue contains less osteocytes than newer bone tissue (Vashishth et al, 2000b) so it would be of interest to model the specific locations of osteocytes in a model of a bone trabecula.

The method for calculating resorption and formation rates, described in 3.7.2.1, may also be a limitation of this model. However, in the absence of experimental data on specific osteoclast/osteoblast activity rates, it allows for approximation of remodelling rates for use in this model. It would be of interest to experimentally investigate the rates of activity of osteoclasts and osteoblasts in response to altered strains and the presence of microdamage in vivo.

For the implementation of trabecular remodelling, a simplified 2D geometry was chosen to represent a bone trabecula in these analyses. As is illustrated in section 4.2 of this thesis, trabeculae have complex geometries and, as such, it is obvious that a 2D model is only a schematic representation of this aspect of trabecular bone behavior. If bone remodelling were indeed a mechano-regulated phenomenon then the geometry of a bone trabeculum would certainly play a role in dictating the development of a BMU. Nonetheless, the model serves well to illustrate the potential applicability of a mechano-regulation rule to model BMU activity. The use of a simplified 2D model also allows for investigation of the possible relevance of certain parameters such as resorption depth and osteocyte sensory capacity by removing the complexity due to geometric non-linearity. It should be noted that, by comparison of the 2D analysis to the 3D models of single trabeculae with resorption lacunae (section 4.2), it is found that the locations of elevated stress and strain are similar to those observed in 3D models with elevated stresses at the base of the resorption lacunae. However the magnitudes of the elevated stress and strain are more severe in the 3D models, see Table 5.1. This suggests that the remodelling activity in the real trabecula may be higher than predicted for our 2D model.

Model	**Trabecula 1**	**Trabecula 3**	**Trabecula 4**	**2D representation***
Mean Stress (MPa)	10.4	8.6	10.8	2.2
Maximum Stress (MPa)	93.4	123.1	148.4	7.27
Volume < 10MPa	62.6%	73.9%	65.6%	100%
Volume > 30 MPa	2.4%	2.1%	14.6%	-
Mean Strain (με)	4,906.0	4042.0	6054.9	1,538
Maximum Strain (με)	40,685	53,573	64,179	22,830

Table 5.1: *Comparison of mean, maximum and distribution of principal stress and strain within the tissue volume of the trabecular specimens to the 2D approximation of trabecular geometry.*

Another limitation of the 2D representation is that physiologically the osteocyte sensory system is a 3D network. It is therefore reasonable to assume that a 3D model may result in differences in the remodelling behavior. However, Van Rietbergen *et al* (1995) showed that the osteocyte based regulation process behaves similarly in a three dimensional model.

In this analysis the bone tissue was modeled as linear elastic with isotropic material properties. In reality bone tissue is a composite material consisting of lamellae of old and new bone, which are at different stages of mineralization and therefore may have different material behavior and extent of damage present. The next step will be to apply this model to a model of the composite nature of bone tissue including the different lamellae of new and aged bone tissue, which have different extents of mineralization and microdamage. If this material behavior were to be included in this model then it would certainly affect the pattern of development of a BMU cycle. In fact the effect of different lamellae was investigated to a certain extent by modeling a region of damaged material and observing the development of a BMU in response to this damage.

Square elements were used to represent the trabecular geometry in this analysis. This limits the development of the BMU shape to the size and shape of the elements. To attempt to overcome this issue mixture elements were used at the resorption/formation surfaces so that the elements at these surfaces were of material properties that were intermediate between bone and marrow.

The assumption was made that osteoclast and osteoblasts are both regulated by mechanical stimuli, but that formation is only stimulated by the presence of elevated strain. It is conceivable that bone is capable of resorbing bone tissue in response to the presence of under loaded bone tissue and microdamage. The mechanisms that initiate osteoblasts bone formation are not as clear. The activity of osteoblasts may be governed by one of two mechanisms (1) physiological coupling to the osteoclast bone resorption or (2) mechano-regulation of osteoblast bone formation. The behavior of bones under conditions of weightlessness suggest that osteoblast bone formation is

also a mechano-regulated phenomenon and that the assumption made in the development of this model that no direct physiological coupling exists may be valid.

5.3 Comparison to previous observations

In this section the results obtained throughout the work of this study are compared to similar studies and also to known in vivo quantities to which these observations are related.

5.3.1 Stress analyses of bone trabeculae

The magnitudes of the strains observed in the finite element analysis of single bone trabeculae are corroborated by a study by Van der Linden *et al.*, 2001, who observed peak strains in excess of 10,000 με within individual trabeculae with active resorption lacunae. In the analysis of Smit and Burger (2000), peak strains of 1800 με were predicted at the bottom of the lacuna where resorption is stopped and osteoblasts are recruited to fill the gap, and 2270 με perpendicular to the direction of loading. In the direction of loading the strain levels were reduced to as low as 130 με, see Figure 5.1.

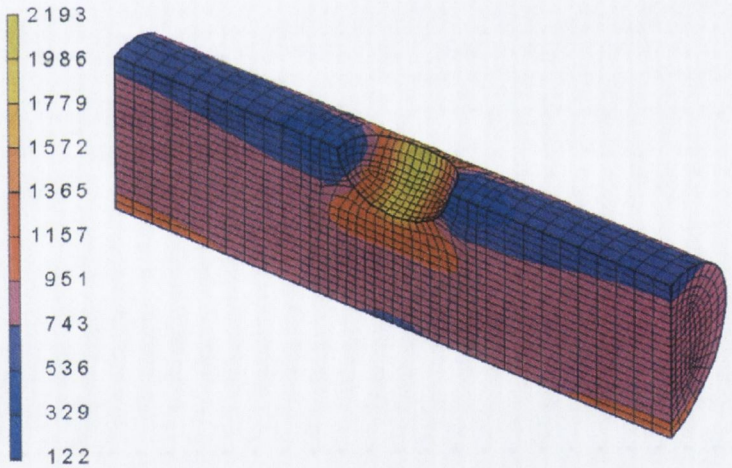

Figure 5.1: *Distribution of strain (με) about idealised lacuna (Smit and Burger, 2000)*

They concluded from these observations that low strain levels activate osteoclast resorption activity and that high strains activate osteoblast bone formation. In the analysis presented in this thesis, while lower strain in the direction of loading was observed (Fig. 4.9 (d) section 2), peak strains ahead of the resorption cavity in the direction of loading were also predicted (Fig. 4.9 (a) section 9; Fig. 4.8 (c) section 11; Fig. 4.9 (d) section 6). Elevated strains were predicted in the analyses presented in this thesis at the base of the resorption cavity (Fig. 4.9 (a) section 7; Fig. 4.9 (c)

section 12; Fig. 4.9 (d) section 4), but these were not the peak strains observed in the trabeculae. Therefore, despite the differences in magnitude, the analysis of resorption lacunae within real trabeculae does support the conclusions of Smit and Burger (2000) that were made based on an idealised hemispherical lacuna. This also explains the difference in magnitudes between the present analysis and their study, as is illustrated in Table 4.5.

5.3.2 Mechanical testing of bone trabeculae

Previous mechanical tests of single bone trabeculae have reported a wide range of elastic moduli for the bone tissue. The variation in reported results may be due to the different test methods applied and the associated errors, as discussed in Chapter 2 and also reviewed by Luchinetti *et al* (2000).

Study	**Specimen Origin**	**Elastic Modulus (Standard deviation)**	**Possible error**
Current study	Rat proximal tibia	2.6 (1.6) GPa	Glue
Townsend and Rose (1975)	Human medial tibia	14.1 GPa(dry); 11.3 GPa(wet)	Epoxy
Runkle and Pugh (1975)	Human subchondral bone	8.7 (3.2) GPa	Cement
Mente and Lewis (1989)	human femora/ tibia	6.2 (1.2) GPa	Epoxy
Kuhn *et al* (1989)	Human iliac crest	3.8 GPa	Machining
Rho *et al* (1993)	Proximal human tibia	10.4 (3.5) GPa	Glue
Choi *et al* (1990)	Proximal tibia.	4.6 (1.3) GPa	Machining
Ryan and Williams (1989)	Bovine femora	0.8 (0.4) GPa	Clamp plates

Table 5.2: *Comparison of results of current study to those obtained through previous mechanical testing of single bone trabeculae.*

The finding reported in section 4.2 above that OVX tissue is stiffer than normal bone tissue is corroborated by the results of a study that found a higher stiffness in trabecular bone samples from subjects with osteoporotic fractures relative to their volume fraction than subjects without disease or fracture (Homminga *et al*, 1998). The reason why osteoporotic trabeculae are stronger and stiffer may be due to

a change in the bone tissue composition, i.e. the content or quality of collagen and mineral in the bone tissue. A number of studies have investigated the possibility of a change in mineral content in osteoporotic bone tissue; some have revealed no change in mineral content (Li and Aspden, 1997) and others reveal an increase in the mineral content and a lack of collagen (Dickenson *et al*, 1981; Boyde *et al*, 1998; Zioupos and Aspden, 2000). A reduction in the ratio of mineral to matrix in the centre of bone trabeculae has been observed in osteoporotic bone tissue (Gadeleta *et al*, 2000). These studies provide strong evidence of tissue-level changes in the composite bone tissue during osteoporosis; the present study additionally shows that these changes have an effect of increasing the mechanical strength of the mineralized matrix.

On the apparent level, previous studies have shown that drug treatment increases the strength structural or bulk mechanical behaviour of osteoporotic bone (Ederveen *et al*, 2001; Teramura *et al*, 2002) and of whole bones (Kasugai *et al*, 1998; Hirano *et al*, 2000; Teramura *et al*, 2002; Sugita *et al*, 1999) relative to untreated ovariectomized bone. Based on the results presented in Chapter 4 it would appear that the increase found in such studies may be due solely to increase in bone mass and maintenance of trabecular architecture, and are not due to an increase in the strength of the mineralised matrix constituting the trabecular tissue itself. The effect of drug treatment for maintaining trabecular architecture has been quantified previously by Yoshitake *et al* (1999) who examined the architecture of bone after drug treatment. They observed a higher bone volume, tissue volume, trabecular number and a decrease in trabecular separation as compared to untreated osteoporotic bone. Their study found that the osteoclast inhibition allowed for maintenance of the structural mechanical behaviour of the matrix. During osteoporosis however, the increased bone turnover leads to trabecular thinning and increases the likelihood of trabecular penetration under physiological loads (Compston *et al*, 1989). There are fewer trabeculae present, and their connectivity is diminished, so there may not be adequate structural support, which would explain the decreased mechanical performance of osteoporotic bone. However, these earlier studies do not impart information about the effect of the disease on the material properties of the mineralized bone matrix.

5.3.3 Computational simulations of bone turnover

The values observed in the 2D representation of the bone trabecula to which the mechano-regulation rules were applied require comparison in order to confirm their

magnitudes. An analysis of the mechanical stimuli local to a tunneling osteon was previously performed by Burger *et al* (2003) who also used a poroelastic material to model the bone tissue. The aim of this study was to propose a mechanism that explains the action of osteoclasts in the cutting cone during a remodelling cycle. They predicted that the magnitude of fluid flow was approximately 20 nm/sec at the base of the resorption cavity at that this value reduced to 0 nm/sec at a depth of approximately 80 μm from the base of the lacuna within the bone tissue, see Figure 5.2 (a) and 5.2 (b). Upon analyzing the strains in these regions they predicted that the strain at the base of the lacuna was approximately – 1000 με, whereas at the cutting tip the strains were of the order of 500 με, see Figure 5.3.

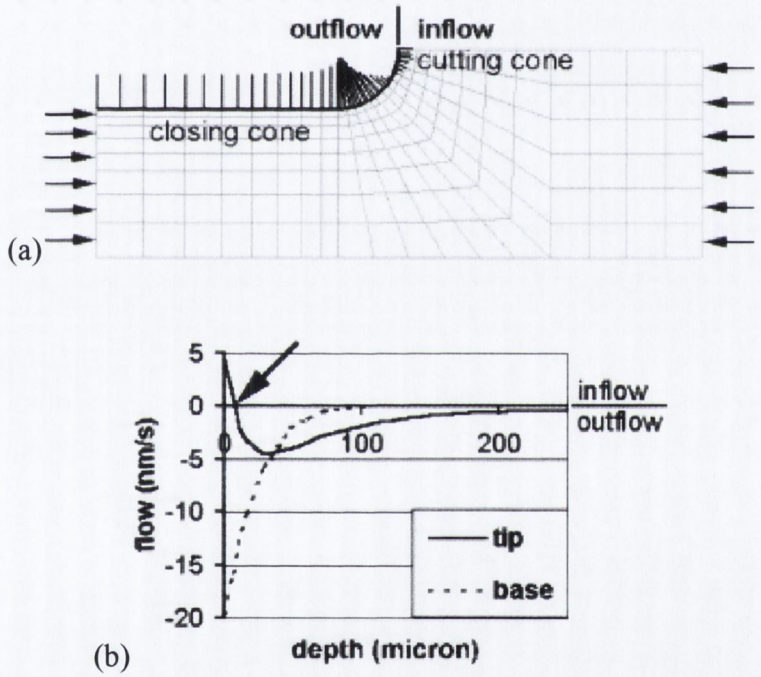

Figure 5.2: **(a)** *Schematic of fluid-flow (με) about lacuna and (b) varying magnitudes of fluid-flow (nm/s) about lacuna of Burger et al (2003)*

In comparison to the results presented in section 4.4, it is seen that the fluid flow was greatest at the base of the resorption lacuna, see Figure 5.4. The maximum fluid flow at this point was 12 nm/sec. If it is assumed that the cutting surface is at the outer surface, it can be seen that the magnitudes of the fluid flow are much lower at these regions, below 0.5 nm/sec. The strain results indicate that at the base of the resorption cavity the strains were elevated to a maximum value of approximately 6700 με. At the

bone surface the strains were lower than 500 με. The magnitudes of the loads employed in the analysis of Burger *et al* (2003) are similar to those of this study, as the maximum load they applied resulted in a deformation of 1500 με of the bone matrix.

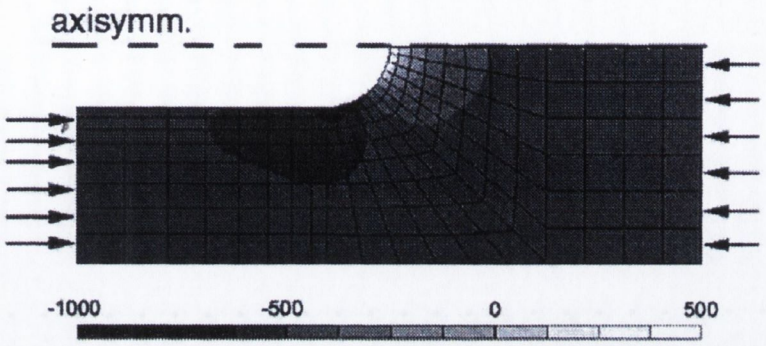

Figure 5.3: *Volumetric strain (με) around the progressing end of an osteonic BMU, Burger et al (2003)*

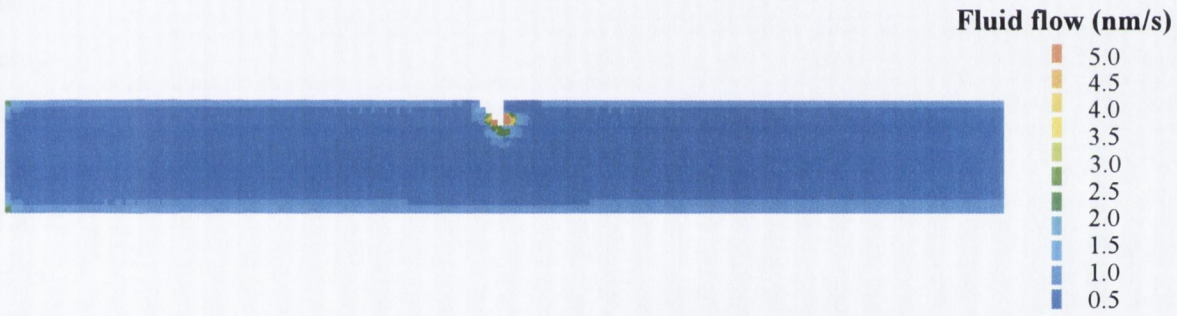

Figure 5.4: *Fluid flow (nm/sec)) around a trabecular resorption cavity*

Previous predictions of bone remodelling have been used to investigate the mechanisms of bone adaptation under altered loading conditions (Weinans *et al*, 1992, Huiskes *et al*, 2000; Mullender *et al*, 1994,1995,1997)) and in response to the presence of prosthetic implants (Huiskes *et al*, 1987; Carter *et al*, 1989; Beaupre *et al*, 1997). In these models only net bone mass loss or gain was considered. These models were not capable of modelling specific BMU activity due to the resolutions that were used to represent the trabecular geometry. In the model presented in this thesis it was possible to model the separate activity of osteoblasts and osteoclasts.

Thomsen *et al* (1994) developed a computer simulation to assist in predicting the effects of changes in the remodelling process on bone mass, trabecular thickness and perforations. They investigated specifically the affects of osteoporosis and drug

treatment. Their approach was to vary the remodelling parameters; activation frequency, resorption time/depth, formation time and reversal time, based on observations from different types of bone remodelling; normal, osteoporotic and drug-treated. The initiation of remodelling on trabeculae was randomly assigned and the probability of remodelling on a quiescent trabecula was determined by the activation frequency. They predicted that osteoporotic remodelling resulted in a mainly reversible bone loss. However in this model the cause of alteration of activation frequency and other remodelling parameters were not investigated. Etidronate and estrogen were found to cause a slight increase in bone mass and Etidronate was found to be capable of preventing perforations.

5.4 Relevance of observations

5.4.1 Mechanical stimuli for bone remodelling (stress analysis)

In this study it was shown that the stress/strain distribution within individual trabeculae is highly heterogeneous, even under the simplified loading conditions employed in the present analysis. Furthermore it was shown that stress and strain levels within trabeculae are elevated by resorption cavities. In each of the trabeculae, the peak stresses were located ahead of the resorption lacunae. According to Wolff's Law (Wolff, 1892) the architecture of cancellous bone is continuously adapted so that it is optimised to support the loads it bears, throughout life, with minimal weight. If this were true, it might be expected that the stresses and strains in trabeculae should be evenly distributed throughout trabecular architecture. It has been demonstrated clearly that the distributions of stresses within trabeculae are very far from being evenly distributed. This inhomogeneity of stress will be additional to that existing within the trabecular architecture itself (Van Rietbergen *et al.*, 1999).

Given the pattern of stress concentrations predicted in this analysis (very high stress ahead of resorption cavities and elevated stresses at the base of the cavity) it is plausible that, as Smit and Burger (2002) hypothesised, there are different stimuli that govern the activity of osteoblasts and osteoclasts. Smit and Burger (2002) postulated that low strains trigger the osteoclast resorption and that increased strains serve to inhibit the osteoclasts and activate osteoblasts to refill. However the magnitudes of the peak stresses and strains observed in the analysis presented in this thesis suggest that damage would occur, and, as predicted by Prendergast and Huiskes (1996), the

presence of microdamage results in unloading of the osteocyte lacuna local to the damage site and consequently reduced mechanical straining of the osteocytes and resorption. The mechanism by which both damage and strain might initiate a biomechanical signal for bone remodelling is illustrated in Figure 5.5.

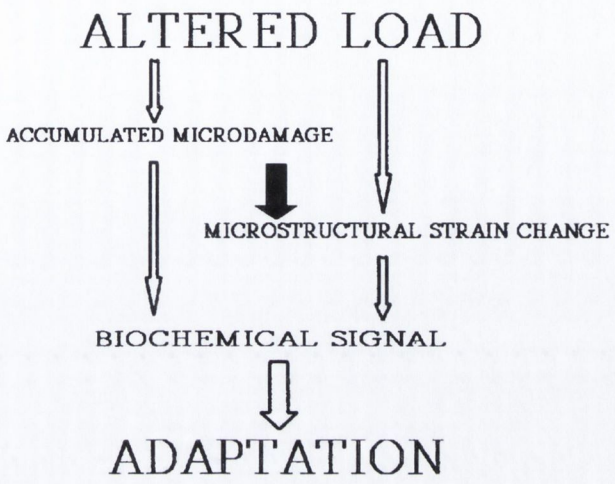

Figure 5.5: *Possible pathways for transducing mechanical load changes into adaptive response to both damage and strain after Prendergast and Huiskes (1995)*

Analyses of the stress distributions local to resorption cavities demonstrate that microdamage may play a role in regulating the movement of resorption lacunae on the surface of a trabeculum. Stress elevations as high as 144 MPa have been predicted local to resorption sites which shows clearly that the creation of a resorption site, whether initiated by damage or not, results in massive elevations of stress in the trabeculum. The magnitudes of these stresses correspond to values associated with fatigue failure of trabecular bone tissue (100-140 MPa) as measured by Choi and Goldstein (1992), who reported that, at these stress levels, the number of cycles to failure was approximately 100,000. This corresponds to approximately five weeks under normal physiological loading conditions (Carter *et al.*, 1981). It has also been shown that the number of cycles to failure of bone decreases rapidly as the stress increases. It is clear also from the magnitudes of the peak strains in trabeculae from the calculations in this study, which are greater than 14,000 με and as high as 64,300 με, would lead to bone microdamage, as bone has been shown to fail in fatigue at strain ranges of 5,000 – 10,000 microstrains in as few as 1,000 – 100,000 cycles (Carter *et al.*, 1981). It is therefore reasonable to assume that the magnitudes of stresses and strains that were calculated around resorption lacunae would cause

further damage to the structure local to the resorption site. The locations of the peak stresses were ahead of resorption lacunae in all of the trabeculae with active resorption lacunae, see sections 4-6 and sections 10-12 in Fig 4.7(a), sections 5-7 in Fig 4.7(c) and sections 5 and 6 in Fig 4.7(d). This evidence leads to the interesting speculation that driving force to propel a BMU along the surface of trabecula may be damage ahead of the resorption cavity, i.e. the BMU cycle develops when osteoclasts "chase" the newly developed damage.

This prediction is supported by a number of studies that have observed that resorption cavities occur preferentially in regions of microdamage in cortical bone (Burr et. al, 1985; Mori and Burr, 1993). Reilly (2000) also noted that diffuse microdamage (<10 μm length) is concentrated around remodelling cavities. In fact, the argument for the targeting of bone remodelling to regions of damage in bone have been strengthened by recent experiments that have demonstrated that there is a time dependent migration of osteoclasts into regions of cortical bone containing experimentally induced microdamage in rats. In these studies it was demonstrated that osteocyte apoptosis, induced by bone fatigue, is localized to regions of bone that contain microcracks and that osteoclastic resorption after fatigue also coincides with regions of osteocyte apoptosis. It has also been observed that there is an increased microdamage burden in regions of bone tissue that have a low density of osteocytes (Mori *et al*, 1997)

A number of questions are as yet unanswered with respect to the activity of BMU remodelling on the surface of an individual trabecula. If a microcrack is present in bone, it weakens the bone and the resulting bone is fragile and has a propensity to failure. In this study the author investigated whether bone remodelling, stimulated by the presence of microdamage and/or strain, removes damaged bone only if the amount of microdamage/strain has exceeded some critical value. This may explain the stimuli for propagation, direction of travel and termination of BMU's, which has not be previously researched.

5.4.2 Mechanical effects of osteoporosis and drug treatment on the mechanical behavior of bone tissue

This is the first study to quantify the effect of osteoporosis and drug treatment on the mechanical behaviour of bone tissue from individual trabeculae. It was found that ovariectomy in rats increases the strength and stiffness of the mineralized tissue that

constitutes trabecular bone relative to normal. It was also found that drug treatment inhibits this increase and normalizes it to control levels; this inhibition was found to be significant at 14, 34 and 54 weeks.

It is perhaps surprising that osteoporotic trabecular bone tissue of individual trabeculae shows a higher yield strength and stiffness than both normal and drug-treated bone tissue. It might be expected that the tissue would become more brittle as a result, and consequently may be less functional in responding to loads. On the contrary however, the results presented in this thesis indicate that, at 34 and 54 weeks post-ovariectomy, the OVX tissue has a significantly higher yield strain than the control bone tissue and there is no difference between the post-yield strain of the OVX tissue compared to control over the course of 54 weeks.

It is intriguing to speculate that the increase in trabecular stiffness may actually cause the degradation of the trabecular architecture during osteoporosis. It is widely accepted that bone remodelling is regulated by mechanical stimuli (Frost, 1986; Lanyon *et al*, 1993; Carter *et al*, 1987; Prendergast and Huiskes, 1996; Huiskes *et al*, 2000; Martin, 2002), and that bone cells are driven to adapt trabecular architecture when changes in loading conditions occur. It is therefore believed that bone cells are sensitive to local changes in either strain or microdamage (Lanyon *et al*, 1993; Huiskes *et al*, 2000; Carter *et al*, 1987; Frost, 1986; Martin, 2002; Prendergast and Huiskes, 1996). If this is true then, when the strength and elasticity are increased during osteoporosis as has been found in this study, the magnitudes of the strain local to the bone cells will change and the bone architecture will adapt as a consequence. Of course the converse situation may equally well be true; i.e. that the increase in the yield strength and stiffness may be due to some mechanism where bone compensates for the decrease in mass by increasing the mechanical properties of the tissue. However, Van der Linden *et al* (2004) undertook computational simulations of bone adaptation and found that, if the stiffness of the bone tissue was increased, the resulting adaptation created a bone structure with lower mass and increased anisotropy. Both of these observations are common features of osteoporotic trabecular architecture, and therefore Van der Linden *et al* (2004) would appear to corroborate the finding that stiffer tissue is an inherent part of osteoporotic bone and that this pathological change in the material may be the root cause of the adaptation of the trabecular architecture that is observed during osteoporosis.

A concern with some HT drugs is that they inhibit the remodelling process resulting in an increase in the amount of old bone, so that, although bone mass is maintained, bone strength at the tissue-level may be impaired. It has been previously been shown that suppressing bone turnover causes an increase in the degree of mineralization of bone tissue (Meunier *et al*, 1997; Boivin *et al.*, 2000) As the degree of mineralization of bone tissue has been previously been linked to bone strength (De Paula *et al*, 2002), this infers that the strength of the drug-treated bone tissue should be stronger than the control bone tissue. However, in this study it was found that the drug-treated bone tissue tended to lower in strength than both the control and OVX bone tissue. This may be an effect of the suppression of osteoclast activity by the hormone treatment (Hall *et al* 1995; Bord *et al*, 2001). Osteoclast activity is believed to preferentially remove aged bone and regulate damage generation in bone tissue (Burr *et al*, 1985; Carter *et al*, 1987; Prendergast and Taylor, 1994). Therefore, suppressing osteoclast activity may cause damage to accumulate in the bone tissue. It has previously been found that accumulation of microdamage reduces bone elastic modulus (Burr *et al*, 1998). Therefore it is proposed that the reduction in strength and elasticity of the drug-treated bone tissue observed in this thesis may be an effect of suppressing osteoclast removal of microdamage. This is corroborated by a study by Hirano *et al* (2000) who observed that suppressing the normal bone remodelling process in bisphosphonate-treated dogs resulted in impaired mechanical strength in lumbar vertebrae, and that this was accompanied by a significant increase in the amount of damage. In the same study they found that a decrease in strength of the rib was not accompanied with a change in the amount of damage; however it should be noted that the vertebrae are important weight-bearing structures in the body, and as such may be subjected to higher loads and consequently more damage than the ribs. Also, in the study of Hirano *et al* (2000), the drug treatment was administered to intact animals that had not undergone ovariectomy. Given that these drugs are administered at the onset of the menopause, i.e. at the onset of estrogen deficiency, it would have been better if the study had compared drug-treated to untreated *osteoporotic* bone tissue.

However, it must be noted that a study by Ederveen *et al* (2001) showed the use of tibolone at a dose equal to that used in this study, resulted in significantly higher (equal to the control-group) compression strength of the vertebral body than the OVX group. This study was performed for 16 months and it would be of interest

to investigate whether longer treatment would result in a reduction in the compression strength of the vertebral body due to drug treatment.

The processes by which osteoporosis and ageing lead to a reduction in bone strength are not well understood. In order to address this problem it is imperative that biomechanical engineers develop an understanding of how the normal bone renewal process maintains bone strength, the mechanism by which a breakdown in this process occurs during osteoporosis, and finally the extent to which conventional drug treatments are capable of halting osteoporosis.

5.4.3 Comparison of mechano-regulation rules for bone remodelling

In this section the four mechano-regulation rules that were proposed in section 4.4 are compared. This allows the adaptation process to be viewed and observations of which mechano-regulation rule allows for the best optimisation of mechanical performance. In each case the use of an osteocyte model over a model where the actor cells are the sensors are compared. Successful bone remodelling is characterised by the following factors:

i. Initiation of a resorption cavity in response to a region of damaged tissue
ii. Refilling of resorption cavity by new bone tissue,
iii. Removal of accumulating micro-damage in order to maintain microdamage burden below homeostatic levels,
iv. Attaining or maintaining homeostatic strain levels (1500 με).

5.4.3.1 Osteocytes vs. Surface cells as mechano-sensors

It was found through these analyses that the osteocyte sensor model was incapable of simulating bone remodelling according to the above criteria. The use of osteocyte sensor cells resulted in incomplete removal of damaged bone tissue and convergence to an unfilled configuration, see Figure 5.6 (a). On the other hand, the surface sensor model was capable of resorbing damaged tissue in all the models investigated and also showed refilling of the cavity in the models that were regulated with strain as part of the remodelling stimulus, see Figure 5.6 (b) for example.

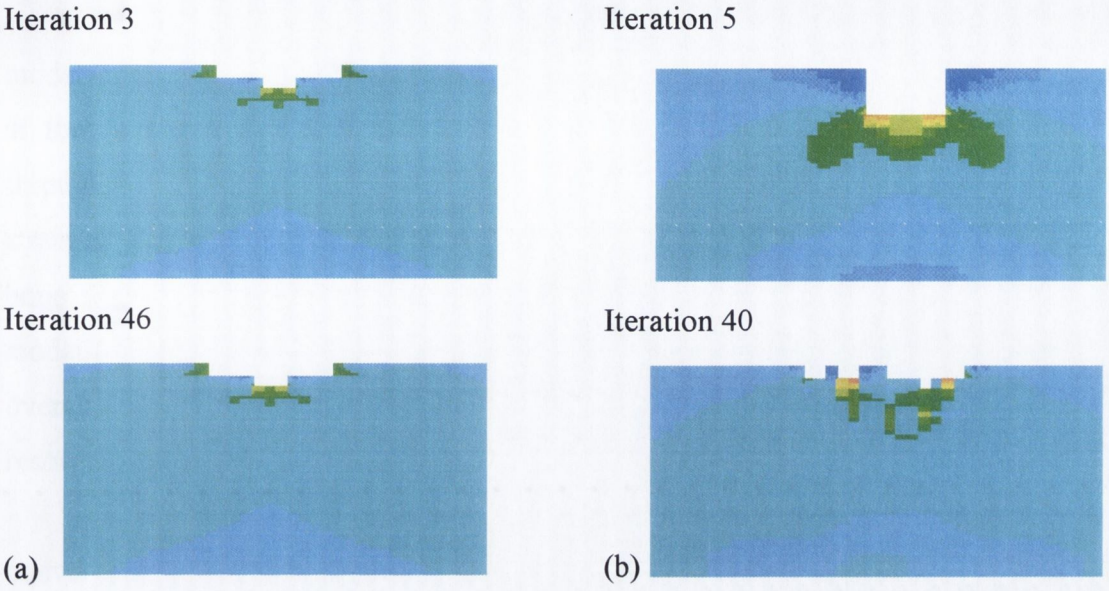

Figure 5.6: *Comparison of remodelling with (a) osteocyte sensors and (b) surface sensors*

The time to perforation of a trabeculum with a critically large resorption cavity took longer than was predicted for the osteocyte sensor model than the surface sensor model. However, it must be noted that the use of osteocyte sensors was capable of responding to the occurrence of damage deep within the bone trabeculum, see Figure 5.7, whereas the surface sensor model was not.

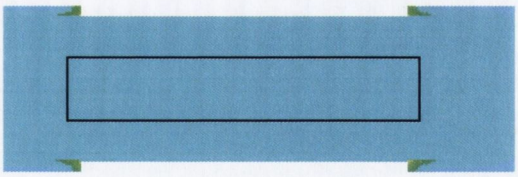

Figure 5.7: *Initiation of resorption due to damaged region deep within trabecular tissue (indicated by box)*

This is important in so far as; in vivo, newer bone tissue is located at the surface of bone trabeculae whereas aged/damaged tissue is deeper within structure. Therefore the osteocyte network could initiate a process of repairing it whereas the surface sensors would not. However, it may be possible that once a BMU is activated the

actor cells themselves regulate the amount of bone resorption and formation that occurs, and effectively take over the role of regulation of BMU activity.

The main difference between these two models is that in the surface based model each cell is only responsive to the mechanical stimulus at its location whereas in the osteocyte based model each actor cell is responsive to mechanical stimuli throughout the tissue. Therefore, for surface based remodelling, if the strain/microdamage in the cell is of sufficient value to signal either bone resorption or bone formation then this process is carried out. However, in the osteocyte-based model, if the strain/microdamage at a particular location is of sufficient value, but the overall stimulus from the entire osteocyte network is not sufficient, then bone resorption or formation is not predicted.

It must be noted that, for the osteocyte based model (Figure 4.32), convergence was predicted while the stimulus was still of value to require bone remodelling. This may be explained by the fact that the signal is additive for the osteocyte model. Therefore, while the signal at a particular location may be sufficient to require bone resorption, the use of an additive signal results in the signal being negated by the signals from other sensor cells in the model where formation or quiescence is predicted. It may be that the choice of the region of influence parameter D was incorrect, and allowed sensor cells at a great distance from the actor cell to have too much of an influence on the actor cell. This question should be tested by variation of the parameter D in future studies. However, the real question about the range of influence can only be addressed by physiological tests.

5.4.3.2 Damage as a mechano-regulatory stimulus

In damage-regulated remodelling, bone resorption only occurs in response to damage. Thus predicted no refilling was possible and complete perforation of the trabecular strut would always occur. It was seen that after 113 iterations perforation of a 10 μm strut occurred. The mechano-regulation governed by damage only is thus incapable of refilling a resorption cavity initiated in response to damage. In the surface sensor model, regardless of the size of the resorption cavity there will always be a resorption process initiated by damage only-regulated model due to the stress concentration at the base of the cavity that may lead to damage in that particular element, see Figure 5.8.

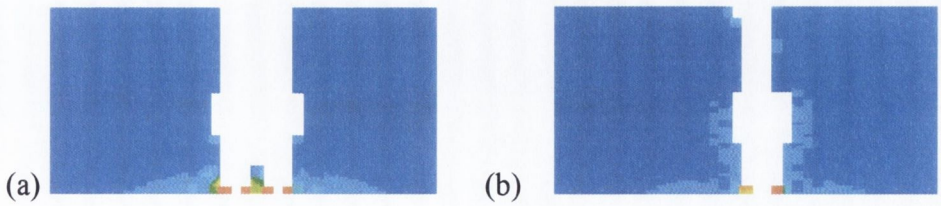

Figure 5.8: *Damage based remodelling with surface sensors of (a) damage region and (b) existing resorption cavity*

For osteocyte-regulated remodelling the damage based remodelling does not completely resorb the damaged region, see Figure 5.9(a) and an existing resorption cavity does not lead to perforation after 100 iterations, see Figure 5.9(b).

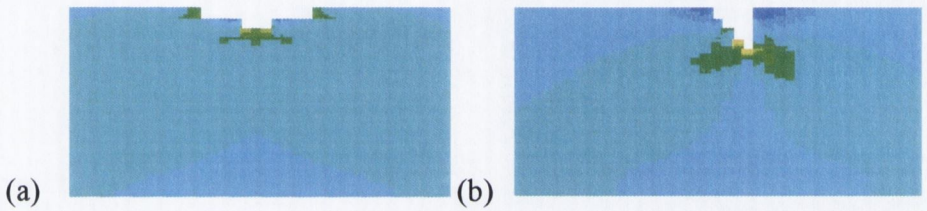

Figure 5.9: *Damage based remodelling with osteocyte sensors of (a) damage region after 30 iterations and (b) existing resorption cavity after 100 Iterations*

5.4.3.3 Strain as a mechano-regulatory stimulus

The strain only model was incapable of responding to regions of damage in the bone tissue. This would result in accumulation of microdamage throughout our lifetime. However it has been observed through experimental testing that bone is capable of repairing regions of damaged tissue. However this model was capable of refilling an existing bone cavity with new bone tissue, but complete refilling was not achieved after 50 iterations, see Figure 5.10.

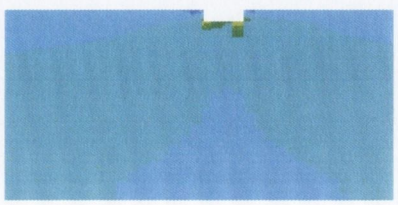

Figure 5.10: *Strain based remodelling with surface sensors of existing resorption cavity (20 μm depth) after 50 iterations*

5.4.3.4 Combination of strain and damage as a mechano-regulatory stimuli

It was predicted that the combined strain and damage mechano-regulation was incapable of fully responding to a region of damaged tissue, and that while resorption did occur it was inhibited by a formation response before all the damage was completely removed. While it was capable of initiating a resorption cavity in response to region of damaged tissue, it was not capable of continuing resorption to the point where all damaged tissue was removed, see Figure 5.11.

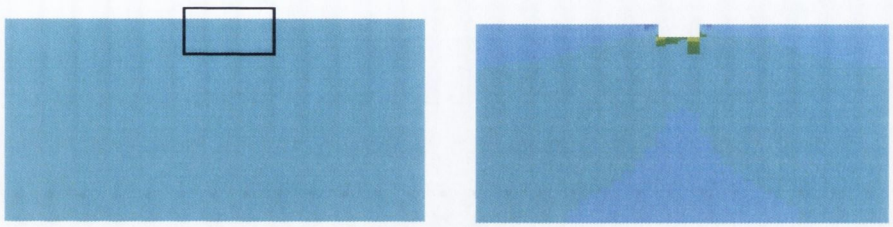

(a) (b)

Figure 5.11: *Combined strain and damage based remodelling with surface sensors of damage region (a) after 50 iterations (b)*

5.4.3.5 Either strain or damage as a mechano-regulatory stimuli, where damage is prioritized

Mechano-regulation in response to *either* strain or microdamage, with damage prioritized when it accumulated above a threshold level, was capable of initiating a resorption cavity, resorbing the complete region of damaged tissue and then refilling the cavity with new bone tissue.

It was predicted that through the use of a surface sensor model in which the stimulus was either strain or damage, and damage was prioritized was capable of

i. Initiating a resorption cavity in response to damage, Figure 5.12(a)
ii. Maintaining microdamage burden below homeostatic levels,
iii. Achieving homeostatic strains,
iv. Refilling an existing cavity, see Figure 5.12(b)

There was a critical depth to which the surface sensor model could repair a resorption cavity.

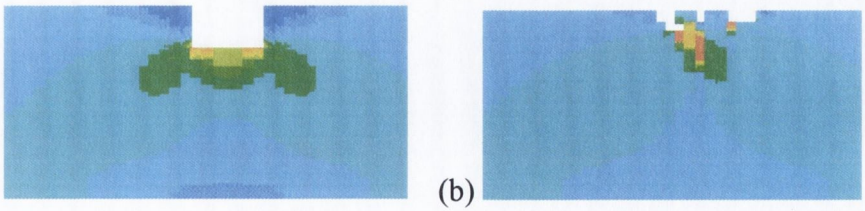

Figure 5.12: *Strain or damage based remodelling with damage as a priority surface in response to (a) damaged region and (b) existing resorption cavity (20 μm depth) after 50 iterations*

5.4.3.6 Critical resorption depth

It was predicted through the results presented in Chapter 4, that a critical resorption depth exists for both of the mechano-regulation rules that include damage. It is interesting that the bone tissue can tolerate resorption cavities to a certain depth but that beyond this, the resorption of bone tissue to remove damage leads to a cascade effect where bone resorption continues until trabecular perforation. The mechanism of trabecular perforation has not been described before and the evidence of the existence of a critical resorption depth that can be repaired by the normal bone remodelling process appears to be strong. This is discussed further in section 5.5.

5.5 On the biomechanics of bone remodelling and osteoporosis

In this thesis, it has been shown experimentally that there is a change in the material properties of the mineralized matrix constituting trabecular bone tissue during osteoporosis. It would appear that the bone tissue during osteoporosis is in fact mechanically stronger than that of healthy bone. Thus the mechanism by which failure occurs may be due only to the deteriorated architecture being incapable of supporting offset loads. This is corroborated by Homminga *et al* (2004) who observed that the osteoporotic trabecular structure behaves similarly to the healthy under loading conditions that represent peak loads during walking, with 8% of trabeculae overloaded in the healthy structure and 9% overloaded in the osteoporotic structure, see Figure 5.13. However under "error loads" as would be generated during forward flexion and lifting they observed that only 4% of trabeculae were overloaded in the healthy bone whereas 13% of trabeculae were overloaded in the osteoporotic bone,

see Figure 5.14. This suggests that the issue of osteoporotic fractures may be due to offset loading conditions that the deteriorated architecture is incapable of supporting.

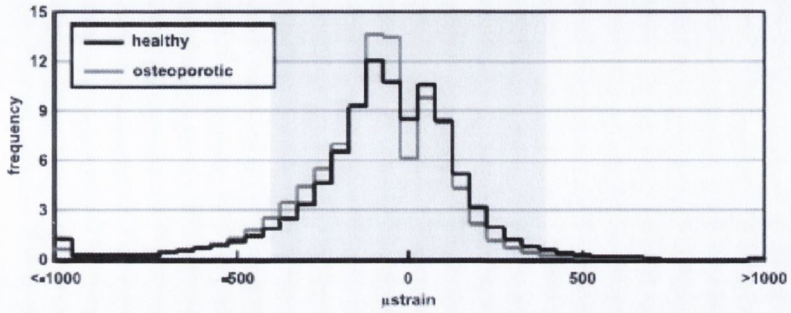

Figure 5.13: *Comparison of strain distribution in healthy and osteoporotic bone under daily loading conditions (Homminga et al, 2004)*

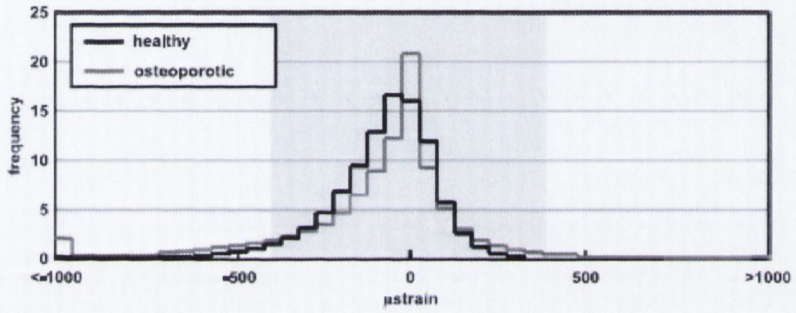

Figure 5.14: *Comparison of strain distribution in healthy and osteoporotic bone under "error" loading conditions (Homminga et al, 2004)*

Through the work of this thesis it has been predicted that, by using an elastic modulus from mechanical testing of osteoporotic bone trabeculae in combination with a mechano-regulation rule that incorporates both strain and microdamage as stimuli for bone turnover, the behaviour of osteoporotic remodelling can be simulated. It is thus proposed that this change in stiffness may alter the stimuli to mechano-sensitive bone cells and cause them to adapt the trabecular architecture erroneously.

A model by Van der Linden *et al* (2003) investigated the effects of different tissue stiffness on trabecular adaptation. Using a mechano-regulation rule that used strain as a stimulus they predicted that the adaptation of trabecular architecture was similar to osteoporotic behaviour if a higher elastic modulus was used to model the constituent bone tissue, see Fig. 5.15. Their findings were that a loss of bone mass and increase in trabecular perforation resulted if the elastic modulus were higher.

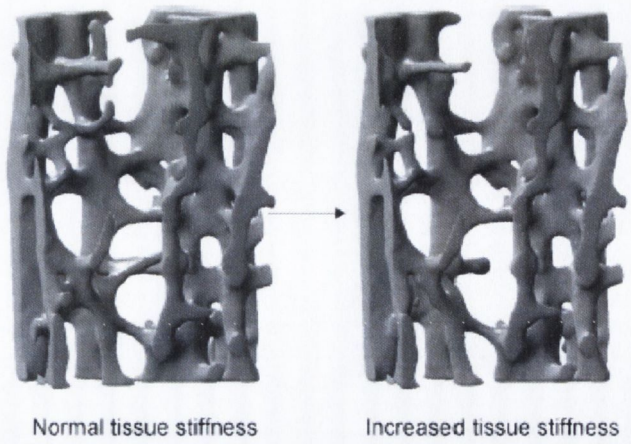

Figure 5.15: *Comparison of remodelling of trabecular architecture of normal and osteoporotic bone after Van der Linden et al (2004)*

In the damage-based mechano-regulation models proposed above, it was observed that the use of a higher elastic modulus resulted in easier trabecular perforation in response to an existing resorption cavity of 20 μm; such a cavity was capable of being refilled if normal tissue properties were used, see Figure 5.16. This perforation is a common observation during osteoporosis (Ito *et al*, 2002).

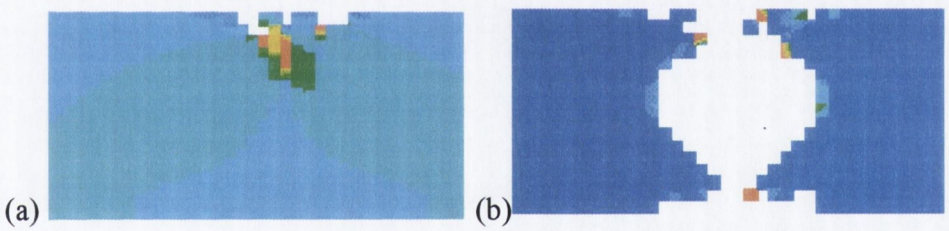

Figure 5.16: *Comparison of predicted remodelling of existing resorption cavity of 20 μm depth using normal and osteoporotic bone material properties*

The mechanism by which osteoporosis may cause a change in material properties is unknown. It is known that during osteoporosis the levels of circulating estrogen are reduced (Rosen, 2000) and that a large increase in osteoclast activity occurs after withdrawal of estrogen (Lane *et al*, 1998; Tremollieres *et al*, 2001). It has been observed that the ratio of mineral to collagen is altered during osteoporosis (Gadeleta *et al*, 2000). Further investigations into how this relationship determines the mechanical performance of the trabecular strut are required to develop a comprehensive understanding of the biomechanics of osteoporotic bone.

The specific problem of the biomechanics of trabecular bone during osteoporosis is that microstructural deterioration of the trabecular architecture occurs by means of trabecular perforation and subsequent disappearance of trabeculae (Ito et al, 2002). Following perforation trabecular connectivity cannot be regained and the

mechanisms that result in trabecular perforation are not fully understood. This leads to a significant reduction in bone strength and ultimately results in fractures of the spine, hip and wrist in sufferers.

Through the simulations presented in section 4.4 it is predicted that two separate mechanisms may be responsible for trabecular perforation during osteoporosis.

The first mechanism is due to an increase in resorption depth. The proposed mechano-regulation rule developed, which is best capable of simulating BMU activity, has a critical resorption depth to which it can refill the resorbed tissue. For larger cavities due to a combination of an increase in microdamage burden and unloading of the trabecular strut perforation occurs. This is interesting if osteoporosis is indeed due to the previously proposed mechanism (Lane *et al*, 1998; Tremollieres *et al*, 2001) of an increase in osteoclast activity by reduction in circulating estrogen levels in the blood following the menopause. This would serve to explain why trabecular perforation occurs during osteoporosis.

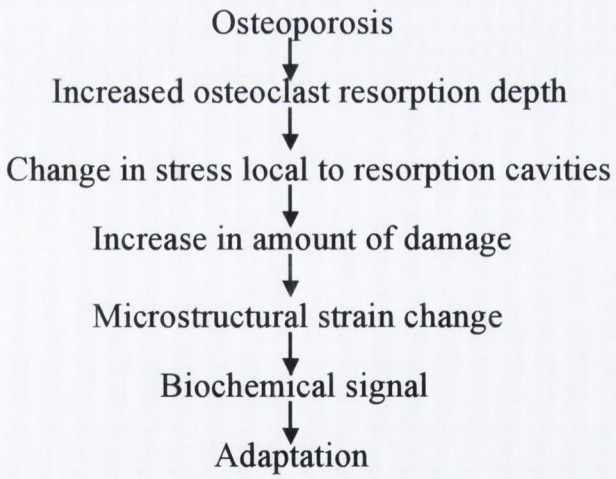

Figure 5.17: *Possible mechanism by which change in resorption depth drives trabecular perforation during osteoporosis*

The second mechanism predicted to result in trabecular perforation is a change in material properties during osteoporosis. If the bone remodelling cells retain their adaptive capacity during osteoporosis and some pathological change alters the material properties then it is predicted that the bone cells will adapt the architecture and lead to perforation of struts that would normally be refilled. This suggests that the initial step of osteoporosis may be due to a change in the material constituting the bone tissue. This also serves to explain why trabecular perforation occurs during

osteoporosis. This biomechanical basis for osteoporosis is supported by the fact that a change in material behaviour was indeed observed in the mechanical testing that was carried out through the work of this thesis.

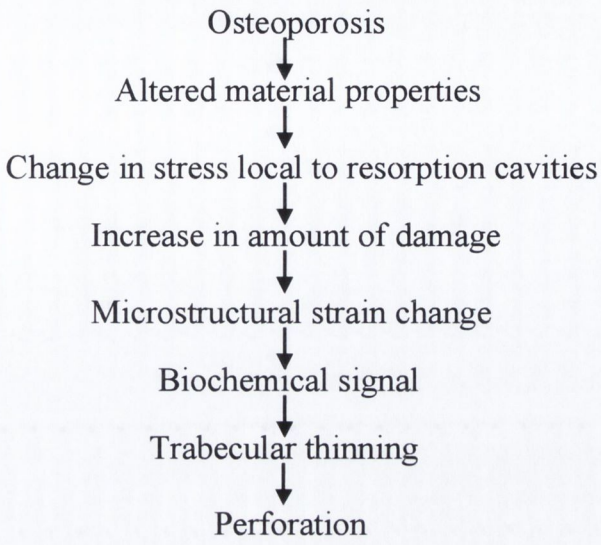

Figure 5.18: *Possible mechanism by which change in mechanical properties drives trabecular adaptation*

5.6 Conclusions

Through mechanical testing an increase in the stiffness and strength of bone tissue during osteoporosis has been observed. The results of the mechanical testing presented in this thesis ultimately require experimental investigation into the degree of differences in mineral and collagen content during osteoporosis and also investigations into the extent of damage present between normal, osteoporotic and drug-treated bone tissue. Such experiments are planned to be part of the Trinity Centre for Bioengineering "Bone for Life" project.

Despite the simplifications and assumptions made in the finite element model of the single bone trabeculae it is clear that the individual bone trabeculae is not an optimised structure and that the variety of stresses and strains observed may certainly play a role in mechano-regulation of BMU's.

The development of a simplified mechano-regulation model of bone remodelling incorporating both strain and microdamage as stimuli has provided evidence to confirm the hypotheses that bone remodelling is driven by a combination of strain and microdamage. A mechano-regulatory rule using both strain and microdamage has successfully predicted many features of the bone remodelling process observed during normal physiology and also during osteoporosis. The model will have to be continually tested by attempting to simulate bone remodelling under a variety of different circumstances; however it does strongly suggest that the mechano-regulation model can be used as a tool to evaluate the mechanisms that drive the normal bone remodelling process.

The model has been used to study the breakdown in the remodelling process during osteoporosis. It has been concluded that the use of this model in conjunction with a change in material properties during osteoporosis is capable of simulating the behaviour of trabecular remodelling during osteoporosis.

From the results of these simulations it is proposed that trabecular perforation during osteoporosis occurs either (i) through an increase in osteoclast activity and subsequently resorption depth that is greater than critical or (ii) through a change in material properties that alter the mechanical stimuli to bone remodelling cells and drive them to perforate for resorption cavities of depths that can be repaired during normal remodelling.

The further applications of a mechano-regulation model that includes both strain and damage responses are immense, and could be used for example in predicting bone remodelling around orthopaedic implants or investigating possible interventions to the bone remodelling process during osteoporosis that might prevent loss of bone strength. New insights into mechano-biology will increase the predictive power of computational models such as that presented here, making them an invaluable tool in the future design of drug treatments and orthopaedic implants.

6. Conclusions

6.1 Main results of this thesis

Using a combination of (a) finite element analyses, (b) mechanical testing and (c) computational simulations three hypotheses were tested and the following results were obtained.

During osteoporosis there is a change in the material properties of bone tissue (stiffness and strength). Suppressing bone turnover using Tibolone treatment normalizes the bone tissue properties (stiffness and strength) of single trabeculae on or slightly below normal levels.

The distribution of stress and strain within individual bone trabeculae is highly heterogeneous. Furthermore stress and strain levels within trabeculae are elevated by resorption cavities to magnitudes that may cause damage. This suggests that the mechanical stimuli that drive bone multi-cellular units (BMUs) to remodel bone trabeculae during normal remodelling may be a combination of damage and local strains.

A mechano-regulation rule that incorporates both strain and damage as stimuli for bone remodelling is capable of initiating a BMU cycle to remove microdamage and refill an existing resorption cavity. This further corroborates the idea that bone cells are sensitive to both strain and microdamage. The results of the application of such a mechano-regulation rule also indicate that, while osteocytes may act as sensors to initiate bone remodelling, the regulation of the BMU activity along a bone trabeculum is governed by the surface cells.

A change in either the mechanical properties or the resorption depth during osteoporosis alters the mechanical stimuli to bone remodelling cells. Simulations of the remodelling process during osteoporosis demonstrate that these changes initiate an over-adaptation of the trabecular architecture and result in trabecular perforation.

6.2 Conclusions

i. Aside from the consequences of osteoporosis on the architecture of bone tissue, there are also more subtle processes ongoing that cause stiffening of bone tissue during osteoporosis.

ii. During normal remodelling a combination of damage and local strains generated 'up and down stream' of resorption lacunae act as mechanical

stimuli to propel the continued activity of a BMU until such a time as a significant amount of the trabeculum is remodelled.

iii. Osteocytes act as sensor cells to initiate the remodelling process, but thereafter the surface cells are capable of regulating the amount of bone resorption and bone formation activity that occurs.

iv. The change in material behaviour during osteoporosis alters the mechanical stimuli received by bone remodelling cells and subsequently drives the defective adaptation of the trabecular architecture that is seen during osteoporosis.

v. Anti-resorptive therapy normalizes the effect of osteoporosis on bone tissue properties.

6.3 *Future Work*

The following recommendations are made for future work on the subject of this thesis:

- Determination of the effect of changes in the levels of estrogen in the blood during osteoporosis on the mineral content in the bone tissue using techniques such as ash content analysis
- Quantify the integrity of the collagen, the quality and the degree of cross-linking between collagen bundles during osteoporosis using histological techniques
- Investigation of the amount of damage generated in drug-treated bone tissue relative to untreated osteoporotic bone tissue using histological techniques. The aim would be to determine whether the normalizing of tissue properties observed in this study is due to an inhibition of bone resorption and subsequent increase in damage burden similar to other anti-resorptive drugs.
- Quantification of the strain in bone trabeculae during tensile testing using high-resolution video microscopy to record specimen displacements.
- Fatigue testing of bone trabeculae to determine the effects of osteoporosis and subsequent drug-treatment on the fatigue behaviour of bone trabeculae
- Quantify comprehensively the biological parameters of bone remodelling using histological techniques
- Incorporate the biological parameters into bone remodelling algorithms

- Investigation of the effects of different loading conditions and magnitudes on the remodelling activity predicted using the proposed mechano-regulation rule. This would perhaps also give an insight into the mechanisms that allow damage accumulation and result in stress fractures under high frequency loading conditions.
- Application of mechano-regulation rule to 3D models of trabecular bone volumes with osteoporotic tissue material properties to determine whether adaptation of the architecture occurs in the same manner as is observed during osteoporosis
- Develop an understanding of the optimal interventions that are necessary for an effective drug treatment to maintain bone strength during osteoporosis, such as inhibiting/promoting bone cell activity or perhaps attempting to change the composition of the tissue.

References

Aspden, R.M., Biomechanics of osteoporotic bone, in Orthopaedic Issues in Osteoporosis, CRC Press, 2003

Bartl, R., 1998, Bisphosphonate, In: Recommendations regarding the diagnostics, therapy and aftercare Multiple Myelom (title translated from German), Bartl, R., Dietzfelbinger, H., Eds, Tumor center Munich

Beaupre, G.S., Orr, T.E., and Carter, D.R., 1990a, An approach for time-dependant bone modeling and remodeling – Theoretical development, Journal of Orthopaedic Research, **8**, 651-661

Beaupre, G.S., Orr, T.E., and Carter, D.R., 1990b, An approach for time-dependant bone modeling and remodeling – Application: A preliminary remodeling simulation, Journal of Orthopaedic Research, **8**, 662-670

Bell, K.L., Loveridge, N. Lunt, M., Lindsay, P. C. and Reeve, J., Oestrogen suppression increases Haversian resorption depth as well as remodelling activity in women with endometriosis, 1996, Bone, **19**, 3, Supplement 1, p. 131S

Birkenhaeger-Frenkel, D., 1987, A significant lack of collagen in osteoporotic bone. In: C. Christiansen, J. Johansen and B. Riis, Editors, International Symposium on Osteoporosis, Norhaven A/S, Denmark, 443–445.

Birkenhager-Frenkel, D.H., Nigg, A.L., Hens, C.J., Birkenhager, J.C., 1993, Changes of interstitial bone thickness with age in men and women, Bone, **14**,3, 211-6.

Boivin, G.Y., Chavassieux, P. M., Santora, A. C., Yates, J. and Meunier, P. J., 2000, Alendronate increases bone strength by increasing the mean degree of mineralization of bone tissue in osteoporotic women, Bone, **27**, 5, 687-694

Bord, S., Beavan, S., Ireland, D., Horner, A. and Compston, J. E., 2001, Mechanisms by which high-dose estrogen therapy produces anabolic skeletal effects in postmenopausal women: role of locally produced growth factors, Bone, **29**, 3, 216-222

Bourrin, S., Ammann, P., Bonjour, J. P. and Rizzoli, R., 2002, Recovery of proximal tibia bone mineral density and strength, but not cancellous bone architecture, after long-term bisphosphonate or selective estrogen receptor modulator therapy in aged rats, Bone, **30**, 1, 195-200

Boyde, A., Compston, J. E., Reeve, J., Bell, K. L., Noble, B. S., Jones, S. J. and Loveridge, N., 1998, Effect of estrogen suppression on the mineralization density of iliac crest biopsies in young women as assessed by backscattered electron imaging, Bone, **22**, 3, 241-250

Boyde, A., Elliott J.C., Jones, S.J., 1993, Stereology and histogram analysis of backscattered electron images: age changes in bone, Bone, **14**,3, 205-10.

Burger, E.H., Klein-Nulend, J. and Smit, T.H., 2003, Strain-derived canalicular fluid flow regulates osteoclast activity in a remodelling osteon—a proposal, 2003, Journal of Biomechanics, **36**, 10, 1453-1459

Burger, E.H., Klein-Nulend, J., 1999, Mechanotransduction in bone--role of the lacuno-canalicular network, FASEB J.; **13,** Suppl: S101-12. Review.

Burr, D.B., Martin, R.B., Schaffler, M.B., Radin, E.L., 1985, Bone remodeling in response to in vivo fatigue microdamage, Journal of Biomechanics, **18**,3, 189-200

Burr, D.B., Turner, C.H., Naick, P., Forwood, M.R., Ambrosius, W, Sayeed Hasan, M. and Pidaparti, R., 1998, Does microdamage accumulation affect the mechanical properties of bone?, Journal of Biomechanics, **31**, 4, 337-345

Carter, D.R. and Caler, W.E, 1981, Uniaxial fatigue of human cortical bone. The influence of tissue physical characteristics, Journal of Biomechanics, **14**, 461-470

Carter, D.R., 1984, Mechanical loading histories and cortical bone remodelling, Calcified Tissue International, **36**, S9-S24

Carter, D.R., Caler, W.E, Spengler, D.M., and Frankel, V.H., 1981, Fatigue behaviour of adult cortical bone: the influence of mean strain and strain rate, Acta Orthop Scand, **52**, 491-490

Carter, D.R., Fyhrie, D.P., and Whalen, R.T., 1987, Trabecular bone density and loading history: regulation of connective tissue biology by mechanical energy, Journal of Biomechanics, **20**, 785-794

Carter, D.R., Hayes, W.C., Schurman, D.J., 1976, Fatigue life of compact bone--II. Effects of microstructure and density, Journal of Biomechanics, **9**, 4, 211-8.

Carter, D.R., Orr, T.E., Fyhrie, D.P., 1989, Relationships between loading history and femoral cancellous bone architecture, Journal of Biomechanics, **22**,3,231-44

Chambers, T.J., Fox, S., Jagger, C.J., Lean, J.M. and Chow, J.W.M., 1999, The role of prostaglandins and nitric oxide in the response of bone to mechanical forces, Osteoarthritis and Cartilage , **7,** 4, 422-423

Choi, K., and Goldstein, S.A., 1992, A comparison of the fatigue behaviour of Human trabecular and cortical bone tissue, Journal of Biomechanics, **25**, 12, 1371-1381

Choi, K., Kuhn, J.L., Ciarelli, M.J., Goldstein, S.A., 1990, The elastic moduli of human subchondral, trabecular, and cortical bone tissue and the size-dependency of cortical bone modulus, Journal of Biomechanics, **23**, No. 11, 1103-1113

Cohen-Solal, M.E., Shih, M.S., Lundy, M.W. and Parfitt AM., A new method for measuring cancellous bone erosion depth: application to the cellular

mechanisms of bone loss in postmenopausal osteoporosis, 1991, Journal of Bone and Mineral Research; **6**, 12,1331-8

Compston, J.E., Mellish, R.W.E., Croucher, P.I., and Garrahan, N.J., 1989, Structural mechanisms of trabecular bone loss in man, Bone Miner, **6**: 339-350

Compston, J.E., Rosen, C.J., 2002, Osteoporosis, 3rd Edition, Oxford: Health Press

Cooper, C. and Melton, LJ. III, 1992, Epidemiology of osteoporosis, Trends Endocrinol Metab, **3**,224-229

Cowin, S.C., 1999, Bone poroelasticity, Journal of Biomechanics, **32**, 3, 217-238

Cowin, S.C., and Hegedus, D.H., 1976, Bone remodelling I: theory of adaptive elasticity, Journal of Elasticity, **6**, No. 3, 313-326

Cowin, S.C., and Van Buskirk, W.C., 1979, Surface bone remodeling induced by a medullary pin, Journal of Biomechanics, 12,4,269-76

Cowin, S.C., Moss-Salentijn, L., and Moss, M.L., 1991, Candidates for the mechanosensory system in bone, ASME Journal of Biomechanical Engineering, **113**, 191 – 197

Cowin, S.C., Weinbaum, S. and Zeng, Yu, 1995, A case for bone canaliculi as the anatomical site of strain generated potentials, Journal of Biomechanics, **28**, 11, 1281-1297

Cummings, S.R, Kelsey, J.L, Nevitt, M.C., O' Dowd, K.J., 1985, Epidemiology of osteoporosis and osteoporotic fractures. Epdemiol Rev; **7**, 178-208

Cummings, S.R., Melton, L.J., 2002, Epidemiology and outcomes of osteoporotic fractures, Lancet, **18**,359(9319): 1761-7

Currey, J.D, Brear, K., Zioupos, P., 1994, Dependence of mechanical properties on fibre angle in narwhal tusk, a highly oriented biological composite, Journal of Biomechanics, **27**,7, 885-97.

Currey, J.D., 1984, Bones: structure and mechanics, Princeton, N.J. ;Oxford: Princeton University Press, re-published 2002

Currey, J.D., 1984b, Effects of differences in mineralization on the mechanical properties of bone, Philosophical Transactions of the Royal Society of London, Series B., Biological Sciences, **304**, 1121, 509-518

Dalle Carbonare, L., and Giannini, S., 2004, Bone microarchitecture as an important determinant of bone strength, Journal of Endocrinological Investigations, 27, 1, 99 – 105

Dempster DW, Shane E, Horbert W, Lindsay R., 1986, A simple method for correlative light and scanning electron microscopy of human iliac crest bone biopsies: qualitative observations in normal and osteoporotic subjects, Journal of Bone and Mineral Research; **1**, 1, 15-21.

Dempster W.T., Liddicoat, R.T., 1952, Compact bone as a non-isotropic material, Am Journal of Anatomy. 1952; **91,**3,331-62

DePaula, C.A., Abjornson, C., Pan, Y., Kotha, S.P., Koike, K. and Guzelsu, N., 2002, Changing the structurally effective mineral content of bone with in vitro fluoride treatment, Journal of Biomechanics, **35**, 3, 355-361

Dickenson, R.P., Hutton, W.C. and Stott, J.R., 1981, The mechanical properties of bone in osteoporosis. Journal of Bone and Joint Surgery British, **63**-B 2, 233–238.

Ederveen, A.G.H., Spanjers, C.P.M., Quaytaal, J.H.M. and Kloosterboer, H.J., 2001, Effect of 16 months of treatment with tibolone on bone mass, turnover, and biomechanical quality in mature ovariectomized rats, Journal of Bone and Mineral Research, **16**, 1674–1681

el Haj, A.J., Minter, S.L., Rawlinson S.C., Suswillo, R., Lanyon, L.E., Cellular responses to mechanical loading in vitro, Journal of Bone and Mineral Research, **5**,9, 923-32

Eriksen, E.F., and Kassem, M., The cellular basis of bone remodelling, in The changing Architecture of the skeleton, Triangle, Sandoz Journal of Medical Science, **31**, 2/3, 1992

Flora, L., Hassing, G.S., Cloyd, G.G., Bevan, J.A., Parfitt, A.M., Villanueva, A.R., 1981, The long-term skeletal effects of EHDP in dogs, Metab Bone Dis Relat Res.; **3**,4-5, 289-300

Frost, H.L, 1960, Presence of Microscopic Cracks in Vivo in Bone, Henry Ford Hospital Med. Bulli, **8**, 25-35

Frost, H.M., 1986, Intermediary Organization of the Skeleton, CRC Press, Boca Raton, FL

Fyhrie, D.P. and Carter, D.R., Femoral head apparent density distribution predicted from bone stresses, 1990, Journal of Biomechanics, **23**,1,1-10.

Gadeleta, S.J., Boskey, A.L., Paschalis, E., Carlson, C., Menschik, F., Baldini, T., Peterson, M. and Rimnac, C.M., 2000, A physical, chemical, and mechanical study of lumbar vertebrae from normal, ovariectomized, and nandrolone decanoate-treated cynomolgus monkeys (macaca fascicularis), Bone, **27**, 4, 541-550

Goldstein S.A, Goulet R, McCubbrey D., 1993, Measurement and significance of three-dimensional architecture to the mechanical integrity of trabecular bone, Calcified Tissue International; **53**, Suppl 1:S127-32; discussion S132-3

Gottesman, T. and Hashin, Z., 1980, Analysis of viscoelastic behaviour of bones on the basis of microstructure, Journal of Biomechanics; **13**,2, 89-96

Guo, X.E., McMahon, T.A., Keaveny, T.M., Hayes, W.C., Gibson, L.J., 1994, Finite element modeling of damage accumulation in trabecular bone under cyclic Loading, Journal of Biomechanics, **27**, 2, 145-155

Hall, T.J., Nyugen H., Schaueblin M. and Fournier B., 1995, The bone-specific estrogen centchroman inhibits osteoclastic bone resorption in vitro, Biochemical and Biophysical Research Communications, **216**, 2, 662-668

Harrigan, T.P., Jasty, M., Mann, R.W., Harris, W.H., 1988, Limitations of the continuum assumption in cancellous bone. Journal of Biomechanics; 21, 4, 269-75

Hart, R.T, 2001, Bone modeling and remodeling, theories and computation, in: Cowin, S.C. (ed.), Bone Mechanics Handbook, Chapter 31, CRC Press, Boca Raton

Hertzberg, R.W., Tensile response of materials, in Deformation and Fracture Mechanics of Engineering Materials, Fourth Edition, 1996

HIPE (Hospital In-Patient Enquiry) Report 2002, Activity in acute public hospitals in Ireland, 1990 –1999, The Economic and Social Research Institute, ISBN: 0707002087

Hirano, T., Turner, C.H., Forwood, M.R., Johnston, C. C. and Burr, D. B., 2000, Does suppression of bone turnover impair mechanical properties by allowing microdamage accumulation?, Bone, **27**, 1, 13-20

Hodgskinson, R., Currey, J.D., Evans, G.P., 1989, Hardness, an indicator of the mechanical competence of cancellous bone, Journal of Orthopaedic Research; 7,5, 754- 8.

Homminga, J., Mccreadie, B.R., Weinans, H., Huiskes, R., 2003, The dependence of the elastic properties of osteoporotic cancellous bone on volume fraction and fabric, Journal of Biomechanics, **36**, 10, 1461-1467

Homminga, J., Van-Rietbergen, B., Lochmüller, E. M., Weinans, H., Eckstein, F. and Huiskes, R., 2004, The osteoporotic vertebral structure is well adapted to the loads of daily life, but not to infrequent "error" loads, Bone, **34**, 3, 510-516

Homminga, J., Weinans, H., van Rietbergen, B., Ruegsegger, P. and Huiskes, R., 1998, Trabecular bone from osteoporotic patients is stiffer than expected, Journal of Biomechanics, **31**, 1, p. 153

Hu, J. H., Ding, M., Søballe, K., Bechtold, J. E., Danielsen, C. C., Day, J. S. and Hvid, I., 2002. Effects of short-term alendronate treatment on the three-dimensional microstructural, physical, and mechanical properties of dog trabecular bone, Bone, **31**, 5, 591-59

Huiskes, R., and Hollister, S.J., 1993, From structure to process, from organ to cell: Recent developments of FE-analysis in orthopaedic biomechanics. ASME Journal of Biomechanical Engineering, **115**, 520-527

Huiskes, R., Ruimerman, R., van Lenthe, G.H., Janssen, J.D., 2000, Effects of mechanical forces on maintenance and adaption of form in trabecular bone, Nature, **405**, 704-706

Huiskes, R., Weinans, H., Grootenboer, H.J., Dalstra, M., Fudala, B., Slooff, T.J., 1987, Adaptive bone-remodeling theory applied to prosthetic-design analysis, Journal of Biomechanics, **20**, 11-12,1135-50

Huja, S.S., Sayeed Hasan, M., Pidaparti, R.M, Turner, C.H., Garetto, L.P., Burr, D.B., 1999, Development of a fluorescent light technique for evaluating Microdamage in bone subjected to fatigue loading, Journal of Biomechanics, **32**, 1243-1249

Ito, M., Nishida, A., Nakamura, T., Uetani, M. and Hayashi, K., 2002, Differences of three-dimensional trabecular microstructure in osteopenic rat models caused by ovariectomy and neurectomy, Bone, **30**, 4, 594-598

Jaworski, Z.F.G., Lok, E. and Wellington, J.L., 1975, Impaired osteoclastic function and linear bone erosion rate in secondary hyperparathyroidism associated with chronic renal failure, Clinical Orthopedics, 107, 298-310

Jee, W.S.S., 2001, Integrate Bone Tissue Physiology, In: Bone Mechanics Handbook, Cowin, S.C. (Ed.), Chapter 1, CRC Press, Boca Raton

Jessop, H.L., Suswillo, R.F., Rawlinson, S.C., Zaman, G., Lee, K., Das-Gupta, V., Pitsillides, A.A., and Lanyon, L.E., 2004, Osteoblast-like cells from estrogen receptor alpha knockout mice have deficient responses to mechanical strain, Journal of Bone and Mineral Research, **19**, 6, 938 - 946

Kanis, J.A., 1998, Pathophysiology of osteoporosis, Pathophysiology, **5**, 1, June 1998, p. 129

Kasugai, Y., Ikegami, A., Matsuo, K., Ohashi, M., Sukamoto, T., Hosoi, T., Ouchi, Y. and Orimo, H., 1998, Effects of tibolone (Org OD14) treatment for 3 Months on ovariectomy-induced osteopenia in 8-month-old rats on a low-calcium diet: Preventive Testing for 3 Months, Bone, **22**, 2, 119-124

Keaveny, T.M., 2001, Strength of trabecular bone, In: Bone mechanics handbook, Cowin, S.C. (Ed.), Chapter 16, CRC Press, Boca Raton

Keaveny, T.M., Borchers, R.E., Gibson, L., and Hayes, C., 1993, Trabecular bone modulus and strength can depend on specimen geometry, Journal of Biomechanics, **26**, 8, 991-1000

Keaveny, T.M., Pinilla TP, Crawford RP, Kopperdahl DL, Lou, A., 1997, Systematic and random errors in compression testing of trabecular bone, Journal of Orthopaedic Research; **15**,1, 101-10

Keaveny, T.M., Wachtel, E.F., Ford, C.M. and Hayes, W.C., 1994, Differences between the tensile and compressive strengths of bovine tibial trabecular bone depend on Modulus, Journal of Biomechanics, **27**, 9, 1137-1146

Kimmel, D.B., 1996, Animal models for in vivo experimentation in osteoporosis research, In: Osteoporosis, Marcs, R., Feldman, D., and Kelsey, J., Eds., Academic Press, San Diego, Chapter 33

Kloosterboer, H.J. and Ederveen, A.G.H., 2002, Pros and cons of existing treatment modalities in osteoporosis: a comparison between tibolone, SERMs and estrogen (±progestogen) treatments, The Journal of Steroid Biochemistry and Molecular Biology, **83**, 1-5, 157-165

Kopperdahl, D.L. and Keaveny, T.M., 1998, Yield strain behaviour of trabecular bone, Journal of Biomechanics, **31**, 601-608

Kothari, M., Keaveny, T.M., Lin, J.C., Newitt, D.C., and Majumdar, S., 1999, Measurement of intraspecimen variations in vertebral cancellous bone architecture, Bone. **25**, 2, 245-250

Kuhn, J.L., Goldstein, S.A., Choi, K., London, M., Feldkamp, L.A., and Matthews, L.S., 1989, Comparison of the trabecular and cortical tissue moduli from human iliac crests, Journal of Orthopaedic Research, 7, 876-884

Lane, N.E., Thompson, J.M., Haupt, D., Kimmel, D.B., Modin, G., Kinney, J.H., 1998, Acute changes in trabecular bone connectivity and osteoclast activity in the ovariectomized rat in vivo, Journal of Bone and Mineral Research, **13**, 2, 229-36

Lanyon, L.E., 1993, Osteocytes, strain detection, bone modelling and remodelling. Calcified Tissue International, **53**, Suppl 1: S102-S106

Lee, T.C., Arthur. T.L., Gibson, L.J. and Hayes, W.C., 2000, Sequential labelling of microdamage in bone using chelating agents, Journal of Orthopaedic Research, **18**, 322-325

Lee, T.C., O'Brien, F.J., Taylor, D., 2000, The nature of fatigue damage in bone, International Journal of Fatigue, **22**, 847-853

Lee, T.C., Staines, A., and Taylor, D., 2002, Bone adaptation to load: microdamage as a stimulus for bone remodelling, Journal of Anatomy, **201**, 436-446

Li, B. and Aspden, R.M., 1997a, Material properties of bone from the femoral neck and calcar femorae of patients with osteoporosis or osteoarthritis, Osteoporosis International, 7, 5, 450–456

Li, B. and Aspden, R.M., 1997b, Mechanical and material properties of the subchondral bone plate from the femoral head of patients with osteoarthritis or osteoporosis, Ann Rheum Dis.; **56**,4, 247-54.

Linde, F., and Sorensen, H.C., 1993, The effect of different storage methods on the Mechanical Properties of Trabecular Bone, Journal of Biomechanics, **26**, 10, 1249-1252

Lucchinetti, E., Dense bone tissue as a molecular composite, In: Bone Mechanics Handbook, Cowin, S.C. (Ed.), , Chapter 13, CRC Press, Boca Raton

Lucchinetti, E., Thomann, D., and Danuser, G., 2000, Micromechancial testing of bone trabeculae – potentials and limitations, Journal of Materials Science, **35**, 6057-6064

Manfredini, P., Cocchetti, G., Maier, G., Redaelli, A. and Montevecchi, F. M., 1999, Poroelastic finite element analysis of a bone specimen under cyclic loading, Journal of Biomechanics, **32**, 2, 135-144

Martin, R.B., 2002, Is all cortical bone remodelling initiated by microdamage?, Bone, **30**, 1, 8-13

Martin, R.B., and Burr, D.B., 1989, The structure, function and adaptation of cortical bone, Raven Press, New York

Martin, R.B., and Burr, D.B., 1998, Skeletal biology, In: Skeletal tissue mechanics, Springer, New York

Martini, F., 1998, The Skeletal System, In: Fundamentals of Anatomy & Physiology, Prentice Hall, New Jersey

McNamara, B.P., Taylor, D., Prendergast, P.J., 1997, Computer prediction of adaptive bone remodelling around noncemented femoral prostheses: the relationship between damage-based and strain-based algorithms, Medical Engineering & Physics; **19**,5, 454-63.

McNamara, L.M., Prendergast, P.J., Lyons, C.J., Ederveen, A.G.H. and Weinans, H., 2003, Strength of single rat trabeculae in normal, ovariectomized and drug treated bone during ageing, accepted for oral presentation at the 50th Annual Meeting of the Orthopaedic Research Society, San Francisco, California, 2004

McNamara, L.M., Prendergast, P.J., O Kelly, K., and Lyons, C.J., Micro-mechanical, 2002, Micro-tensile testing of individual trabeculae from normal, ageing and ovarectomized rat bones, Proceedings of the 4th World Congress of Biomechanics, Calgary, Canada

McNamara, L.M., Van der Linden, J. C. Weinans, H. and Prendergast, P.J., 2003, Stresses high enough to cause microdamage occur near resorption cavities in rat

trabeculae and suggest that trabecular remodelling may be damage driven, Journal of Biomechanics (submitted)

Mente, P.L., and Lewis, J.L., 1989, Experimental method for the measurement of the elastic modulus of trabecular bone tissue, Journal of Orthopaedic Research, **7**, 456-461

Meunier, P.J. and Boivin, G., 1997, Bone mineral density reflects bone mass but also the degree of mineralization of bone: Therapeutic Implications, Bone, **21**, 5, 373-377

Michel, M.C, Guo, X.D, Gibson, L.J, McMahon, T.A, Hayes, W.C., 1993 Compressive fatigue behavior of bovine trabecular bone, Journal of Biomechanics; **26**, 4-5, 453-63

Mori, S., Burr, D.B., 1993, Increased intracortical remodeling following fatigue damage, Bone, 14, 2,103-9.

Mori, S., Harruff, R., Ambrosius, W. and Burr, D. B., 1997, Trabecular bone volume and microdamage accumulation in the femoral heads of women with and without femoral neck fractures, Bone, **21**, 6, 521-526

Mosekilde, L., Danielsen, C.C. Søgaard, C.H. McOsker, J.E. and Wronski, T.J., 1995, The anabolic effects of parathyroid hormone on cortical bone mass, Dimensions and Strength--Assessed in a Sexually Mature, Ovariectomized Rat Model, Bone, **16**, 2, 223-230

Mullender, M.G., and Huiskes, R., 1997. Osteocytes and bone lining cells: which are the best candidates for mechano-sensors in cancellous bone?, Bone, **20**, No.6, 527-532

Mullender, M.G., Huiskes, R. and Weinans, H., 1994. A physiological approach to the simulation of bone remodelling as a self-organizational control process, Journal of Biomechanics, **27**, 1389-1394

Muller, R. and Ruegsegger, P., 1995, Three-dimensional finite element modelling of non-invasively assessed trabecular structures, Medical Engineering & Physics, **17**, 2, 126-133

Muller, R., and Ruegsegger, P., 1996, Analysis of mechanical properties of cancellous bone under conditions of simulated bone atrophy, Journal of Biomechanics, **29**, 8, 1053-1060

Nicholson, P.H., Cheng, X.G., Lowet, G., Boonen, S., Davie, M.W., Dequeker, J. and Van der Perre, G., 1997, Structural and material mechanical properties of human vertebral cancellous bone, Medical Engineering & Physics, **19**, 8, 729-737

Noble, B., 2003, Bone microdamage and cell apoptosis, Eur Cell Mater, 21; 6:46-55

O'Brien, F.J., Taylor, D., Dickson, G.R. and Lee, T.C., 2000, Visualisation of three dimensional microcracks in compact bone, Journal of Anatomy, **197**, 413-420

Odgaard, A., 1997, Three dimensional methods for quantification of cancellous bone architecture, Bone, **20**, 4, 315-328

Papathanasopoulou, V.A., Fotiadis, D.I., Foutsitzi, G. and Massalas, C.V., A poroelastic bone model for internal remodeling, 2002, International Journal of Engineering Science, **40**, 5, 511-530

Parfitt, A.M., 1984, The cellular basis of bone remodelling: The quantum concept re-examined in light of recent advances in the cell biology of bone, Calcified Tissue International, **36**, S37-S45

Parfitt, A.M., Mundy, G.R., Roodman, G.D., Hughes, D.E., Boyce, B.F., 1996, A new model for the regulation of bone resorption, with particular reference to the effects of bisphosphonates, Journal of Bone and Mineral Research, **11**,2, 150-9

Pidaparti, R.M., Chandran, A., Takano, Y., Turner, C.H., 1996, Bone mineral lies mainly outside collagen fibrils: predictions of a composite model for osteonal bone, Journal of Biomechanics, **29**,7, 909-16.

Pidaparti, R.M.V, 1997, Microdamage simulation in a bone tissue using finite element analysis, Computers and Structures, **62**, 3, 463-466

Pietschmann, P., Resch, H., and Peterlik, M., 2003, Etiology and pathogenesis of osteoporosis, in: An, Y.H. (ed.), Orthopaedic Issues in Osteoporosis, Chapter 1, CRC Press, Boca Raton

Prendergast, P.J. and Taylor, D., 1994, Prediction of bone adaptation using damage accumulation, Journal of Biomechanics, **27**, 8, 1067-1076

Prendergast, P.J., 2002, Mechanics applied to skeletal ontogeny and phylogeny, Meccanics, **37**, 317-334

Prendergast, P.J., and Huiskes, R., 1996, Microdamage and osteocyte-lacuna strain in bone: A microstrucutral finite element analysis, 1996, J Biomech Eng., **118**,2, 240-6.

Prendergast, P.J., Huiskes R, 1995, Mathematical modelling of microdamage in bone remodelling and adaptation, In Bone Structure and Remodelling [ISBN 981-02-2190-8]. A. Odgaard & H. Weinans (Eds.), 213-224, World Scientific Publishers: Singapore

Randell, K.M., Honkanen, R.J., Kroger, H., Saarikoski, S., 2002, Does hormone-replacement therapy prevent fractures in early postmenopausal women? , Journal of Bone and Mineral Research; **17**,3, 528-33

Recker, R.R., 1993, Architecture and vertebral fracture, Calcified Tissue International, **53**, Supplement 1: S139 –142

Reilly, G.C, 2000, Observations of microdamage around osteocyte lacunae in bone, Journal of Biomechanics, **33**, 1131-1134

Reilly. D.T. and Burstein, A.H., The elastic and ultimate properties of compact bone tissue, Journal of Biomechanics, **8**,6, 393-405

Rho, J.Y., Ashman, R.B., and Turner, C.H., 1993, Young's modulus of trabecular and cortical bone material: Ultrasonic and microtensile measurements, Journal of Biomechanics, **26**, 2, 111-119,1993

Rho, J.Y., Tsui, T.Y. and Pharr, G.M., 1997, Elastic properties of human cortical and trabecular lamellar bone measured by nanoindentation, Biomaterials; **18**, 20, 1325-30.

Rho, Jae-Young, Kuhn-Spearing, Liisa and Zioupos, Peter, Mechanical properties and the hierarchical structure of bone, 1998, Medical Engineering & Physics, **20**, 2, 92-102

Rosen, C.J., 2000, Pathogenesis of osteoporosis, Baillieres Best Pract Res Clin Endocrinol Metab; **14**,2, 181-93.

Runkle, J.C., and Pugh, J., 1975, The micro-mechanics of cancellous bone: II. Determination of the elastic modulus of individual trabeculae by a buckling analysis, Bulletin of the Hospital of Joint Disorders, 36, 2-10

Ryan, S.D, and Williams, J.L., 1989, Tensile testing of rodlike trabeculae excised from bovine femoral bone, Journal of Biomechanics, **22**, 4, 351-355

Samelin, N., Koller, W., Ascherl, R. and Gradinger, R., 1996. A method of determining biomechanical properties of trabeculae and other tissue obtained from cancellous bone, Biomedizinische Technik, **41**, 7-8, 203-208

Seeman, E., 2003, The structural and biomechanical basis of the gain and loss of bone strength in women and men, Endocrinology and metabolism clinics of North America, **32**, 1, 25 - 38

Seeman, E., Tsalamandris, C., Bass, S. and Pearce, G., 1995, Present and future of osteoporosis therapy, Bone, **17**, 2, Supplement 1, S23-S29

Smit, T.H, and Burger, E.H., 2000, Is BMU-coupling a strain-regulated phenomenon? A finite element analysis, Journal of Bone and Mineral Research, **15**, 2, 301-307

Smit, Theo H., Huyghe, Jacques M. and Cowin, Stephen C., Estimation of the poroelastic parameters of cortical bone, 2002, Journal of Biomechanics, **35**, 6, 829-835

Steck, R., Niederer, P. and Knothe Tate, M. L., 2000, A finite difference model of load-induced fluid displacements within bone under mechanical loading, Medical Engineering & Physics, **22**, 2, 117-125

Sugita, H., Oka, M., Toguchida, J. Nakamura, T., Ueo, T. and Hayami, T., 1999, Anisotropy of osteoporotic cancellous bone, Bone, **24**, 5, 513-516

Taylor, D., Hazenberg, J.G., Lee, T.C., 2003, The cellular transducer in damage-stimulated bone remodelling: a theoretical investigation using fracture mechanics, Journal of Theoretical Biology, **225**, 1, 65 - 75

Taylor, D., Stress fractures in bone: Predicting incidence and risk factors, 2004, Proceedings of the Tenth Annual Conference of the Section of Bioengineering of the Royal Academy of Medicine in Ireland, p. 1

Teramura, K., Fukushima, S., Iwai, T., Nozaki, K., Kokubo, S. and Takahashi, K., 2002, Incadronate inhibits osteoporosis in ovariectomized rats, European Journal of Pharmacology, **457**, 1, 51-56

Thomsen, J.S., Mosekilde, L., Boyce, W., and Mosekilde, E., 1994, Stochiastic simulation of vertebral trabecular bone remodelling, Bone, **15**, 6, 655-666

Townsend, P.R., Rose, R.M., and Radin, E.L., 1975. Buckling studies of single human trabeculae, Journal of Biomechanics, **8**, 199-201

Tremollieres, F.A., Pouilles, J.M., Ribot, C., 2001, Withdrawal of hormone replacement therapy is associated with significant vertebral bone loss in postmenopausal women, Osteoporosis International, **12**, 5, 385-90

Turner, C.H., Rho, J., Takano, Y., Tsui, T.Y., Pharr, G.M., 1999, The elastic properties of trabecular and cortical bone tissues are similar: results from two microscopic measurement techniques, Journal of Biomechanics; **32**,4,437-41

Ulrich, D., van Rietbergen, B., Weinans, H. and Rüegsegger, P., 1998, Finite element analysis of trabecular bone structure: a comparison of image-based meshing techniques, Journal of Biomechanics, **31**, 12, 1187-1192

Van der Linden, J.C., 2002, PhD Thesis, Interactions between remodeling, architecture and tissue properties, Chapter 5, Erasmus University Rotterdam

Van der Linden, J.C., Birkenhager-Frenkel, D.H., Verhaar, J.A., Weinans, H., 2001a, Trabecular bone's mechanical properties are affected by its non-uniform mineral distribution, Journal of Biomechanics; **34**,12, 1573-80

Van der Linden, J.C., Day, J.S., Verhaar, J.A.N. and Weinans, H., 2004, Altered tissue properties induce changes in cancellous bone architecture in aging and diseases, Journal of Biomechanics, **37**, 3, 367-374

Van der Linden, J.C., Homminga, J., Verhaar, J.A, Weinans, H., 2001b, Mechanical consequences of bone loss in cancellous bone, Journal of Bone and Mineral Research, **16**, 3, 457-65.

Van Rietbergen, B., Müller, R., Ulrich, D., Rüegsegger, P. and Huiskes, R., 1999, Tissue stresses and strain in trabeculae of a canine proximal femur can be quantified from computer reconstructions, Journal of Biomechanics, **32**, 2, 165-173

Van Rietbergen, B., Weinans, H., Huiskes, R. and Odgaard, A., 1995, A new method to determine trabecular bone elastic properties and loading using micromechanical finite-element models, Journal of Biomechanics, **28**, 1, 69-81

Vashishth, D., Koontz, J., Qiu, S.J., Lundin-Cannon, D., Yeni, Y.N., Schaffler, M.B., and Fyhrie, D.P., 2000a, In vivo diffuse damage in human vertebral trabecular bone, Bone, **26**, 2, 147-152

Vashishth, D., Verborgt, O., Divine, G., Schaffler, M.B., Fyhrie, D.P., 2000b, Decline in osteocyte lacunar density in human cortical bone is associated with accumulation of microcracks with age, Bone, 26,4,375-80

Verborgt, O., Gibson, G.J., Schaffler, M.B., 2000, Loss of osteocyte integrity in association with microdamage and bone remodeling after fatigue in vivo, Journal of Bone and Mineral Research; **15**,1, 60-7.

Waarsing, J.H., Day, J.S., van der Linden, J.C., Ederveen, A.G., Spanjers, C., De Clerck, N., Sasov, A., Verhaar, J.A.N. and Weinans, H., 2004, Detecting and tracking local changes in the tibiae of individual rats: a novel method to analyse longitudinal in vivo micro-CT data, Bone, **34**, 1, 163-169

Weinans, H., Huiskes, R., Grootenboer, H.J., 1992, The behavior of adaptive bone-remodeling simulation models, Journal of Biomechanics, **25**,12,1425-41.

Weinbaum, S., Cowin, S.C., Zeng, Y., 1994, A model for the excitation of osteocytes by mechanical loading-induced bone fluid shear stresses, Journal of Biomechanics; **27**,3,339-60

Wenzel, T.E., Schaffler, M.B., and Fyhrie, D.P., 1996, In vivo trabecular microcracks in human vertebral bone, Bone, **19**, 2, 89-95

Wolff, J. Das Gesetz der Transformation der Knochen. A. Hirschwald: Berlin, 1892, Translated by Manquet, P. and Furlong, R. as The Law of Bone Remodelling. Springer: Berlin, 1986

Yoshitake, K., Yokota, K., Kasugai, Y., Kagawa, M., Sukamoto, T., and Nakamura, T., 1999, Effects of 16 weeks of treatment with tibolone on bone mass and bone mechanical and histomorphometric indices in mature ovariectomized rats with established osteopenia on a low-calcium diet, Bone, **25**, 3, 311-319

Zioupos, P., and Aspden, R.M., 2000, Density, material quality and quantity issues in OP cancellous bone, in Proceedings of the 12th Conference of the European Society of Biomechancis, Prendergast, P.J., Lee, T.C., and Carr, A.J., Eds., Royal Academy of Medicine in Ireland, Dublin, 2000, 327

Appendix A

Modelling bone as a poroelastic material

Poroelasticity is a theory developed (Biot, 1935, 1941) to model the mechanical behaviour of bi-phasic materials, consisting of a solid phase and a fluid phase. According to Biot's theory, the following basic properties for the porous saturated material are assumed: (1) isotropy, (2) reversibility of the stress-strain relations, (3) linearity of stress-strain relations, (4) small strains, (5) an incompressible fluid phase, (6) the fluid may contain air bubbles, (7) fluid flow through the porous skeleton according to Darcy's Law.

Consider a small cubic element of such a fluid-infiltrated solid, its sides been parallel with the coordinate axes. The element is taken to be large enough compared to the size of pores so that it may be treated as homogenous, and at the same time small enough, compared to the scale of the macroscopic phenomena of interest, so that it may be considered infinitesimal in the mathematical treatment. The average stress condition in the fluid-infiltrated solid is represented by forces distributed uniformly on the faces of this cubic element, which must satisfy the equilibrium conditions of a stress field.

$$\begin{aligned}
&\frac{\partial \sigma_x}{\partial x}+\frac{\partial \tau_{xz}}{\partial y}+\frac{\partial \tau_{xy}}{\partial z}=0\\
&\frac{\partial \tau_{yz}}{\partial x}+\frac{\partial \sigma_y}{\partial y}+\frac{\partial \tau_{yx}}{\partial z}=0\\
&\frac{\partial \tau_{zy}}{\partial x}+\frac{\partial \tau_{zx}}{\partial y}+\frac{\partial \sigma_z}{\partial z}=0
\end{aligned} \qquad (1)$$

Physically the stresses may be considered to be composed of two parts, one that is caused by the hydrostatic pressure of the water filling the pores, the other caused by the average stress in the porous material.

The strain in the soil (e_x, e_y, e_z, γ_{xy}, γ_{xz}, γ_{yz}) can be related to the component of displacement in the material (u, v, w). In order to completely describe the macroscopic condition of the saturated material an additional variable θ, the variation in water content, must be considered. The increment of water pressure may be denoted by σ. Assuming the water pressure to be uniform throughout the element, the macroscopic conditions of the soil (e_x, e_y, e_z, γ_{xy}, γ_{xz}, γ_{yz}, θ) must be functions of the stresses in the

material and water pressure (σ_x, σ_y, σ_z, τ_{xy}, τ_{xz}, τ_{yz}, σ). If the soil is assumed to be isotropic, the water pressure cannot produce any shearing strain, and for the same reason its effect will be the same on all three components of strain e_x, e_y, e_z. Therefore the stress-strain relations reduce to Hooke's law for an isotropic material, with the addition of an extra term relating the water pressure σ to the normal strain:

$$\begin{aligned} e_x &= \frac{\sigma_x}{E} - \frac{v}{E}(\sigma_y + \sigma_z) + \frac{\sigma}{3H}, \\ e_y &= \frac{\sigma_y}{E} - \frac{v}{E}(\sigma_z + \sigma_x) + \frac{\sigma}{3H}, \\ e_z &= \frac{\sigma_z}{E} - \frac{v}{E}(\sigma_x + \sigma_y) + \frac{\sigma}{3H}, \\ \gamma_{xy} &= \frac{\tau_{xy}}{G},\ \gamma_{xz} = \frac{\tau_{xz}}{G},\ \gamma_{yz} = \frac{\tau_{yz}}{G}, \end{aligned} \tag{2}$$

where E is the Young's modulus, G is the shear modulus, v is the Poisson's ratio and H is an additional physical constant. The shear modulus G can be related to the Young's Modulus and the Poisson's ratio,

$$G = \frac{E}{2(1+v)}. \tag{3}$$

Equation 2 expresses the six strain components as a function of the stresses in the soil and the pressure of the water in the fluid. The relationship between the water content θ on these same variables must also be considered. The most general relationship is

$$\theta = a_1\sigma_x + a_2\sigma_y + a_3\sigma_z + a_4\tau_{xy} + a_5\tau_{xz} + a_6\tau_{yz} + a_7\sigma \tag{4}$$

Due to isotropy the shear stress (τ_{xy}, τ_{xz}, τ_{yz}) cannot affect the water content, therefore $a_4 = a_5 = a_6 = 0$. Furthermore all three directions x, y, z must have equivalent properties $a_1 = a_2 = a_3$. Therefore equation 3 may be written as

$$\theta = \frac{1}{3H_1}(\sigma_x + \sigma_y + \sigma_z) + \frac{\sigma}{R}, \tag{5}$$

where H_1 and R are physical constants. If it is assumed that the existence of potential energy in the soil then $H = H_1$ (Proof not shown). Therefore equations 2 and 5 are the fundamental relations describing the properties of the saturated material, for strain and water content, under equilibrium conditions. They contain four distinct physical constants G, v, H and R.

The differential equations for the transient analysis are established by solving equation 1 with respect to the stresses as follows

$$e = e_x + e_y + e_z = (\sigma_x + \sigma_y + \sigma_z)\left(\frac{1-2v}{E}\right) + \frac{\sigma}{H} \tag{6}$$

$$\Rightarrow \quad \frac{1}{E}(\sigma_y + \sigma_z) = \frac{-\sigma_x}{E} + \frac{e}{1-2v} - \frac{\sigma}{H(1-2v)} \tag{7}$$

Substituting equation 6 into the first line of equation 1

$$e_x = \frac{\sigma_x}{E} - v\left(\frac{-\sigma_x}{E} + \frac{e}{1-2v} - \frac{\sigma}{H(1-2v)}\right) + \frac{\sigma}{3H} \tag{8}$$

$$\Rightarrow \quad \sigma_x \frac{(1+v)}{E} = e_x + \frac{ve}{1-2v} - \frac{v\sigma}{H(1-2v)} - \frac{\sigma}{3H} \tag{9}$$

$$\Rightarrow \quad \sigma_x = \frac{E}{1+v}\left(e_x + \frac{ve}{1-2v}\right) - \frac{E}{1+v}\left(\frac{\sigma(v+1)}{3H(1-2v)}\right) \tag{10}$$

Letting $\alpha = \dfrac{2(1+v)G}{3(1-2v)H}$ and given that $G = \dfrac{E}{2(1+v)} \quad \Rightarrow$

$$\sigma_x = 2G(e_x + \frac{ve}{1-2v}) - \alpha\sigma$$

Similarly

$$\sigma_y = 2G(e_y + \frac{ve}{1-2v}) - \alpha\sigma$$

$$\sigma_z = 2G(e_z + \frac{ve}{1-2v}) - \alpha\sigma \tag{11}$$

$$\tau_{xy} = G\gamma_{xy}, \ \tau_{xz} = G\gamma_{xz}, \ \tau_{yz} = G\gamma_{yz},$$

In the same way the variation in water content (equation 5) can be expressed as

$$\theta = \alpha e + \frac{\sigma}{Q} \tag{12}$$

where

$$\frac{1}{Q} = \frac{1}{R} - \frac{\alpha}{H}.$$

Substituting equation 7 for the stresses into equation 2, the equilibrium conditions, it is found that

$$G\nabla^2 u + \frac{G}{1-2v}\frac{\partial e}{\partial x} - \alpha\frac{\partial \sigma}{\partial x} = 0,$$
$$G\nabla^2 v + \frac{G}{1-2v}\frac{\partial e}{\partial y} - \alpha\frac{\partial \sigma}{\partial y} = 0, \qquad (13)$$
$$G\nabla^2 w + \frac{G}{1-2v}\frac{\partial e}{\partial z} - \alpha\frac{\partial \sigma}{\partial z} = 0,$$
$$\nabla^2 = \partial^2/\partial x^2 + \partial^2/\partial y^2 + \partial^2/\partial z^2.$$

There are three equations in four unknowns u, v, w, σ. In order to have a complete system one more equation is needed. This is done by introducing Darcy's law governing fluid flow in a porous medium. According to Darcy's law the rate of flow (V_x, V_y, V_z) is related to the water pressure σ by the relations

$$V_x = -k\frac{\partial \sigma}{\partial x},\ V_y = -k\frac{\partial \sigma}{\partial y},\ V_z = -k\frac{\partial \sigma}{\partial z}, \qquad (14)$$

where k is the permeability of the soil. If the water is incompressible, the rate of change of water content must be equal to the volume of water entering per second through each of the surfaces of the element, hence

$$\frac{\partial \theta}{\partial t} = -\frac{\partial V_x}{\partial x} - \frac{\partial V_y}{\partial y} - \frac{\partial V_z}{\partial z}. \qquad (15)$$

Combining equations 12, 14 and 15 the following expression is obtained

$$k\nabla^2 \sigma = \alpha\frac{\partial e}{\partial t} + \frac{1}{Q}\frac{\partial \sigma}{\partial t} \qquad (16)$$

There are now four equations, equations 13 and 16, satisfied by four unknowns u, v, w, σ.